Austrian Journal of Technical and Natural Sciences

2024, No 7–8

PREMIER Publishing

Vienna
2024

Austrian Journal of Technical and Natural Sciences

Scientific journal

№ 7–8 2024

ISSN 2310-5607

Proofreading Kristin Theissen

Cover design Andreas Vogel

Additional design Stephan Friedman

Editorial office Premier Publishing s.r.o.

Praha 8 – Karlín, Lyčkovo nám. 508/7, PSČ 18600

E-mail: pub@ppublishing.org

Homepage: ppublishing.org

Austrian Journal of Technical and Natural Sciences is an international, English language, peer-reviewed journal. The journal is published in electronic form.

The decisive criterion for accepting a manuscript for publication is scientific quality. All research articles published in this journal have undergone a rigorous peer review. Based on initial screening by the editors, each paper is anonymized and reviewed by at least two anonymous referees. Recommending the articles for publishing, the reviewers confirm that in their opinion the submitted article contains important or new scientific results.

Premier Publishing is not responsible for the stylistic content of the article. The responsibility for the stylistic content lies on an author of an article.

Instructions for authors

Full instructions for manuscript preparation and submission can be found through the Premier Publishing home page at: http://ppublishing.org.

Material disclaimer

The opinions expressed in the conference proceedings do not necessarily reflect those of the Premier Publishing, the editor, the editorial board, or the organization to which the authors are affiliated.

Premier Publishing is not responsible for the stylistic content of the article. The responsibility for the stylistic content lies on an author of an article.

Included to the open access repositories:

TOGETHER WE REACH THE GOAL SJIF 2024 = 6.62 (Scientific Journal Impact Factor Value for 2024).

Included to the Uzbekistan OAK journals bulletin.

The Austrian Journal of Technical and Natural Sciences, No 7–8
ISSN 2310-5607

PREMIER Publishing
ppublishing.org

Section 1. Biology

DOI:10.29013/AJT-24-7.8-3-7

IMPROVING EXTERNAL RESPIRATORY FUNCTION IN PRIMARY SCHOOL CHILDREN IN THE CONDITIONS OF THE REPUBLIC OF KARAKALPAKSTAN

Naubahar Orazbaeva [1]

[1] Department of Sports Psychology, Socio-Natural Sciences, Nukus Branch of the Institute for Retraining and Professional Development of Specialists in Physical Education and Sports

Cite: *Orazbaeva N. (2024). Improving external respiratory function in Primary school Children in the Conditions of the Republic of Karakalpakstan. Austrian Journal of Technical and Natural Sciences 2024, No 7–8.* https://doi.org/10.29013/AJT-24-7.8-3-7

Abstract

The issues of improving external respiratory function in young schoolchildren in the conditions of the Republic of Karakalpakstan are considered. It is shown that there is a high interdependence between the physical development of children and the development of lung ventilation function, as well as the mechanisms of its regulation. The identified relationships in the levels of lung ventilation function development and physical development are consistent and are determined by the heterochrony and unevenness of maturation of each of the studied systems.

Keywords: *external respiration, regulatory mechanisms, Karakalpakstan, reserve capacities, younger generation*

Research in the field of physiology and respiratory biochemistry at the end of the 19th and 20th centuries is known for the development of the diffusion model of gas exchange. The creation of the theory of functional systems and the study of adaptation mechanisms have contributed to the development of various correction methods for respiratory and gas exchange disorders (Minyaev V.I., Minyaeva A.V., Morozov G.I., Petushkov M.N. et al., 2012; Solopov I.N., 2004).

The priority task of society and the state is to preserve and strengthen the health of the younger generation (Kotova A.V., Losevoy T.N., 2011). Children's health reflects the integrated system of material and spiritual relationships existing in society and largely depends on the quality of the natural environment, upbringing conditions, family relationships, the state of the healthcare system, and other factors (Agajanyan N.A., Makarova I.I., 2001; Anokhin P.K., 1978).

The respiratory system is most strongly affected by negative environmental factors, which underlie the high percentage of diseases of the upper respiratory tract, bronchi, and

lungs in children, leading to a decrease in respiratory reserve capacities. It is precisely due to this group of illnesses that children have the highest number of school absences. At the same time, only the school, being the only organized form of social upbringing in the country, covering the entire child population of the country for a long period (from 7 to 17 years), can become the basis for implementing the most modern and effective prevention and health promotion programs (Baevsky P.M., Berseneva A.P., 1997; Berseneva A.P., 2006).

It is known that the respiratory system is one of the leading and largely determining factors of aerobic and anaerobic performance of the body (Dubilei V.V., Dubiley P.V., Kuchinn S.N., 1991; Kabirova E.I., 1989). Breathing is one of the most important forms of constant interaction with the external environment. Attempts to study it and find a connection between breathing, mental state, and health were made in ancient times. Subsequently, at various stages of the development of philosophy and natural science, these attempts received further development (Berseneva A.P., 2006).

Anaerobic capabilities are determined by the ability to use energy in oxygen-deficient conditions, depending on the power of the corresponding enzymatic systems, reserves of energy substances in tissues, the ability to compensate for shifts in the body's internal environment, and the level of tissue adaptation to hypoxic conditions (Breslav I.S., Segizbaeva M.O., Isaev G.G., 2000; Kabirova E.I., 1989).

Aerobic and anaerobic capacities fully characterize the functional "ceiling" of human energy exchange – overall energy capabilities. It should be noted that all bioenergetic reactions that support muscle activity are closely interconnected and typically trigger one another (Kuchkin S.N., 1988; Matyskin A.V., 2006).

There is a high interdependence between the physical development of children and the development of lung function, as well as the mechanisms regulating it. Authors believe that biological age (Bezrukikh, M.M., Farber D.A., 2010), somatotype characteristics, child's adaptive response type (Rubanovich V.B., Girienko L.A., Aizman R.I., 2003), nature of motor activity, environmental and genetic factors significantly influence the pace of physical development and the level of respiratory system functioning (Berseneva A.P., 2006), (Breslav I.S., Segizbaeva M.O., Isaev G.G., 2000; Kabirova E.I., 1989). Between 8 and 9 years of age, against the backdrop of intensified bronchial tree growth, relative alveolar lung ventilation significantly decreases along with the relative oxygen content in the blood. After 10 years, following the relative stabilization of functional indicators, age-related transformations intensify – lung volumes and elasticity increase, relative lung ventilation and oxygen absorption by the lungs decrease even more, and functional indicators start to differ between boys and girls (Bezrukikh, M.M., Farber D.A., 2010). The abundance of interstitial tissue with numerous bronchioles in children's lungs is also a characteristic feature of the respiratory organs, associated with frequent inflammatory processes in the lungs. This necessitates constant care for air cleanliness in educational institutions, proper ventilation, humid cleaning of premises, and adherence to sanitary and hygienic rules (SanPiN No. 0341–16).

The study of the respiratory function of primary school children was carried out using the portable spirometer "SPIROVIT SP-1 – Schiller" (with a pneumotachometer SP-20) manufactured in Switzerland according to standard methods. The following types of spirometric tests were performed with each child: quiet breathing, vital capacity, forced vital capacity, maximum lung ventilation, and functional tests (Bezrukikh, M.M., Farber D.A., 2010; Gamza N.A., Solyanko G.R., Zhukova T.V., 2010).

It is known that the main indicator of spirometry is the vital capacity of the lungs (FVC), which represents the maximum volume of air that can be inhaled (inspiratory FVC) or exhaled (expiratory FVC). The main requirement for measuring FVC is the completeness of the maneuver, not the speed of its execution (Anokhin P.K., 1978; Solopov I.N., 2004). With coordinated work of individual systems, each of which includes its reserves, we can talk about a system of reserves of functioning systems, the level of which follows certain regularities of adaptive processes (Kulikov V. Yu., Pikovskaya N.B. 2011).

The results obtained indicate that during children's development, the indicators of vital lung capacity (FVC) tend to increase (table 1).

Table 1. *Age dynamics of respiratory function indicators in children living in the South Aral region (M±m) (n=125)*

age	gender	FVC	PEF	FEF-75	FEF-25
8	b (n = 11)	1.94 ± 0.08	3.77 ± 0.1	3.33 ± 0.1	1.26 ± 0.07
	g (n =18)	1.72 ± 0.08	4.06 ± 0.2	3.53 ± 0.2	1.36 ± 0.1
9	b (n = 10)	2.18 ± 0.08	4.49 ± 0.2	3.78 ± 0.2	1.33 ± 0.07
	g (n = 12)	1.85 ± 0.06	4.24 ± 0.1	3.86 ± 0.1	1.42 ± 0.1
10	b (n = 11)	2.34 ± 0.07	4.91 ± 0.2	4.23 ± 0.1	1.54 ± 0.1
	g (n = 14)	2.07 ± 0.07	5.17 ± 0.1	4.31 ± 0.2	1.76 ± 0.01

Note: g – girls, b – boys, FVC – forced vital capacity (liters); FEF-75 – forced expiratory flow at 75% of FVC (liters/second); FEF-25 – forced expiratory flow at 25% of FVC (liters/second), PEF – peak expiratory flow (liters/second)

During the conducted research, it was found that in boys aged 6 and 7 years, the FVC values were 1.90 ± 0.07 L and 1.93 ± 0.02 L respectively. The greatest increase in FVC was observed in children aged 9 and 10 years, with boys showing FVC values of 2.18 ± 0.08 L and 2.34 ± 0.07 L ($p < 0.001$) respectively.

Analysis of the data revealed that in girls aged 6 and 7 years, the FVC values were 1.60 ± 0.04 L and 1.62 ± 0.08 L respectively. The highest increase in FVC was observed in girls aged 9 and 10 years, with absolute FVC values of 1.85 ± 0.06 L and 2.07 ± 0.07 L ($p < < 0.001$) respectively. In girls aged 10 years, the FVC was significantly higher at 2.07 ± 0.07 L ($p < 0.001$) compared to girls aged 6 years and not significantly different from girls aged 8 years ($p > 0.05$).

Examination of the patency of various parts of the tracheobronchial tree showed that in boys, there is a tendency towards increased bronchial patency with age. In boys aged 9 and 10 years, the patency of large bronchi (FEF-75) was 3.78 ± 0.2 L/s and 4.23 ± ± 0.1 L/s respectively compared to 3.33 ± 0.1 L/s for boys aged 7 and 8 years (respectively) ($p < 0.001$). In girls aged 9 and 10 years, the absolute values of FEF-75 were significantly increased to 4.31 ± 0.2 L/s compared to values of 3.48 ± 0.2 L/s and 3.53 ± 0.2 L/s in girls aged 7 and 8 years ($p < 0.001$).

It should be noted that the absolute values of small airway flow rates (FEF-25) in boys aged 9 and 10 years were significantly higher at 1.33 ± 0.07 and 1.54 ± 0.1 L/s, respectively, compared to boys aged 6–8 years ($p < 0.05$). As for girls, in the 9–10 age group, small airway flow rates (FEF-25) were significantly increased to 1.42 ± 0.1 and 1.76 ± 0.01 L/s ($p < 0.001$) compared to girls aged 7– –8 years, and significantly higher than the 1.23 ± 0.1 L/s in girls aged 6 years ($p < 0.001$).

It is known that the movement of airflow during breathing is associated with a considerable expenditure of energy by the respiratory muscles. During inhalation, the elastic resistance of the lungs and chest tissues, the elastic resistance of the organs in the chest and abdominal cavities moving during breathing, as well as the resistance of the tracheobronchial tree have to be overcome (Kabirova E. I., 1989; Kuznetsova T. D., 1983; Kuznetsova T. D., 1986). Since muscular activity is the most powerful natural stimulus for breathing, we attached great importance to the dynamics of ventilation parameters after light physical exertion on the subjects (Garkavi L. Kh., Glanz S., 1999; Kabirova E. I., 1989; Kuznetsova T. D., 1983). Impulses from the sensorimotor cortex to the working muscles simultaneously have a direct influence on the respiratory center through corticobulbar pathways. In addition, breathing is stimulated by afferent impulses coming from the proprioceptors of the working muscles (Kuznetsova T. D., 1986). As soon as muscular load is initiated, breathing becomes faster and deeper. At the same time, the variability of ventilation parameters increases, which is apparently related to the different individual sensitivity of chemoreceptors and the respiratory center to humoral factors regulating breathing, as well as to the different intensity of metabolic processes in children of the same calendar age (Matyskin A. V., 2006; Ustyushin B. V., Istomin A. V., 1996).

All examined children show a relatively favorable dynamic of maximal lung ventilation (MLV) after the performed load: at 8 years old, it is 98.8%, at 9 years old, it is 106.8%, and at 10 years old, it is 102.4% of the resting level. If the testing of MLV in the first 60 seconds of the recovery period reveals that its value has not changed or has decreased but has not reached zero, then the performed load is considered relatively adequate. Such changes in the respiratory system are observed in examined 8–9-year-old children. In examined 10-year-old children, the response to this load is favorable, and adaptation to it occurs without additional strain on the external respiratory system, without signs of respiratory muscle fatigue.

It is well known that static and dynamic lung volumes increase with the age of children. This increase is provided by greater lung compliance with increasing age and the ability of muscles to produce maximum changes in thoracic cavity volume. Periods of maximal growth in these indicators are noted between 5 and 7 years old, i.e., at the age of 6 years, due to the predominance of the process of airway expansion over their elongation, bronchial resistance decreases intensively, breathing rates increase, and, accordingly, dynamic lung volumes increase. Under conditions of rest and breathing with atmospheric air, the functional indicators of the examined children correspond to age norms.

However, the respiratory reserve after performing the MLV test in these children falls into the category of high values. This fact, during the examination of the external respiratory system, is not considered a sign of any respiratory function-related disease but rather an individual reaction of the child to the load presented to them, indicating processes of adaptive response (Skoblina N.A., 2008; Ustyushin B.V., Istomin A.V., 1996). In this case, the activity of the autonomic systems, including the respiratory system, changes to create optimal conditions for supplying working muscles with energy and minimizing negative shifts in the body's internal environment that may arise due to metabolic processes in the muscles (Kuchkin S.N., 1988; Matyskin A.V., 2006; Skoblina N.A., 2008; Ustyushin B.V., Istomin A.V., 1996).

The identified relationships between the levels of lung ventilation function development and physical development are consistent and determined by the heterochrony and uneven maturation of each of the studied systems. Ventilation in 8–9-year-old children during exercise is provided solely by an increase in breathing rate, while in 10-year-old children, an increase in tidal volume is also slightly involved.

Therefore, considering the high pollution levels in the lower atmospheric layer in the Southern Aral Sea region, the observed increase in bronchial patency in children was interpreted by us as an undesirable reaction and one of the factors contributing to bronchopulmonary pathology development. Increasing bronchial patency in dusty atmospheric conditions is physiologically irrational. When assessing the levels of lung ventilation function development and physical development, it is important to consider the influence of environmental factors and heredity, especially in children who fall outside the average level of physical development. The use of developed assessment tables can help identify the nature and extent of deviations in the functional development of the respiratory system and physical development, determine ways and methods for their correction.

References:

Minyaev V.I., Minyaeva A.V., Morozov G.I., Petushkov M.N., et al. Features of functional relationships between the respiratory and circulatory systems // Bulletin of Tver State University. Series: Biology and Ecology, 2012.– No. 3.– P. 19–27. (In Russian)

Solopov I.N. Physiological effects of methods of targeted impact on human respiratory function: monograph.– Volgograd, 2004.– 220 p. (In Russian)

Physiology and Basics of Anatomy: student / ed. A.V. Kotov, T.N. Loseva.– M.: Medicine, 2011.– 1056 p. (In Russian)

Agadzhanyan N.A., Makarova I.I. Habitat and reactivity of the organism.– Tver, 2001. – 176 p. (In Russian)

Anokhin P.K. Systemogenesis as a General Law of the Evolutionary Process // Philosophical Aspects of the Theory of a Functional System.– Moscow: Nauka, 1978.– P. 125–150. (In Russian)
Baevsky R.M., Berseneva A.P. Assessment of the Adaptive Capacities of the Body and the Risk of Disease Development.– Moscow, 1997.– 180 p. (In Russian)
Berseneva A.P. Problems of Adaptation and the Study of Health. – Moscow: RUDN University Press, 2006.– 284 p. (In Russian)
Dubiley V.V., Dubiley P.V., Kuchkin S.N. Physiology and Pathology of the Respiratory System in Athletes.– Kazan, 1991.– 146 p. (In Russian)
Kabirova E.I. Function of External Respiration and the Health Status of Senior Preschool Children // Hygienic and Medico-Biological Aspects of Population Health: Collection of Scientific Papers.– L., 1989.– P. 46–49. (In Russian)
Breslav I.S., Segizbaeva M.O., Isaev G.G. Does the respiratory system limit human aerobic performance? // Human physiology.2000.– Vol. 26.– No. 4.– P. 115–122. (In Russian)
Kuchkin, S.N. Respiratory system reserves and aerobic performance of the body: author's abstract. diss. ... doctor of medical sciences.– Kazan, 1988.– 48 p. (In Russian)
Matyskin A.V. Parameters of external respiration under dust pollution conditions // Abstract of the annual scientific and practical conference of young scientists dedicated to the 30 th anniversary of the State Research Institute of Medical Problems of the North, Siberian Branch of the Russian Academy of Medical Sciences.– Krasnoyarsk, 2006.– P. 98–99. (In Russian)
Physiology of child development. Handbook of Age Physiology / Ed. by M.M. Bezrukikh, D.A. Farber.– M.: MPSI, 2010.– 768 p. (In Russian)
Rubanovich V.B., Giryenko L.A., Aizman R.I. Features of morphofunctional development of boys aged 7–14 years of different types of adaptive response // Human Physiology. 2003.– Vol. 29.– No. 3.– P. 48–53. (In Russian)
Sanitary and epidemiological requirements for the conditions and organization of education in comprehensive schools (SanPiN No. 0341–16) of the Republic of Uzbekistan. (In Russian)
Gamza N.A., Solyanko G.R., Zhukova T.V. Functional tests in sports medicine.– Minsk: BSUPC, 2010.– 57 p. (In Russian)
Kuznetsova T.D. Development of respiratory function of the lungs / Physiology of child development.– M.: Pedagogy, 1983.– P. 115–133. (In Russian)
Kuznetsova T.D. Age-related features of breathing in children and adolescents.– M.: Medicine, 1986.– 128 p. (In Russian)
Garkavi L. Kh., Glanz S. Adaptive reactions of training, activation and stress, principles of their formation and role in maintaining health Medical and biological statistics / – M.: Praktika, 1999.– 459 p. (In Russian)
Ustyushin B.V., Istomin A.V. et al. Features of the state of health and adaptive reactions of the child's body in the North // Pediatrics. 1996. No. 1.– P. 56–59. (In Russian)
Skoblina N.A. Physical development of children in different social conditions // Russian Pediatric Journal. 2008.– No. 3.– P. 29–31. (In Russian)
Kozinets G.I. Physiological systems of the human body, main indicators.– M.: Triada-X, 2000.– 384 p. (In Russian)
Kozlikina N.B., Gainanova N.K. Some features of physical development of children (6–10 years old) with different rates of growth processes // Biological science and education in pedagogical universities: materials of the VII All-Russian scientific and practical conference "Problems of biological science and education in pedagogical universities" Issue. 7.– Novosibirsk: Publ. NSPU, 2011.– P. 98–102. (In Russian)
Resolution of the Committee for Sanitary and Epidemiological Welfare and Public Health under the Ministry of Health of the Republic of Uzbekistan, dated 09.15.2023 No. 22. (In Russian)

submitted 14.07.2024;
accepted for publication 29.07.2024;
published 28.09.2024

Contact: gayrat-n@bk.ru

The Austrian Journal of Technical and Natural Sciences, No 7–8
ISSN 2310-5607

PREMIER Publishing
ppublishing.org

Section 2. Chemistry

DOI:10.29013/AJT-24-7.8-8-13

STUDYING THE BIOLOGICAL ACTIVITY OF ISOMERIC N-(TOLYL)-α-PICOLINAMIDES IN THE PASS ONLINE PROGRAM

Burieva Dilnoza Madarttovna [1], Abdushukurov Anvar Kabirovich [1], Yusufov Mukhriddin Saidovich [1]

[1] National University of Uzbekistan, Tashkent

Cite: *Burieva D.M., Abdushukurov A.K., Yusufov M.S. (2024). Studying the Biological Activity of Isomeric N-(Tolyl)-A-Picolinamides in the Pass Online Program. Austrian Journal of Technical and Natural Sciences 2024, No 3–4.* https://doi.org/10.29013/AJT-24-7.8-8-13

Abstract

The biological activity of the isomers of toluidine and N-(tolyl)-α-picolinamides synthesized on the basis of picolinic acid was studied in the PASS online program (https://www.way2drug.com/PassOnline/index.php). Indicators of the biological activity of isomeric amides in relation to certain diseases, adverse and toxic effects on the body, negative effects of drugs on the cardiovascular and hepatobiliary systems, cytotoxic effects on cancer cells and human breast cancer cell lines were obtained. The results are summarized in a table. Judging by the tables above, the biological activity of isomeric N-(tolyl)-α-picolinamides showed very similar results compared to each other

Keywords: *PASS online program, N-(tolyl)-α-picolinamide, Pa and Pi values, toxicity, cancer cells, prognosis*

Introduction

Today, the development of new, more effective and safe drugs is one of the priorities of organic chemistry, and in the production of such drugs PASS, GUSAR and Pharma Expert programs are used, which make it possible to accurately predict various types of biological activity based on structural formulas of compounds of different chemical classes. On the basis of these programs, the initial approximate primary biological properties of organic compounds are revealed and used in the practical study of biological properties of substances. This helps save time and money.

One of the most important properties of chemical compounds is their biological activity, the presence of which allows or prevents the practical application of a chemical compound in medicine, cosmetics, food industry, agricultural chemistry and other fields (Barenboim G.M., Malenkov A.G., 1986). By using the PASS (Prediction of Activity Spectra for Substances) program, the pharmacotherapeutic effect, biochemical mechanisms of action, toxic and adverse effects, interaction

characteristics with antitargets, drug metabolism for a given compound can be determined. It is possible to estimate the properties associated with the transporter proteins, the parameters of the interaction and the changes in the expression of certain genes. The GUSAR program allows prediction of acute toxicity in mice and rats with four types of administration, interactions with antitargets, and certain characteristics of ecotoxicology. PharmaExpert software is designed to analyze the results of PASS and GUSAR predictions, to see the relationships between different activities and to search for chemical compounds with the required bio-logical activity profiles (Druzhilovskiy D.S., Rudik A.V., Filimonov D.A., Gloriozova T.A., Lagunin A.A., Dmitriev A.V., Poroikov V.V., 2017). As part of the collaborative work of the Institute of Chemical and Energy Technology Problems (Siberian branch of the Russian Academy of Sciences) and the Novosibirsk Institute of Organic Chemistry (Siberian branch of the Russian Academy of Sciences), the biological activity spectra of a number of compounds in the hexaazaisowurtzitane structure (the biological activity spectrum of a chemical compound is the spectrum of various biological properties of this compound a set of different types of biological activity reflecting the results of interaction with objects (URL: https://www.way2drug.com/passonline/index.php) predicted and the results of in vivo analysis reviewed by scientists of the Siberian Department of the Russian Academy of Sciences of the compounds studied in the PASS program confirmed the predicted activity (Tolstikova T.G., Morozova E.A., Sysolyatin S.V., Kalashnikov A.I., Zhukova Yu.I., Surmachev V.N., 2010). The biological activity spectra of the hexaazaizawurtzitan structure according to PASS Online program analyzes predicted nootropic and analgesic activity with high probability (Pa = 0.881–0.956) and their subsequent pharmacological in vivo analysis confirmed only analgesic activity for these compounds and studies two patents were obtained as a result (RF Patent No. 2558148; Byul. Izobret. [Invention Bulletin], 2015, 21; RF Patent No. 2565766; Byul. Izobret. [Invention Bulletin], 2015, 29).

Amide functionalities attract much attention in current chemical and industrial research, not only because of their wide biological and pharmacological activity, but also because they are versatile reagents for the synthesis of various useful molecules. A review of the literature shows that more than 50% of known drugs contain amide units. Among bioactive compounds, N-hetero-aryl amides are widely distributed as an important class of medicinal compounds. Recently, pyridyl benzamide derivative (1) has been reported as Trypanosoma brucei inhibitors (Ferrins L., Gazdik M., Rahmani R., Varghese S., Sykes M.L., Jones A.J., Avery V.M., White K.L., Ryan E., Charman S.A., Kaiser M., Bergström C.A.S. and Baell J.B., 2014), tubulin (2) polymerization inhibitor – tumor growth reduction (Colley H.E., Muthana M., Danson S.J., Jackson L.V., Brett M.L., Harrison J., Coole S.F., Mason D.P., Jennings L.R., Wong M., Tulasi V., Norman D., Lockey P.M., Williams L., Dossetter A.G., Griffen E.J. and Thompson M.J. 2015), thiazolyl amides (3) as protein methyltransferase selective inhibitors (Gao C., Margolis B.J., Strelow J.M., Vidler L.R. and Mader M.M., 2016).

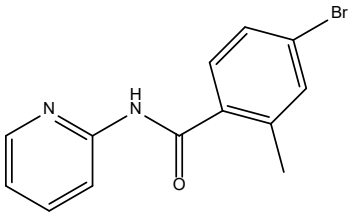

1

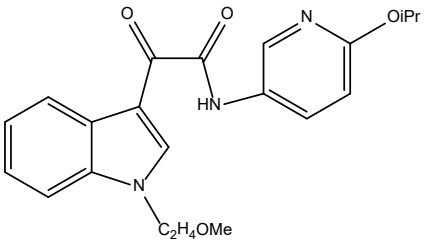

2

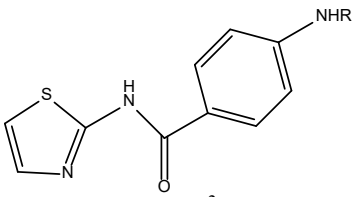

3

Research methodology

In this article, N-(tolyl)-α-picolinamides were synthesized from toluidine isomers and picolinic acid, and how the position of the methyl ($-CH_3$) group in the benzene ring in the N (tolyl)-α-picolinamide molecule affects the biological activities of amides PASS online (https://www.way2drug.com/PassOnline/

index.php) was studied using the program. The PASS online program is a software product designed as a tool to assess the overall biological potential of an organic drug-like molecule. The PASS program provides simultaneous prediction of many types of biological activity based on the structure of organic compounds. Thus, PASS can be used for chemical synthesis of virtual molecules and evaluation of biological activity profiles prior to biological testing. PASS results are expressed as Pa (probability of active compound) and Pi (probability of inactive compound). If Pa > 0.7 according to the results of PASS, the possibility of finding the activity experimentally is high. 0.5 < Pa < 0.7 indicates moderate therapeutic potential. Pa < 0.5 indicates weak pharmaceutical activity and the activity is less likely to be found experimentally (URL: https://www.way2drug.com/passonline/index.php; Abe Kawsar S.M., Hosen Mohammed A., Tasneem Sultana Chowdhury, Kazi Masud Rana, Yuki Fujii, Yasuhiro Ozeki, 2021).

Results and discussion

Three isomeric amides are formed from the reaction of toluidine isomers and picolinic acid.

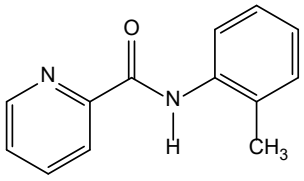

N-(o-tolyl)-α-picolinamide

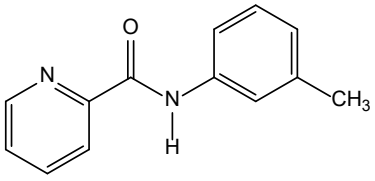

N-(m-tolyl)-α-picolinamide

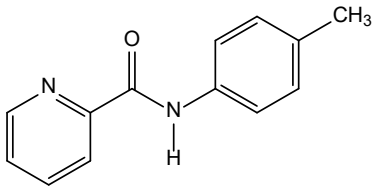

N-(p-tolyl)-α-picolinamide

In the PASS online program, indicators of biological activity of isomeric N-(tolyl)-α-picolinamides against some diseases, adverse and toxic effects on the body, adverse drug effects on the cardiovascular and hepatobiliary systems, cancer cell lines the cytotoxic effect of chemical compounds and the cytotoxicity of the substance against human breast cancer cell lines were obtained and the obtained results were compared in the form of a table. The results show that the biological activities of amides synthesized from picolinic acid and toluidine isomers are close to each other.

The N-(tolyl)-α-picolinamide isomers obtained using the program are mainly 5-hydroxytryptamine release inhibitor, amine dehydrogenase inhibitor, membrane integrity agonist, mucosa protector, platelet-derived growth factor receptor kinase inhibitor, taurine dehydrogenase inhibitor, urethanease inhibitor, indications of biological activity against some diseases such as an insulin inhibitor (https://www.way2drug.com/passonline). The Pa value of the obtained results shows a close value in isomeric amides (Table 1).

Table 1. *Predicted biological activities of N-(tolyl)-α-picolinamides against some diseases using PASS online program*

Biological activity	Molecules					
	N-(o-tolyl)-α-picolinamide		N-(m-tolyl)-α-picolinamide		N-(p-tolyl)-α-picolinamide	
	Pa	Pi	Pa	Pi	Pa	Pi
5-Hydroxytryptamine release inhibitor	0.776	0.004	0.791	0.004	0.788	0.004
Amine dehydrogenase inhibitor	0.718	0.007	0.663	0.010	0.718	0.007
Membrane integrity agonist	0.661	0.062	0.690	0.057	0.762	0.044
Mucous membrane protector	0.684	0.064	0.777	0.025	0.769	0.028

Biological activity	Molecules					
	N-(o-tolyl)-α-picolinamide		N-(m-tolyl)-α-picolinamide		N-(p-tolyl)-α-picolinamide	
	Pa	Pi	Pa	Pi	Pa	Pi
Platelet-derived growth factor receptor kinase inhibitor	0.768	0.005	0.794	0.004	0.777	0.004
Taurine dehydrogenase inhibitor	0.781	0.016	0.745	0.023	0.781	0.016
Urethanease inhibitor	0.707	0.008	0.556	0.021	0.618	0.015
Insulin inhibitor	0.583	0.028	0.698	0.009	0.686	0.010

On the basis of the PASS online program, along with the results of the activity of chemical compounds against certain diseases, it is possible to obtain estimates about the adverse and toxic effects of the chemical compound on the body, and preliminary information about the negative and toxic effects of the studied compound (https://www.way2drug.com/passonline) (Table 2). Estimated results are sometimes based on clinical manifestations observed in a few or even a single patient.

Table 2. *Adverse and toxic effects of N-(tolyl)-α-picolinamides studied in the PASS online program*

Biological activity	Molecules					
	N-(o-tolyl)-α-picolinamide		N-(m-tolyl)-α-picolinamide		N-(p-tolyl)-α-picolinamide	
	Pa	Pi	Pa	Pi	Pa	Pi
Crampy syndrome	0.888	0.006	0.840	0.021	0.858	0.014
Hematemesis	0.813	0.012	0.779	0.016	0.813	0.012
Stomach ulcer, aphth	0.735	0.034	0.757	0.028	0.787	0.021
Bleeding from the gastrointestinal tract	0.750	0.014	0.719	0.020	0.750	0.014
Neutrophil dermatosis (Sweet's syndrome)	0.653	0.068	0.685	0.056	0.723	0.044

The results of predicting the adverse effects of drugs based on N-(tolyl)-α-picolinamides on the cardiovascular and hepatobiliary systems (https://www.way2drug.com/adverpred/) Pa value for isomeric amides range from 0.600 to 0.413 showed activity in (Table 3).

Table 3. *Results of predicting adverse effects of drugs based on N-(tolyl)-α-picolinamides on cardiovascular and hepatobiliary systems*

Biological activity	Molecules					
	N-(o-tolyl)-α-picolinamide		N-(m-tolyl)-α-picolinamide		N-(p-tolyl)-α-picolinamide	
	Pa	Pi	Pa	Pi	Pa	Pi
Myocardial infarction	0.562	0.034	0.600	0.028	0.599	0.028
Heart failure	0.538	0.040	0.553	0.034	0.556	0.033
Arrhythmia	0.537	0.080	0.413	0.175	0.432	0.162
Hepatotoxicity	0.428	0.238	0.619	0.134	0.570	0.160

Simultaneous quantitative and qualitative predictions of IC_{50} and IG_{50} values were obtained for each isomeric amide to predict the cytotoxic effects of chemical compounds on cancer cell lines and drug-like compound cytotoxicity against nine breast cancer cell lines (https://www.way2drug.com/Cell-line/). Cytotoxic effects of isomeric amides on cancer cell lines Pa and Pi values are 0.533 and 0.027 for N-(o-tolyl)-α-picolinamide. 0.525 and 0.031 for N-(m-tolyl)-α-picolinamide and N-(β-tolyl)-α-picolinamides. The obtained results are presented in tables 4 and 5.

Table 4. *Cytotoxic effects of N-(tolyl)-α-picolinamides on cancer cell lines*

Pa	Pi	Cell line	Cell-line Full name	Tissue	Tumor type
0.533 – – 0.525	0.027 – –0.031	Kasumi 1	Childhood acute myeloid leukemia with maturation	Haematopoietic and lymphoid tissue	Leukemia

Table 5. *Cytotoxic effects of N-(tolyl)-α-picolinamides against breast cancer cell lines*

Breast cancer cell name	Classification				Quantitative			
	IC_{50}		GI_{50}		pIC_{50}		pGI_{50}	
	Value	AD	Value	AD	Value	AD	Value	AD
N-(o-tolyl)-α – picolinamide								
Bcap37	inactive	+						
BT-20	inactive	+	active	+			5.5762	+
Hs-578T	inactive	+	inactive	+				
MCF7			inactive	+	4.7098	+	4.9716	+
MCF7-DOX	active	+			5.7560	+		
MCF7R	inactive	+			4.5544	+		
MX-1	inactive	+			6.3299	+		
T47D	inactive	+	active	+	5.3721	+	5.8061	+
ZR-75–1	inactive	+	inactive	+	5.6109	+	4.7132	+
N-(m-tolyl)-α – picolinamide								
Bcap37	inactive	+						
BT-20	inactive	+	active	+			5.5155	+
Hs-578T	inactive	+	inactive	+				
MCF7			inactive	+	4.7823	+	4.9231	+
MCF7-DOX	active	+			5.6372	+		
MCF7R	inactive	+			4.4986	+		
MX-1	inactive	+			6.4528	+		
T47D	inactive	+	active	+	5.2233	+	5.6010	+
ZR-75–1	inactive	+	inactive	+	5.5816	+	4.7709	+
N-(p-tolyl)-α – picolinamide								
Bcap37	inactive	+						
BT-20	inactive	+	active	+			5.5144	+
Hs-578T	inactive	+	inactive	+				
MCF7			inactive	+	4.7705	+	4.7912	+
MCF7-DOX	active	+			5.4059	+		
MCF7R	inactive	+			4.5290	+		
MX-1	inactive	+			6.3985	+		
T47D	inactive	+	active	+	5.3755	+	5.4059	+
ZR-75–1	inactive	+	inactive	+	5.5704	+	4.7616	+
Bcap37	inactive	+						

Conclusion

Based on the given tables, the biological activities of N-(tolyl)-α picolinamides showed very close results when compared to each other. The position of the methyl ($-CH_3$) group in the benzene ring of the N-(tolyl)-α-picolinamide molecule does not affect the biological activity of the molecule, and the biological activity is similar regardless of the position of the methyl group in the ring. The results obtained in the PASS online program serve as a basis for studying the biological activity of substances in practice.

References

Barenboim G. M., Malenkov A. G. Biologicheski aktivnye veshchestva. Novye printsipy poiska [Biologically Active Substances. New Principles of Search] // Nauka,– Moscow, 1986.– 363 p.

Druzhilovskiy D. S., Rudik A. V., Filimonov D. A., Gloriozova T. A., Lagunin A. A., Dmitriev A. V., Poroikov V. V. Computational platform Way2Drug: from the prediction of biological activity to drug repurposing // J. Russian Chemical Bulletin, International Edition, 2017.– Vol. 66(10).– P. 1832–1841.

URL: https://www.way2drug.com/passonline/index.php

Tolstikova T. G., Morozova E. A., Sysolyatin S. V., Kalashnikov A. I., Zhukova Yu.I., Surmachev V. N. Khimiya v Interesakh Ustoichivogo Razvitiya [Chemistry in Interests of Stable Development] // 2010.– Vol. 18.– 511 p.

RF Patent No. 2558148; Byul. Izobret. [Invention Bulletin], 2015, 21.

RF Patent No. 2565766; Byul. Izobret. [Invention Bulletin], 2015, 29.

Ferrins L., Gazdik M., Rahmani R., Varghese S., Sykes M. L., Jones A. J., Avery V. M., White K. L., Ryan E., Charman S. A., Kaiser M., Bergström C. A.S. and Baell J. B. Pyridyl Benzamides as a Novel Class of Potent Inhibitors for the Kinetoplastid Trypanosoma brucei // J. Med. Chem., 2014.– Vol. 57.– P. 6393–6402.

Colley H. E., Muthana M., Danson S. J., Jackson L. V., Brett M. L., Harrison J., Coole S. F., Mason D. P., Jennings L. R., Wong M., Tulasi V., Norman D., Lockey P. M., Williams L., Dossetter A. G., Griffen E. J. and Thompson M. J. An Orally Bioavailable, Indole-3-glyoxylamide Based Series of Tubulin Polymerization Inhibitors Showing Tumor Growth Inhibition in a Mouse Xenograft Model of Head and Neck Cancer // J. Med. Chem., 2015.– Vol. 58.– P. 9309–9333.

Gao C., Margolis B. J., Strelow J. M., Vidler L. R. and Mader M. M. Beyond PAINs: Chemotype Sensitivity of Protein Methyltransferases in Screens // J. ACS Med. Chem. Lett., 2016.– Vol. 7.– P. 156–161.

Abe Kawsar S. M., Hosen Mohammed A., Tasneem Sultana Chowdhury, Kazi Masud Rana, Yuki Fujii, Yasuhiro Ozeki. Thermochemical, PASS, Molecular Docking, Drug-Likeness and In Silico ADMET Prediction of Cytidine Derivatives Against HIV-1 Reverse Transcriptase // Rev. Chim., 2021.– Vol. 72(3).– P. 159–178.

submitted 09.07.2024;
accepted for publication 24.07.2024;
published 28.09.2024

Contact: dilnozaboriyeva133@gmail.com

The Austrian Journal of Technical and Natural Sciences, No 7–8
ISSN 2310-5607

PREMIER Publishing
ppublishing.org

DOI:10.29013/AJT-24-7.8-14-17

ANALYSIS OF THE QUANTITY OF MICRO AND MACRO ELEMENTS IN THE ALHAGI MAURORUM PLANT GROWN IN THE KASHKADARYA REGION BY MASS SPECTROMETRY (ICP-MS) METHOD

Baltabaev Ulugbek Narbaevich [2], Kholmurodov Bahodir [1], Sa'dullayeva Shahribonu [1], Nasriddinov Jaloliddin [1], Choriyev Abdusattor [2]

[1] Tashkent Chemical Technology Institute of Shahrisabz branch. Republic of Uzbekistan. Shahrisabz

[2] Tashkent Chemical Technology Institute. Republic of Uzbekistan. Tashkent

Cite: *Baltabaev U. N., Kholmurodov B., Sa'dullayeva Sh., Nasriddinov J., Choriyev A. (2024). Analysis of the Quantity of Micro and Macro Elements in the Alhagi Maurorum Plant Grown in the Kashkadarya Region by Mass Spectrometry (Icp-Ms) Method. Austrian Journal of Technical and Natural Sciences 2024, No 3–4.* https://doi.org/10.29013/AJT-24-7.8-14-17

Abstract

A review of the literature on the significance of Alhagi maurorum and its importance was carried out. The amount of macro and microelements in the upper parts of Alhagi maurorum, i.e., seeds and leaves, was determined and analyzed using inductively coupled plasma mass spectrometry (ICP-MS) for 61 elements. According to the results, the amount of P, K, Ti, Cr, Ni, Cu, Zn, and Rb elements is higher in the seed part of Alhagi maurorum than in the leaf part, and in the leaf part, Li, Be, B, Na, Mg, Al, Ca, Sc, V, Mn, Fe, Co, Ga, As, Se, Sr, Y, Zr, Nb, Mo, Ag, Cd, In, Sn, Cs, Ba, Ce, Pr, Nd, Sm, Eu, The abundance of Gd, Dy, Re, Pb, Th, and U elements was determined. It was observed that the amount of other elements is close to each other.

Keywords: *Alhagi maurorum, micro and macro elements, coupled plasma mass spectrometry, ISPMS, grain, leaf, and seed of Alhagi maurorum plant*

Introduction

Alhagi maurorum is a wild herb with many medicinal properties. Belongs to the kingdom Plantae, order Fabales, family Fabaceae, and genus Alhagi. Since ancient times, people have used Alhagi maurorum to treat many ailments related to the respiratory, liver, cardiovascular, gastrointestinal, immune, and genitourinary systems. (Awaad Amani A.S., Maitland D.J., Soliman G.A., 2006).

The anti-infective effects of Alhagi maurorum extract (AME), a traditional Middle Eastern medicinal plant, on biofilm-forming Proteus mirabilis isolates were investigated by in vitro adhesion assay in cell culture and agar overlay assay using Janthinobacterium lividum (ATCC12472). Mainly, AME reduced biofilm formation in P. mirabilis by targeting genes, and AME showed anti-P. mirabilis and anti-QS activity (Arezoo, Mirzaei., Bahram, Nasr, Es-

fahani., Mustafa, Ghanadian., Sharareh, Moghim., 2022).

Literature Review

The phytochemical composition of the ethanol extract of Alhagi maurorum root was studied using gas chromatography-mass spectroscopy (GC–MS). 32 chemical compounds identified in A. maurorum root extract with medicinal benefits, and anti-inflammatory, antibacterial, and anti-cancer effects have been identified (Mohammed R. K., Noor, Alzahraa, Dheaa, Abd-alkadhemand, 2022).

Dehydroquercetin, rutin, quercetin, lutein, and seneroside substances belonging to the class of flavonoids were analyzed by chromatography of leaves, stems, and seeds of Alhagi maurorum. These flavonoids are natural antioxidants. The above-ground parts of Alhagi maurorum leaves, stems and seeds have been recommended for general use (Kholmurodov B. B., 2023).

The chemical composition and mineral content of the bread samples with Alhagi maurorum powder, based on the analysis results, showed that the Alhagi maurorum powder contains a large amount of protein and raw fiber, in addition to some important minerals such as calcium, phosphorus, and iron. Alhagi maurorum powder increased fiber, ash, and lipids and decreased moisture, protein, and carbohydrates. The addition of Alhagi maurorum powder improved the nutritional content but decreased the intake (wad, Allah., Usama, El-Sayed, Mostafa., I. M., Abd, El-Razik., W., K., Abou, El, Ahmed, 2022).

Minerals are an important component of our body. They perform a variety of functions, including building materials for our bones, influencing muscle and nerve function, and regulating the body's water balance. They are also a component of hormones enzymes and other biologically active compounds. Some minerals also play an important role in the optimal functioning of the immune system. This applies to both the innate defense system and adaptive immunity. Accordingly, mineral supply may affect susceptibility to infections, but it also affects the development of chronic diseases. (Calder P. C., Carr A. C., Gombart A. F., Eggersdorfer M., 2020).

Methods

The mineral content of the Alhagi maurorum plant grown in the Kashkadarya region of the Republic of Uzbekistan in terms of dry mass was analyzed in the central laboratory of JSC "Uzbek Geological Research".

In the process of sample preparation, an exact sample of 0.0500–0.5000 g of the tested substance is weighed on an analytical scale and transferred to Teflon autoclaves. The autoclaves are then filled with an appropriate amount of purified concentrated mineral acids (nitric acid (n/s) and hydrogen peroxide (n/s)). The autoclaves are sealed and placed in a Berghofc microwave digester using MWS-3+ software or a similar microwave digester. Depending on the type of the studied substance, the decomposition program is determined, and the degree of decomposition and the number of autoclaves are indicated (up to 12 pieces).

After disintegration, the contents of the autoclaves are quantitatively transferred to 50 or 100-ml volumetric flasks, and the volume is adjusted to the mark with 0.5% nitric acid.

The detection of the substance under study is carried out using an ISPMS device or a similar optical emission spectrometer device with an inductively coupled argon plasma. The optimal wavelength of micro- or macroelements to be detected in the detection method is indicated, at which they have maximum emission.

Results and discussion

After receiving the information, the actual quantitative composition of the substance in the test sample is automatically calculated by the device and entered in the form of mg/kg or μg / g with error limits – in RSD%.

Based on the results of the analysis, the amount of P, K, Ti, Cr, Ni, Cu, Zn, and Rb elements is more in the seed part of Alhagi maurorum than in the leaf part, and in the leaf part, compared to the seed part, Li, Be, B, Na, Mg, Al, Ca, Sc, V, Mn, Fe, Co, Ga, As, Se, Sr, Y, Zr, Nb, Mo, Ag, Cd, In, Sn, Cs, Ba, Ce, Pr, Nd, Sm, Eu, The abundance of Gd, Dy, Re, Pb, Th, and U elements was determined.

Table 1. *Quantification of micro and macroelements in Alhagi maurorum plant using inductively coupled plasma mass spectrometry (ICP-MS)*

№	Element	Measurement range of detectable elements	Amount, mg/kg	
			Alhagi maurorum seed	Alhagi maurorum leaf
1	**Lithium (Li)**	0.05–4000	2.10	3.80
2	**Beryllium (Be)**	0.05–4000	< 0.05	< 0.05
3	**Boron (B)**	0.10–4000	480	1200
4	**Sodium (Na)**	0.004–11%	1400	4200
5	**Magnesium (Mg)**	0.004–11%	6400	14000
6	**Aluminum (Al)**	0.002–20%	190	320
7	**Phosphorus (P)**	—	8000	2400
8	**Potassium (K)**	0.008–30%	20000	11000
9	**Calcium (Ca)**	0.005–28%	45000	100000
10	**Scandium (Sc)**	0.10–4000	0.160	0.230
11	**Titanium (Ti)**	0.0006–9%	3.90	2.50
12	**Vanadium (V)**	0.10–4000	< 0.10	0.150
13	**Chromium (Cr)**	1.0–4000	1.30	1.20
14	**Manganese (Mn)**	0.002–10%	40.0	77.0
15	**Iron (Fe)**	0.006–30%	410	890
16	**Cobalt (Co)**	0.10–4000	0.300	0.430
17	**Nickel (Ni)**	1.0–4000	5.30	3.30
18	**Copper (Cu)**	1.0–4000	13.0	2.60
19	**Zinc (Zn)**	1.0–4000	94.0	86.0
20	**Gallium (Ga)**	0.10–4000	0.180	0.200
21	**Arsenic (As)**	0.10–4000	1.10	1.60
22	**Celine (Se)**	0.50–4000	< 0.50	< 0.50
23	**Rubidium (Rb)**	0.10–4000	5.90	1.20
24	**Strontium (Sr)**	0.10–4000	230	570
25	**Yttrium (Y)**	0.10–4000	< 0.10	< 0.10
26	**Cerconium (Zr)**	—	0.017	0.025
27	**Niobium (Nb)**	0.005–4000	0.008	0.008
28	**Molybdenum (Mo)**	0.10–4000	0.170	0.380
29	**Silver (Ag)**	0.05–10.0	< 0.05	< 0.05
30	**Cadmium (Cd)**	0.005–4000	0.010	0.007
31	**Indium (In)**	—	< 0.005	< 0.005
32	**Tin (Sn)**	0.10–10	< 0.10	0.100
33	**Antimony (Sb)**	0.10–4000	< 0.10	< 0.10
34	**Tellurium (Te)**	0.30–4000	< 0.30	< 0.30
35	**Cesium (Cs)**	0.02–4000	< 0.02	0.030
36	**Barium (Ba)**	0.10–4000	4.60	17.0
37	**Lanthanum (La)**	0.50–4000	< 0.05	< 0.05
38	**Seriy (Ce)**	0.04–4000	< 0.04	0.100
39	**Prasidiom (Pr)**	0.01–4000	0.010	0.031
40	**Niodymium (Nd)**	0.01–4000	0.038	0.110
41	**Samaria (Sm)**	0.01–4000	< 0.01	0.027
42	**European (Eu)**	0.01–4000	0.006	0.011
43	**Gadolinium (Gd)**	0.01–4000	< 0.01	0.020
44	**Terbiy (Tb)**	0.01–4000	< 0.01	< 0.01

№	Element	Measurement range of detectable elements	Amount, mg/kg	
			Alhagi maurorum seed	Alhagi maurorum leaf
45	**Dysprosium (Dy)**	0.01–4000	< 0.01	0.018
46	**Holmi (Ho)**	0.01–4000	< 0.01	< 0.01
47	**Erbium (Er)**	0.01–4000	< 0.01	< 0.01
48	**Thulium (Tm)**	0.01–4000	< 0.01	< 0.01
49	**Ytterby (Yb)**	0.01–4000	< 0.01	< 0.01
50	**Luticius (Lu)**	0.01–4000	< 0.01	< 0.01
51	**Gafnium (Hf)**	0.05–4000	< 0.05	< 0.05
52	**Tantalum (Ta)**	0.04–4000	< 0.04	< 0.04
53	**Tungsten (W)**	0.08–4000	< 0.08	< 0.08
54	**Rhenium (Re)**	0.01–4000	< 0.01	0.014
55	**Platinum (Pt)**	0.05–4000	< 0.05	< 0.05
56	**Gold (Au)**	0.05–4000	< 0.05	< 0.05
57	**Thallium (Tl)**	0.01–4000	< 0.01	< 0.01
58	**Lead (Pb)**	0.1–4000	0.860	1.30
59	**Bismuth (Bi)**	0.1–4000	< 0.01	< 0.01
60	**Thorium (Th)**	0.01–4000	0.016	0.034
61	**Uranus (U)**	0.01–4000	0.029	0.074

Conclusion

It was found that the calcium element is in the highest concentration in the plant. As a result of the analysis, it was found that the Niobium element is stored in the smallest amount.

References

Awaad Amani A. S., Maitland D. J., Soliman G. A. Antiulcerogenic activity of Alhagi maurorum // Pharmaceutical biology. 2006.– T. 44.– No. 4.– P. 292–296.

Arezoo, Mirzaei., Bahram, Nasr, Esfahani., Mustafa, Ghanadian., Sharareh, Moghim. (2022). Alhagi maurorum extract modulates quorum sensing genes and biofilm formation in Proteus mirabilis. Dental science reports. Doi: 10.1038/s41598-022-18362-x

Mohammed R. K., Noor, Alzahraa, Dheaa, Abd-alkadhemand. (2022). Determination of Active Phytochemical Compounds of Alhagi Maurorum using Gas Chromatography-Mass Spectroscopy (GC–MS). Iraqi journal of science. Doi: 10.24996/ijs.2022.63.1.10

Kholmurodov B. B. *et al.* 2023. *IOP Conf. Ser.: Earth Environ. Sci.* 1284012008. DOI: 10.1088/1755-1315/1284/1/012008

Awad, Allah., Usama, El-Sayed, Mostafa, I. M., Abd, El-Razik., W., K., Abou, El, Ahmed. (2022). Effect of Alhagi Maurorum Powder (Camel Thorn) on Some Chemical and Sensory Properties of Toast Bread. Mağallat¨ Dirāsāt wa Buḥūṯ Al-Tarbiyyat¨ Al-Nawʿiyyat¨. Doi: 10.21608/jsezu.2022.253043

Calder P. C., Carr A. C., Gombart A. F., Eggersdorfer M. Optimal Nutritional Status for a Well-Functioning Immune System Is an Important Factor to Protect against Viral Infections. *Nutrients*. 2020;12:1181. Doi: 10.3390/nu12041181. [PMC free article] [PubMed] [CrossRef] [Google Scholar]

submitted 15.07.2024;
accepted for publication 29.07.2024;
published 28.09.2024

Contact: bahodirxolmurodov1994@gmail.com

The Austrian Journal of Technical and Natural Sciences, No 7–8
ISSN 2310-5607

PREMIER Publishing
ppublishing.org

DOI:10.29013/AJT-24-7.8-18-21

SYNTHESIS OF METHYL ESTERS OF GALLIC ACID AND ITS DERIVATIVES

Kadirova Shokhida Ozotboyevna [1], ***Yuldasheva Mukhabbat Razzoqberdiyevna*** [1], ***Abdumannopova Nasiba Bahodir qizi*** [1]

[1] National University of Uzbekistan, Tashkent

Cite: *Kadirova Sh. O., Yuldasheva M. R., Abdumannopova N. B. (2024). Synthesis of methyl esters of gallic acid and its derivatives. Austrian Journal of Technical and Natural Sciences 2024, No 3–4.* https://doi.org/10.29013/AJT-24-7.8-18-21

Abstract

The article presents information on the method for obtaining esters of gallic acid, syringic acid and 3,4,5-trimethoxybenzoic acid with methanol and the analysis of compounds by IR, 1H and 13C NMR spectroscopy.

Keywords: *Gallic acid, syringic acid, 3,4,5-trimethoxybenzoic acid, methanol, ester*

Introduction

Gallic acid derivatives are commonly found in plants and fruits in nature, and they are currently utilized by humans either directly or indirectly as food products and medicinal substances. These derivatives have been used for various purposes such as treating depression, cancer, microbial infections, and lipid-dependent diseases, as well as exhibiting anticarcinogenic, antimicrobial, antimutagenic, antiangiogenic, and anti-inflammatory properties.

Recent data have shown that alkyl gallates are widely used as antioxidants in the food and cosmetic industries. Furthermore, derivatives of gallic acid, a major component of plant metabolism, are used as raw materials for ink, dye, and colorant manufacturers (Mahmoud N. N., Carothers A. M., Grunberger D., Belinski R. T., Churchill M. R., Martucci C., Newmark H. L., 2000). Pharmacological studies on these compounds have demonstrated that 3,4,5-trihydroxybenzoic acid and its derivative esters possess numerous therapeutic properties, including antioxidant, antifungal, antibacterial, antitumor, antiviral, and antiherpetic effects. There is a growing interest in the antioxidant activity of alkyl gallates due to their ability to absorb and reduce the formation of reactive oxygen species. As a result, scientific studies on gallic acid and its derivatives are being conducted globally, yielding excellent results (Choubey S. et al., 2015; URL: https://doi.org/10.4155/ppa.15.14;

Mahmoud N. N., Carothers A. M., Grun berger D., Belinski R. T., Churchill M. R., Martucci C., Newmark H. L., 2000; URL: https://asianpubs.org/index.php/ajchem/article/view/5556; Kubo, N. Masuoka, P. Xiao and H. Haraguchi, J., 2002; Weetall H. H., 1985; Badhani B., Sharma N., Ka kkar R., 2015; Shi Z., 2015; URL: http://dx.doi.org/10.14233/ajchem.2015.17906; Fer

nandes., Salgado. Gallic Acid:. 2016; Citation: Zheng, Y., Geng, Y., Hou, W., Li, Z., Cheng, C., Wang, X., Yang, Y. 2024; URL: https:// doi.org/10.3390/molecules 29091996; Fernandes, Salgado. (2015); Kadirova Sh., Yuldasheva M., Komilov K., Rakhimov R.; Yuldasheva M., Kadirova Sh. 2023. URL: https: //www.scholarexpress. net).

Gallic acid is a sensitive derivative that is prone to oxidation, therefore it is important to synthesize its ethers through chemical synthesis via fermentative methods. However, this method has several drawbacks including low yield, prolonged processing time, the requirement for specific solutions, and so on (Weetall H. H., 1985; Badhani B., Sharma N., Kakkar R., 2015).

Gallic acid and its derivative esters are known for their strong antioxidant properties. Scientific data highlights the significance of developing natural products based on them. These natural products or their derivatives, with potent antioxidant effects, can help reduce oxidative stress in cells and can also be used as building blocks for creating new drugs to prevent various diseases (Shi Z. et al. 2015; URL: http://dx.doi.org/10.14233/ajchem.2015.17906; Fernandes., Salgado. Gallic Acid: 2016; Citation: Zheng, Y., Geng, Y., Hou, W., Li, Z., Cheng, C., Wang, X., Yang, Y., 1996. URL: https:// doi.org/10.3390/molecules29091996; Fernandes, Salgado. (2015); Kadirova Sh., Yuldasheva M., Komilov K., Rakhimov R.; Yuldasheva M., Kadirova Sh., 2023. URL: https: //www.scholarexpress. net).

Alkyl gallates can be produced by boiling the corresponding acids with alcohols in the presence of various catalysts. Catalysts such as sulfuric acid, hydrogen chloride, boron trifluoride, aluminum chloride, trifluoroacetic anhydride, polyphosphate esters, neodymium oxide, dicyclohexylcarbodiimide, graphite, and bisulfate are commonly used. Toluene is typically used as a solvent in the synthesis of alkyl gallates, and the reactions are carried out with heating for 8–12 hours (Kubo, N. Masuoka, P. Xiao and H. Haraguchi, J. 2002).

Results and discussion:

The esterification of gallic acid, syringic acid, and 3,4,5-trimethoxybenzoic acid with methanol using a sulfuric acid catalyst was conducted at the boiling point of the molar amount of methanol. The study investigated the impact of catalyst concentration, temperature, and molar ratio of reagents on the reaction efficiency. In the esterification reaction, the highest product yield was observed for hydroxybenzoic acid. The reaction equation is as follows:

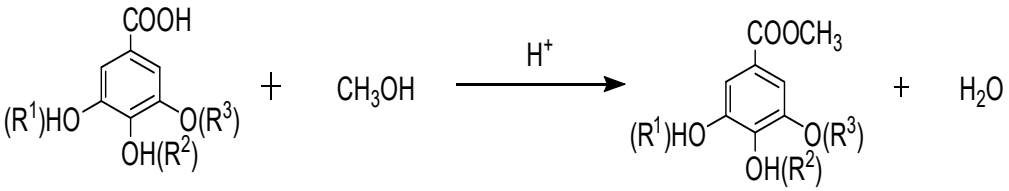

1 = R^1, R^2, R^3 = H; 2 = R^1, R^2, R^3 = CH_3; 3 = R^1, R^3 = CH_3, R^2=H.

The ability of aromatic carboxylic acids to undergo esterification increases in the following order: gallic acid (78%), syringic acid (84%), 3,4,5-trimethoxybenzoic acid (89%). The high yield of the product in the reaction of methanol with 3,4,5-trimethoxybenzoic acid is due to the stabilization of the carbocation formed as a result of proton addition from the catalyst to the carboxyl group, facilitated by the action of the trimethoxy group.

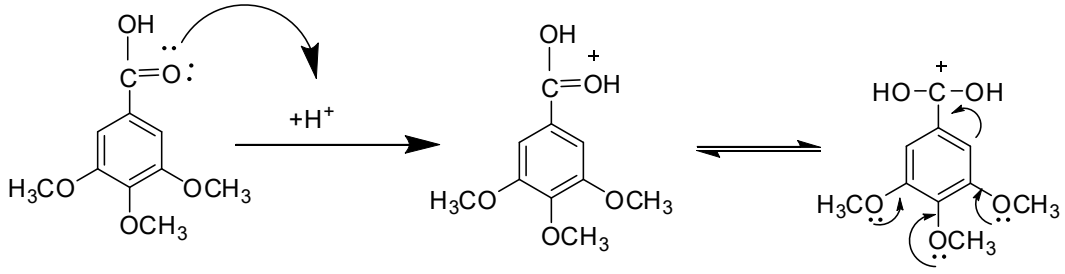

The reaction is catalyzed by sulfuric acid, which protonates the carboxyl oxygen of gallic acid. Then, the electron-deficient carbon undergoes nucleophilic attack by methanol, resulting in a tetrahedral intermediate. Removing a water molecule from the tetrahedral intermediate leads to the formation of an ester. This reaction mechanism can be expressed as follows.

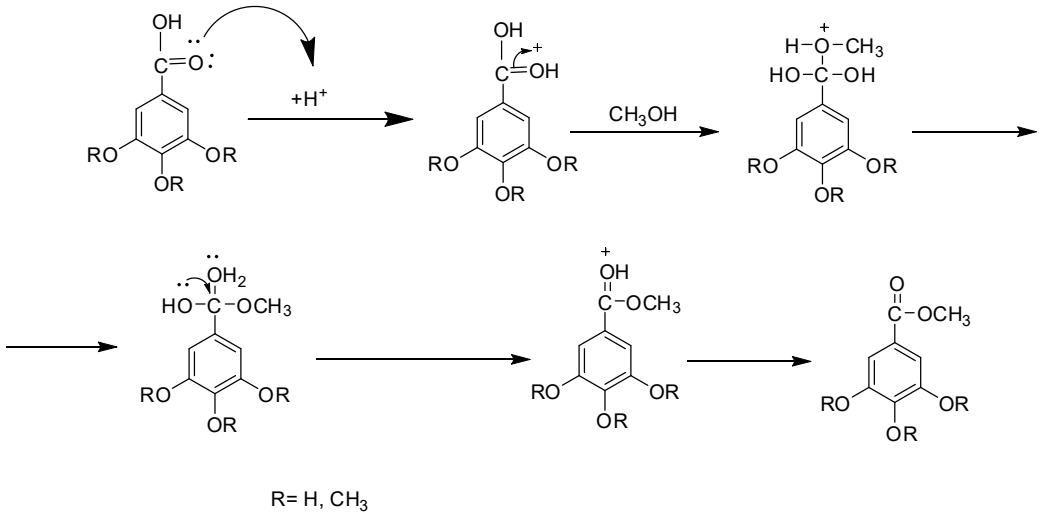

Table 1. *Physical quantities of gallic acid, syringic acid and 3,4,5-trimethoxybenzoic acid*

№	Temperature, °C	Duration of the reaction, hours	Product T(liquid)	Yeild %	Rf
1	68	10	202–203 °C	78	0.75
2	68	10	204–205 °C	84	0.40
3	68	10	168–169 °C	89	0.5

Experimental part: Synthesis of methyl gallate (**1**) 2 g (0.001 mol) of gallic acid and 25 ml (0.78 mol) of methyl alcohol, as well as 3–4 drops of sulfuric acid, were heated in a round-bottomed flask equipped with a reflux condenser. The reaction mixture was heated under reflux for 10 hours. The resulting substance was monitored every hour using TLC. After the reaction was complete, excess alcohol was removed and the residue was washed first with cold water and then with a 5% Na_2SO_4 solution. The white precipitate that settled at the bottom of the vessel was isolated through filtration and recrystallized using ethyl alcohol. Methyl ester of syringic acid and methyl ester of 3,4,5-trimethoxybenzoic acid were also synthesized using this method.

Melting point and thin-layer chromatography were used to determine the obtained product, the gallic acid methyl ester. The product yield was 78%, with a melting point of 203–204 °C and Rf value of 0,75. 1H and 13C NMR were recorded on a JNM-EC Z400R spectrometer (JEOL, Japan) at an operating frequency of 400 MHz for 1H in CD, OD solutions. 1H NMR (400 MHz, DMSO-d6) d 3.79 (3H, s, COOMe), 7.02 (2H, dd, J1=1.88, J2=0.96, Ar-N=2.6). 13C NMR (DMSO-d6): 167.69, 145.16, 138.40, 120.15, 108.72, 50.94, 48.10, 47.96, 47.82, 47.68, 47.53, 47.39, 47.25. IR spectra were recorded on an FT-IR/NIR Spectrum 3 spectrometer (Perkin Elmer, Switzerland) using an ATR system KBr, cm^{-1}, 3514, 3344 cm^{-1} (–OH), 3344, 1468, 1534,1045, 1098, 765, 749 sm^{-1} (Ar-CH), 1468, 1440 sm^{-1} ($–CH_3$), 1686,1612 sm^{-1} (C=O), 1686, 1612 sm^{-1} (COOR).

Synthesis of methyl ester of syringic acid (**2**). Melting point of methyl ester of syringic acid 168–1690 °C, yield 1.68 g (84%), Rf = 0.4. 1H and 13C NMR were recorded on a JNM-EC Z400R spectrometer (JEOL, Japan) at an operating frequency of 400 MHz for 1H in CD, OD solutions. ^{1}H NMR (400 MHz, DMSO-d6) δ 3.84 (3H, c, COOMe), 3.85 (6H, c, OMe-3,5), 7.27 (2H, d, J=1.01, Ar-H=2,6). 13C NMR (DMSO-d6): 167.32, 147.32, 140.84, 119.83, 106.76, 55.45, 51.15, 48.10,

47.96, 47.68, 47.26. IR spectra were recorded on an FT-IR/NIR Spectrum 3 spectrometer (Perkin Elmer, Switzerland) using an ATR system KBr, cm^{-1}, 3554 cm^{-1} (–OH), 2846 sm^{-1} (Ar-OCH_3), 3005, 2950, 1632, 1613, 1107, 1041, 902 sm^{-1} (Ar-CH), 2846, 1446, 1333sm^{-1} (–CH_3), 1682, 1613 sm^{-1} (C=O), 1682, 1613 sm^{-1} (COOR).

Synthesis of methyl ester of 3,4,5-trimethoxybenzoic acid (**3**). Melting point of methyl ester of 3,4,5-trimethoxybenzoic acid is 168–169 º C, yield is 1.78 g (89%), Rf value is 0.5. 1H and 13C NMR were recorded on a JNM-EC Z400R spectrometer (JEOL, Japan) at an operating frequency of 400 MHz for 1H in CD, OD solutions.

1H NMR (400 MHz, DMSO-d6) δ 4.07 (3H, c, COOMe), 4.03 (6H, c, OMe-3,5), 3.78 (3H, c, OMe-4). IR spectra were recorded on an FT-IR/NIR Spectrum 3 spectrometer (Perkin Elmer, Switzerland) using an ATR system KBr, cm^{-1}, 2840 sm^{-1}(Ar-OCH_3), 3015, 1712, 1589, 1507, 1454 sm^{-1} (Ar-CH), 2965 sm^{-1} (–CH_3), 1618sm^{-1} (C=O), 1682, 1622 sm^{-1} (COOR).

Conclusion

Esters were produced by reacting gallic acid, syringic acid, and 3,4,5-trimethoxybenzoic acid with methyl alcohol under the catalysis of sulfuric acid.

The effect of solvent and time on the reaction yield was investigated and the optimum conditions were found. Methods of purification of the obtained substances were determined. The structure of the substances was confirmed by IR and PMR sectors.

References

Choubey S. et al. Medicinal importance of gallic acid and its ester derivatives: a patent review //Pharmaceutical patent analyst. 2015.– T. 4.– № . 4.– P. 305–315. URL: https://doi.org/10.4155/ppa.15.14

Mahmoud N.N., Carothers A.M., Grunberger D., Belinski R.T., Churchill M.R., Martucci C., Newmark H.L. and M.M Microwave.– Assisted Esterification of Gallic Acid Bertagnolli Carcino-genesis,– 21, 921 (2000). URL: https://asianpubs.org/index.php/ajchem/article/view/5556

Kubo, N. Masuoka, P. Xiao and H. Haraguchi, J. Evaluation of the antioxidant and prooxidant actions of gallic acid and its derivatives Food Chem., 2002.– 50.– 3533 p.

Weetall H.H. Appl Enzymatic synthesis of gallic acid esters Biochem. Biotechnol., 1985.– 11,– 25 p.

Badhani B., Sharma N., Kakkar R. Gallic acid: A versatile antioxidant with promising therapeutic and industrial applications // Rsc Advances. 2015.– T. 5.– № . 35.– P. 27540–27557.

Shi Z. et al. Microwave-Assisted Esterification of Gallic Acid //Asian Journal of Chemistry. 2015.– T. 27.– № . 4. URL: http://dx.doi.org/10.14233/ajchem.2015.17906

Fernandes., Salgado. Gallic Acid: Review of the Methods of Determination and Quantification. Crit. Rev. Anal. Chem. 2016.– 46.– P. 257–265.

Citation: Zheng, Y., Geng, Y., Hou, W., Li, Z., Cheng, C., Wang, X., Yang, Y. Study on the Antifungal Activity of Gallic Acid and Its Azole Derivatives against Fusarium graminearum. Molecules 2024, A29, 1996. URL: https:// doi.org/10.3390/molecules29091996

Fernandes, Salgado. (2015). Gallic Acid: Review of the Methods of Determination and Quantification. Critical Reviews in Analytical Chemistry,–46(3).– P. 257–265. Doi:10.1080/10408347.2015.1095064

Kadirova Sh., Yuldasheva M., Komilov K., Rakhimov R. // Peculiarities of binding of tannin isomers obtained from the Euphorbia plant with proteins // Academic Reserch in Educational Sciences,– Vol. 2. Issue 8. ISSN2181–1384, SJIF 5.723, Doi:10.24412/2181-1384-2021-8-231-238

Yuldasheva M., Kadirova Sh. “Gallic acid and its synthesis of propyl ether” World Bulletin of Public Health URL: https: //www.scholarexpress. net Volume-23, June, 2023.

submitted 16.08.2024;
accepted for publication 31.08.2024;
published 28.09.2024

Contact: kadirovasohida6@gmail.com

The Austrian Journal of Technical and Natural Sciences, No 7–8
ISSN 2310-5607

PREMIER Publishing
ppublishing.org

DOI:10.29013/AJT-24-7.8-22-25

MECHANISM OF SYNTHESIS OF QUINAZOLIN-4-THIONE IN A NEW METHOD

Elmuradov Chori Juraevich [1], Qayumova Maftuna Ilxom qizi [3], Saitkulov Foziljon Ergashevich [2], Isaqulova Marxoba Ne'mat qiz [3], Muminova Nigora Kilichovna [3]

[1] Karshi State University, Republic of Uzbekistan, Uzbekistan

[2] Tashkent State Agrarian University of Uzbekistan, Uzbekistan

[3] Institute of Biochemistry of Samarkand State University named after Sh. Rashidov, Uzbekistan

Cite: *Elmuradov Ch.J., Saitkulov F.E., Giyasov K., Muminova N.K. (2024). Mechanism of Synthesis of Quinazolin-4-Thione in a New Method. Austrian Journal of Technical and Natural Sciences 2024, No 3–4.* https://doi.org/10.29013/AJT-24-7.8-22-25

Abstract

In the article, the preparation of quinazolin-4-thione in the presence of quinazolin-4-one by various methods was thoroughly studied, and for the first time, the thionation reaction was carried out in the presence of Lavesson's reagent.

The structure of the quinazoline-4-thione molecule has be en proven using modern physical and chemical research methods.

Keywords: *quinazolin-4-thione, quinazolin-4-one, various methods, thionation reaction, Lavesson's reagent, P_2S_5, in an inert atmosphere (argon), cycloreversion (opposite process to cycloaddition!)*

Introduction

Usually, organic reactions involve step-by-step formation of individual bonds of the target molecule. It is often necessary to isolate and purify intermediate substances, change reaction conditions at subsequent stages of synthesis. Tandem reactions have a number of advantages. Firstly, they allow creating complex structures in a small number of stages. Moreover, the process is often accompanied by high chemo-, regio- and stereoselectivity. It also eliminates the need for purification at each stage. Targeted synthesis of low-toxic biologically active substances based on the study of the "structure-activity" relationship is an important task of organic chemistry. In recent years, priority has been given to the study of substances that are close in structure to natural ones. Anthranilic acid is a product of the metabolism of natural substances in a living organism, and its derivatives exhibit a wide range of pharmacological activity. The search for substances with high anti-inflammatory, analgesic activity and low toxicity is relevant, untimely use of anti-inflammatory agents in systemic inflammatory diseases of connective tissue with a

chronic progressive course can lead to disability of patients (Saitkulov F.E., Elmuradov B. Zh., Sapaev B., 2024; Saitkulov F.E., Elmuradov B.J., Giyasov K., 2023; Saitkulov F.E., Elmuradov B.J., 2024; Saitkulov F. E., Elmuradov B. J., 2022; Saitkulov F., Sapaev B., Nasimov K., Kurbanova D., Tursunova N., 2023).

Finally, tandem reactions allow saving on the cost and quantity of reagents, solvents, adsorbents, reducing the amount of waste generated, energy costs and the number of laboratory operations (Saitkulov F.E., Elmuradov B. Zh., Giyasov K., 2023; Saitkulov F. E., Giyasov K., Elmuradov B. J., 2022; Saitkulov F.E., Tashniyazov A.A., Mamadrahimov A.A., Shakhidoyatov Kh.M., 2014).

Method and results

It is known that heterocyclic compounds containing a thione group are of great interest both theoretically and practically. The reason for this is the high synthetic potential of this group and the abundance of biologically active substances among compounds of this class. Therefore, we considered it appropriate to carry out our dissertation studies on a comparative study of selective methylation reactions with quinazolin-4-thione (2) and its various substituted derivatives. Thionation reactions of quinazolin-4-one (1) were carried out in two ways: in the presence of P_2S_5 and Lawesson's reagent (Lawesson's reagent (LR), 2). Reactions with P_2S_5 are carried out by heating the reagents in an equimolar amount at the boiling temperature of m-xylene for 4 hours, and with LR (2) at the boiling temperature of absolute toluene in an inert atmosphere (argon):

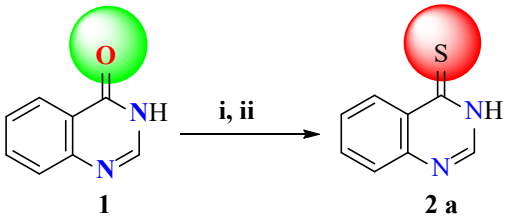

1 2 a

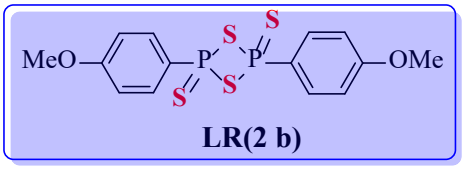

LR(2 b)

The approximate mechanism of the reaction carried out with Lavesson's reagent (LR) can be described as follows:

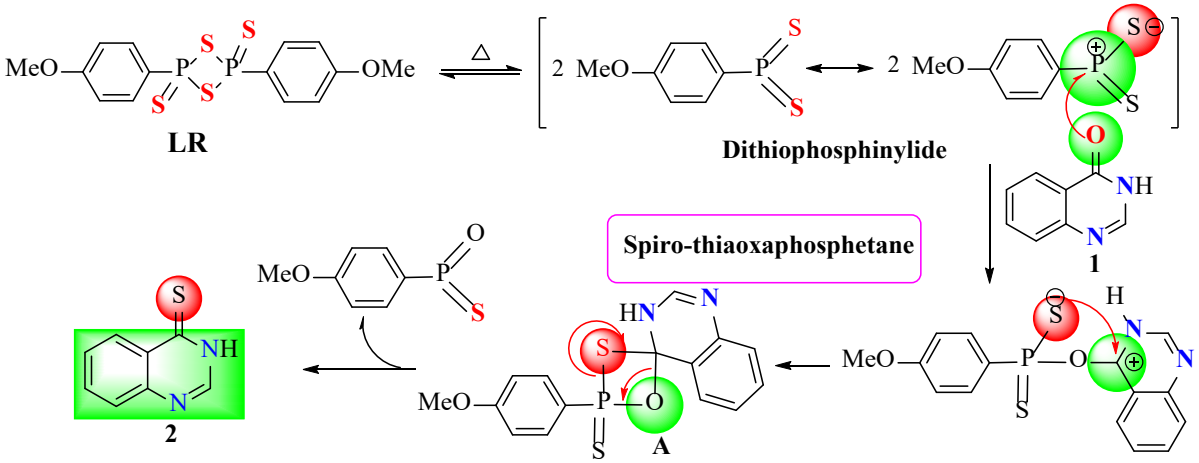

Usually RL is in equilibrium with dithiophosphinylide, which has high reactive activity when heated in an organic solvent. Its reaction with carbonyl compounds can lead to the formation of the intermediate spiro-thioxaphosphetane (A). As a result of thermal cycloreversion (reverse process to cycloaddition!) this cyclic compound (A) leads to the formation of (4-methoxyphenyl)(thioxo)phosphine oxide with a stable P=O bond and the desired thione (2). In the IR spectrum of thione (2) the presence of the absorption frequency corresponding to the C=S bond at 1302 cm^{-1}, in the ^1H NMR spectrum, the one-proton singlet of the NH group at 13.86 ppm, the one-proton doublet signal of the N-2 proton at 8.59 ppm, doublet and triplet signals of 4 aromatic protons of benzene ring appear at 7.62 (t),

7.74 (d), 7.90 (t) and 8.59 (d) ppm (fig-1). In the mass spectrum (M=162), the protonated molecular ion m/z = 163 [M + H]+ was identified, confirming its structure.

Quinazolin-4-one (3) and quinazolin-4-thione (2) contain C=O, C=S, C=N bonds and aromatic ring chromophores. Therefore, their UV spectrum has absorption frequencies specific to these groups. These molecules have absorption frequencies at 220, 311, 330 nm. The longest absorption line at 311 nm corresponds to the n → p* transition. It should be noted that the position of the main absorption lines increases during the transition to the derivatives of quinazolin-4-one (1) and quinazolin-4-thione (2).

Figure 1. *^{1}H NMR spectra of quinazolin-4-thione*

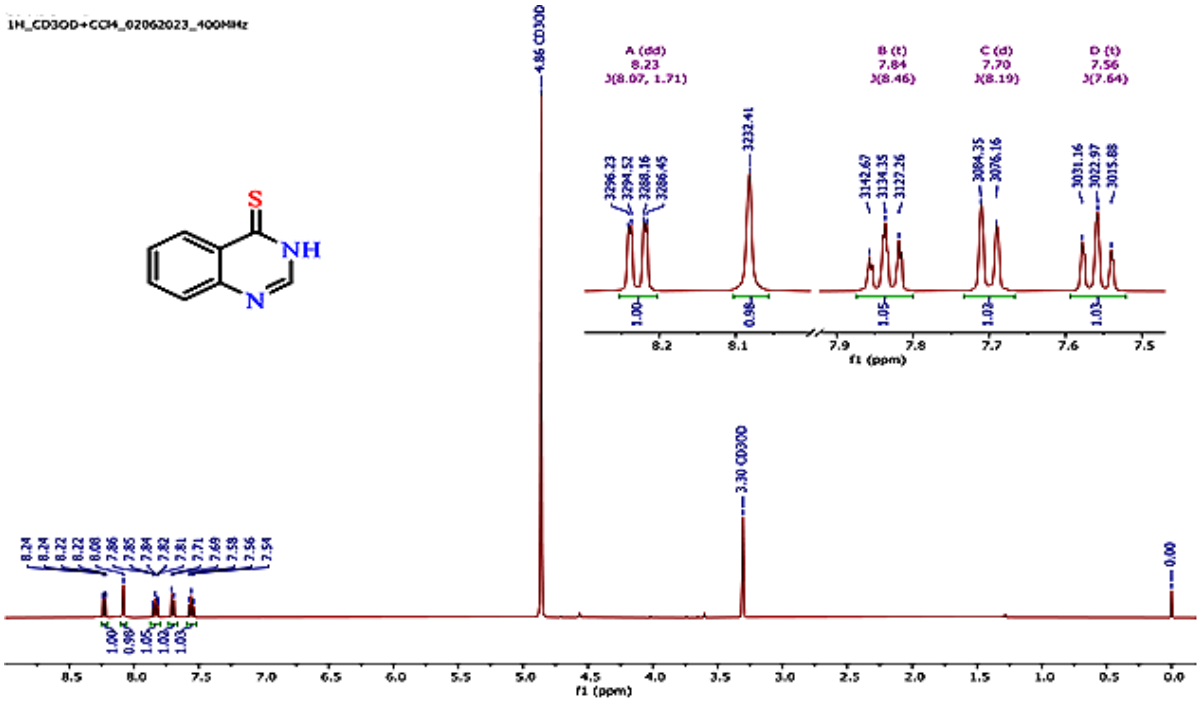

It should be said that the thiolation reactions with LR occur at a relatively low temperature and in a short time, and the product (2) is formed in quantitative yields, as a result, an easy and highly efficient thionation method of quinazolin-4-one (1) was developed.

Experimental part

Quinazolin-4-thione (2). **Method A** (in the presence of P_2S_5): A mixture of 1.46 g (0.01 mol) of quinazolin-4-one (1) and 2.22 g (0.01 mol) of P_2S_5 in 50 ml of absolute m-xylene was refluxed for 4 hours, the mixture was cooled and the reaction mixture was filtered, the filter residue was washed with m-xylene and treated with 7 ml (10%) NaOH. The precipitate was filtered, washed with water and dried under normal conditions, and the substance was recrystallized from hexane. As a result, 1.26 g (78%) of quinazolin-4-thione (2) was obtained, melting point 288–289 °C.

Method B (with Lesson's reagent (LR)): A mixture of 1.46 g (0.01 mol) of quinazolin-4-one and 2.02 g (0.005 mol) of LR in 30 ml of absolute toluene was refluxed for 1 hour (inert gas, Ar). It was cooled to 20–25 °C, the precipitate was filtered and dried. As a result, 1.57 g (97%) of quinazolin-4-thione (2) was obtained, melting point 288–289 °C.

IR (ν, cm^{-1}): 1621 (C=N), 1566 (C=C), 1302 (C=S). ^{1}H NMR (δ, ppm., Gz): 13.86 (1H,.c., NH), 8.59 (1H, d, J = 8.0, H-5), 8.19 (1H, s, H-2), 7.90 (1H, t, J = 7.5, H-7), 7.74 (1H, d, J = 8.0, H-8), 7.62 (1H, t, J = 7.1, H-6). LC–MS: m/z = 163 $[M + H]^+$.

UV spectrum (nm); ethanol 216, 284, 359; ethanol + acid 205, 357; ethanol + acid + base 216, 274, 357; $C_8H_6N_2S$.

Conclusion

A chemical reaction was carried out from quinazolin-4-one with the corresponding quinazolin-4-thione phosphorus V-sulfide and Lavesson's reagent. Reaction mechanisms were studied.

Thionation reactions with Lavesson's reagent occur at relatively low temperature and in a short time, and the product (2) is formed in quantitative yields, resulting in the development of a facile and highly efficient method for thionation of quinazolin-4-one (3).

UF Spectra were first obtained in ethanol, then a shift in the spectral lines was observed when 1–2 drops of 0.1 N HCl solution were added. Then 0.1 N alkali (NaOH) was added and compared with the original spectrum lines, it was found to be compatible.

References

Saitkulov F. E., Elmuradov B. Zh., Sapaev B. Syntheses and biological activity of quyinazolin-4-one hydrochloride // *Austrian Journal of Technical and Natural Sciences*. 2024.– No. 1–2.– P. 28–35.

Saitkulov F. E., Elmuradov B. J., Giyasov K. Alkylation of quinazoline-4-one by "soft" and "hard" alkylating agents // Universum: Chemistry and Biology: – Moscow. 2023.– No. 1.– P. 53–57.

Saitkulov F. E., Elmuradov B. J. Introduction of new methods of studying the methylation reaction of quinazolin-4-one in different solvents. For participation (in) scientific-online conference "Theoretical aspects in the formation of pedagogical sciences". Great Britain. 2024.– No. 3.– Vol. 3.– P. 182–189.

Saitkulov F. E., Elmuradov B. J. Methylation of quinazoline-4-one with "soft" and "hard" methylating agents // Proceedings of the Republican Scientific and practical Conference. IONKH Institute of the Academy of Sciences of the Republic of Uzbekistan. May 12-14, 2022. – Tashkent, Uzbekistan. – 345 p.

Saitkulov F., Sapaev B., Nasimov K., Kurbanova D., Tursunova N. Structure, aromatic properties and preparation of the quinazolin-4-one molecule // E3S Web of Conferences, 2023.– 389, 03075.– P. 1–7.

Saitkulov F. E., Elmuradov B. Zh., Giyasov K. Biological activity of quinazolin-4-one hydrochloride // "Actual problems of chemical science and industry" November 24-25, 2023. – Ferghana.– 160 p.

Saitkulov F. E., Giyasov K., Elmuradov B. J. Methylation of 2-methylquinazoline-4-one by "soft" and "hard" methylating agents // Universum: Chemistry and Biology: – Moscow. 2022.– No. 11.– P. 49–52.

Saitkulov F. E., Tashniyazov A. A., Mamadrahimov A. A., Shakhidoyatov Kh.M., 2,3-Dimethylquinazolin-4(3H)-one // *Acta crystallographica. Section E, Structure reports online*. 2014.– E70,– o788.

submitted 06.08.2024;9
accepted for publication 20.09.2024;
published 28.09.2024

Contact: fsaitkulov@bk.ru

The Austrian Journal of Technical and Natural Sciences, No 7–8
ISSN 2310-5607

PREMIER Publishing
ppublishing.org

DOI:10.29013/AJT-24-7.8-26-29

CONVENIENT SYNTHESIS OF 2-METHYLQUINAZOLIN-4-THIONE BASED ON ANTHRANYL ACID

Elmuradov Chori Juraevich [1], ***Muminova Nigora Kilichovna*** [2], ***Nasimov Khasan Muradovich*** [2], ***Yaxyoeva Maftuna Faxriddin qizi*** [2], ***Saitkulov Foziljon Ergashevich*** [3]

[1] Karshi State University, Republic of Uzbekistan, Uzbekistan

[2] Institute of Biochemistry of Samarkand State University named after Sh.Rashidov, Uzbekistan

[3] Tashkent State Agrarian University of Uzbekistan, Uzbekistan

Cite: *Elmuradov Ch.J., Saitkulov F.E., Giyasov K., Muminova N.K. (2024). Convenient Synthesis of 2-Methylquinazolin-4-Thione Based on Anthranyl Acid. Austrian Journal of Technical and Natural Sciences 2024, No 3–4.* https://doi.org/10.29013/AJT-24-7.8-26-29

Abstract

The synthesis of intermediate products based on anthranilic acid, the reactions of excess amides are justified in the article, and optimal synthesis methods of 2-methylquinazolin-4-thione are well studied. The reaction mechanism was proved on the basis of the corresponding spectra.

Keywords: *Anthranilic acid, intermediate product, synthon, 2-methylquinazolin-4-thione, "structure-activity", 2-methylquinazolin-4-one, N-acetylanthranilic acid, ammonium chloride*

Introduction

The targeted synthesis of low-toxic biologically active substances based on the study of the "structure-activity" relationship is an important task of organic chemistry. In recent years, priority has been given to the study of substances that are close in structure to natural ones. Anthranilic acid is a product of the metabolism of natural substances in a living organism, and its derivatives exhibit a wide range of pharmacological activity. The search for substances with high anti-inflammatory, analgesic activity and low toxicity is relevant, untimely use of anti-inflammatory agents in systemic inflammatory diseases of connective tissue with a chronic progressive course can lead to disability of patients. The search for compounds with a hypoglycemic effect is also relevant. In organic synthesis, anthranilic acid derivatives are used as sources for obtaining various heterocyclic compounds, among which substances with antiviral, antitumor, tuberculostatic and other types of activity have been found (Saitkulov, F.E., Tashniyazov, A.A., Mamadrahimov, A.A., & Shakhidoyatov, K.M., 2014; Sapaev, B., Saitkulov, F.E., Tashniyazov, A.A., & Normurodov, O.U., 2021; Sapaev, B., Sapaev, I.B., Saitkulov, F.E., Tashniyazov, A.A., & Nazaraliev, D., 2022; Saitkulov, F., Farhodov, O., Olisheva, M., Saparboyeva, S., & Azimova, U., 2022; Saitkulov, F.E., Elmuradov, B.J., & Giyasov, K., 2023). Equally

important is the establishment of a quantitative dependence of biological action on structure, since the use of computational methods allows to significantly reduce material costs for the targeted synthesis of biologically active substances (Saitkulov, F.E., Giyasov, K., & Elmuradov, B.J., 2022; Saitkulov, F.E., Elmuradov, B.Z., Giyasov, K., Ruziboev, D.M., & Sultonova, S.X., 2023; Sapayev, B., Saitkulov, F.E., Normurodov, O.U., Haydarov, G., & Ergashyev, B., 2023).

For this purpose, we would like to propose the most convenient and easy method of synthesis of 2-methylquinazlin-4-thione based on anthranilic acid.

Methods and results

N-acetylanthranilic acid is used as the main raw material in the synthesis of 2-methylquinazolin-4-one. In the literature, this compound was synthesized by various methods and the product yield was 65–72%. Anthranilic acid (AA), which we obtained in an equivalent amount, was first completely dissolved in benzene by heating the mixture until boiling (80 °C), then 1 equivalent amount of acetic anhydride was added dropwise. The mixture is cooled and white N-acetylanthranilic acid is obtained:

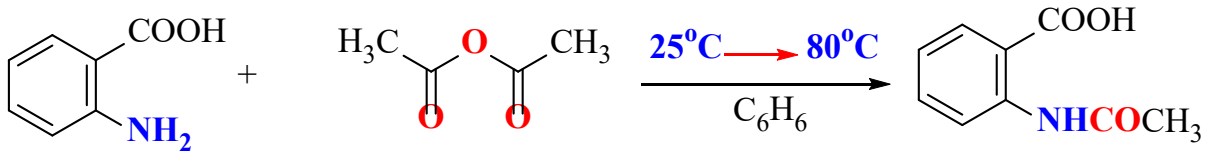

N-acetylanthranilic acid is formed with a high yield (92%).

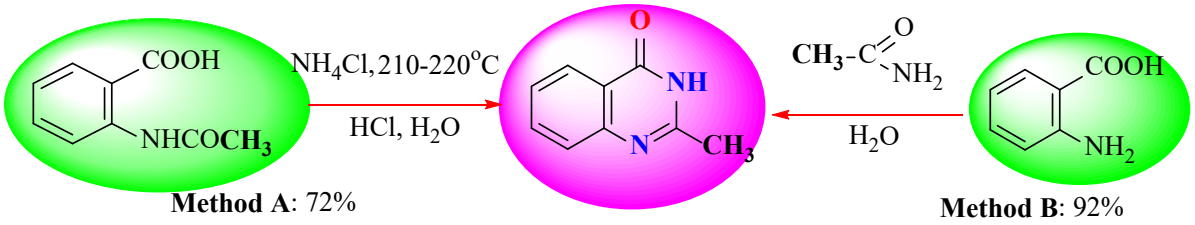

Figure 1. *1P NMR spectrum of 2-Methylquinazolin-4-one.(CD_3OD, 400 MHz)*

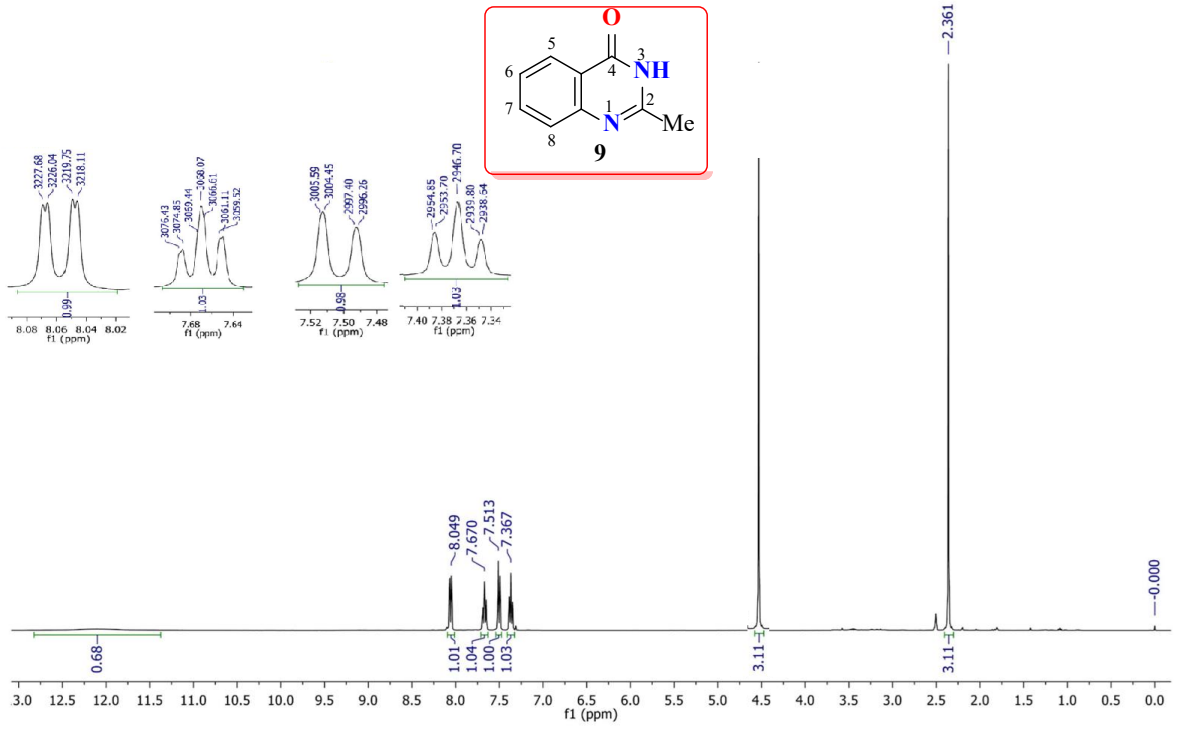

The synthesis of 2-methylquinazolin-4-one needed for research is carried out in two ways (A and B). According to method A: a mixture of initial N-acetylanthranilic acid and ammonium chloride reagents in a ratio of 1:8 is heated at 210–220 °C for 4–5 hours. The yield of 2-methylquinazolin-4-one is 72%:

According to method B: anthranilic acid and acetamide were used as starting raw materials. In this case, a mixture of reagents in a ratio of 1:1 is heated at 210–220 °C for 2 hours. As a result, 2-methylquinazolin-4-one was obtained with a yield of 92%. In the 1H NMR spectrum of the compound, the methyl group is a three-proton singlet (3H, s) at 2.61 parts ppm, 4 aromatic protons in the benzene ring.: 7.33–7.54 ppm. one-proton multiplet at 7.69 ppm. and has one-proton doublets at 7.78 ppm. and one-proton doublet signals at 8.29 ppm., while the N^3-H proton exhibits a singlet signal in the weak region (12.03 ppm.), and these results confirm its structure.

Optimal Synthesis of 2-Methylquinazolin-4-Thione

Theoretically, the introduction of electron-donating or electron-withdrawing substituents into state 2 can affect the direction of the reaction and the yield of the products.

Therefore, in order to synthesize 2-methylquinazolin-4-thion, which has an electron-donating (methyl) group, the reaction of an equimolar mixture of 2-methylquinazolin-4-one and P_2S_5 was carried out. For this, the mixture was boiled in absolute m-xylene for 4 hours.

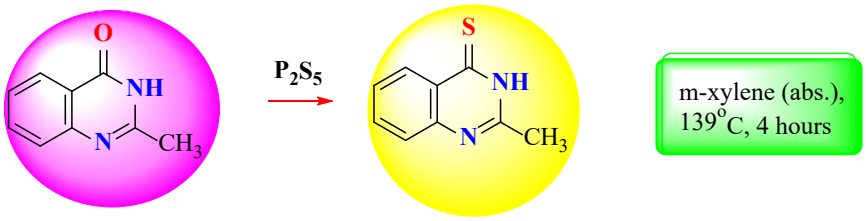

The reaction mixture was filtered, the residue was washed with m-xylene on the filter and treated with aqueous NaOH (10%). The precipitate was filtered, washed with distilled water and dried.

The structure of the synthesized 2-methylquinazolin-4-thione was confirmed by spectral methods. In particular, in its 1H NMR spectrum, the three-proton singlet signal of the methyl group at 2.48 ppt, the aromatic protons H-5, 6, 7, 8 of the benzene ring are 8.55 (d), 7.54 (t), 7.87 (t), 7.64 (d) ppt. presence of doublet and triplet signals, broad singlet signal of endocyclic NH proton at 13.72 ppt. Also, the absorption frequency of the C=S bond at 1292 cm^{-1} is shown in the IR spectrum of the substance, and in the mass spectrum, the detection of the protonated molecular ion m/z 177 $[M^+H]^+$ confirms its structure.

Excremental part

Method A: a mixture of 0.1 mol of N-acetylanthranilic acid with 0.8 mol of NH_4Cl was heated at 210–220 °C for 4–5 hours with the help of a reverse cooler, and then cooled. It was then dissolved in boiling water, adjusted to pH-7.8 (NH_4OH) and cooled. The precipitate was filtered, dried at 20–25 °C. 15.48 g (72%) of 2-methylquinazolin-4-one was obtained, melting point 231 °C.

Method B: a mixture of 0.1 mol of anthranilic acid and 0.1 mol of acetamide was heated at 210–220 °C for 2 hours using a reverse cooler. The mixture was cooled, the precipitate was filtered and dried. 15.48 g (92%) of 2-methylquinazolin-4-one was obtained, melting point 231 °C. 1H NMR (400 MHz, d, $CDCl_3$): 2.61 (s, 3H), 7.33–7.54 (m, 1H), 7.69 (d, 1H, J=7.8), 7.78 (t, 1H, J=7.7), 8.29 (d, 1H, J=7.8), 12.03 (s, 1H). 13C NMR (75 MHz, d, DMSO-d6): 22.4, 120.5, 127.6, 133.4, 138.5, 147.9, 154.9, 163.8. IR spectrum (KBr, cm^{-1}): 1665 (C=O), 3137 (NH); UV spectrum (nm); ethanol 205, 223, 262; ethanol + acid 209, 207, 279; ethanol + acid + base 207, 271.

2-Methylquinazolin-4-thione. 1.6 g (0.01 mol) of 2-methylquinazolin-4-one was refluxed with 2.22 g (0.01 mol) of P_2S_5 in absolute m-xylene for 4 h. The reaction mixture was filtered, the residue was washed with m-xylene on the filter and treated with 7 mL of NaOH (10%). The precipitate was

filtered off, washed with distilled water and dried at room temperature and recrystallized from hexane. 1.58 g (90%) of 2-methylquinazolin-4-thione was obtained, melting point 218 °C. IR (ν, cm^{-1}): 2977 (CH_3), 1607 (C=N), 1568 (C=C), 1292 (C=S). 1H NMR (d, ppt, Hz): 13.72 (1H, broad s., NH), 8.55 (1H, d, J = 8.1, H-5), 7.87 (1H, t, J = 7.6, H –7), 7.64 (1H, d, J = 8.0, H-8), 7.54 (1H, t, J = =7.6, H-6), 2.48 (3H, s, CH_3).

LC–MS: m/z = 177 $[M^+ H]^+$; UV spectrum (nm); ethanol 204, 224, 263, 315; ethanol + acid 211, 221, 281, 310; ethanol + acid + base 202, 226, 263, 315; $C_9H_9N_2S$.

Conclusion

In order to synthesize 2-methylquinazolin-4-thione with an electron-donating (methyl) group, the reaction of mixtures of 2-methylquinazolin-4-one and P_2S_5 in an equimolar ratio of 1:1, 1:2, 1:3, 1:4 was carried out, in which we consider the optimal ratio to be a mixture of 1:1 ratio.

The methyl group in the second position increases the electron density on the pyrimidine ring, which in turn occurs relatively easily in 2-methylquinazolin-4-thione compared to the corresponding 2(H)quinazolin-4-thione.

References

Saitkulov, F. E., Tashniyazov, A. A., Mamadrahimov, A. A., & Shakhidoyatov, K. M. (2014). 2, 3-Dimethylquinazolin-4 (3H)-one. Acta Crystallographica. Section E: Structure Reports Online,– 70(7),– o788-o788.

Sapaev, B., Saitkulov, F. E., Tashniyazov, A. A., & Normurodov, O. U. (2021). Study of methylation reactions of 2-phenylquinazoline-4-tion with “soft” and “hard” methylation agents and determination of its biological activity. In E3S Web of Conferences (Vol. 258, p. 04023). EDP Sciences.

Sapaev, B., Sapaev, I. B., Saitkulov, F. E., Tashniyazov, A. A., & Nazaraliev, D. (2022, June). Synthesis of 2-methylquinazoline-4-thione with the purpose of alkylation of 3-propyl 2-methylquinazoline-4-thione with alkylating agents. In AIP Conference Proceedings (Vol. 2432, No. 1). AIP Publishing.

Saitkulov, F., Farhodov, O., Olisheva, M., Saparboyeva, S., & Azimova, U. (2022). Chemical feeding method of lemon plant using leaf stomata. Academic Research in Modern Science, 1(17), pp. 274-277.

Saitkulov, F. E., Elmuradov, B. J., & Giyasov, K. (2023). Alkylation of quinazoline-4-one by «soft» and «hard» alkylating agents. Universum: Chemistry and Biology, (1-2 (103)). – P. 53-56.

Saitkulov, F. E., Giyasov, K., & Elmuradov, B. J. (2022). Methylation of 2-methylquinazoline-4-one by «soft» and «hard» methylating agents. Universum: Chemistry and Biology, (11-2 (101)).– P. 49–51.

Saitkulov, F. E., Elmuradov, B. Z., Giyasov, K., Ruziboev, D. M., & Sultonova, S. X. (2023). Efficient synthesis and direction of methylation of 2-methylquinazoline-4 (3h)-thione. Theoretical aspects in the formation of pedagogical sciences,– 2(10).– P. 22–26.Sapayev, B., Saitkulov, F. E., Normurodov, O. U., Haydarov, G., & Ergashyev, B. (2023). Studying Complex Compounds of Cobalt (II)-Chlooride Gecsacrystolohydrate with Acetamide and Making Refractory Fabrics from Them.

submitted 06.08.2024;9
accepted for publication 20.09.2024;
published 28.09.2024

Contact: fsaitkulov@bk.ru

The Austrian Journal of Technical and Natural Sciences, No 7–8
ISSN 2310-5607

PREMIER Publishing
ppublishing.org

Section 3. Medical science

DOI:10.29013/AJT-24-7.8-30-36

HYPODYNAMIA – AS A RISK FACTOR FOR CORONARY HEART DISEASE

Rajabova R.Sh. [1]***, Nurillaeva N.M.*** [1]

[1] Tashkent medical academy, Tashkent, Uzbekistan

Cite: *Rajabova R.Sh., Nurillaeva N.M. (2024). Hypodynamia - as a risk factor for coronary heart disease. Austrian Journal of Technical and Natural Sciences 2024, No 3–4.* https://doi.org/10.29013/AJT-24-7.8-30-36

Abstract

As the population's income increases, the proportion of their free time on a particular day increases as well. Many people prefer a sedentary lifestyle and rest in their leisure time. Also, due to the improved transport infrastructure, the indication of people's walking activity is decreasing in developed countries. Despite the many beneficial aspects of physical activity, there is a decrease in the number of people following a physically active lifestyle and an increase in the sedentary lifestyle over the globe. To study physical activity depending on human living conditions 183 patients with coronary artery diseases living in rural and urban areas are involved in the research. The standard treatment regimen was combined with an individually-selected physical activity program and administered to the patients during the 6 months. As a result, positive dynamics were observed in terms of lipid spectrum parameters, heart rate, supraventricular and ventricular arrhythmias in both urban and rural populations.

Keywords: *Coronary artery disease, urban and rural population, hypodynamia, physical activity, lipid spectrum, Holter monitoring examination*

Introduction

According to the World Health Organization (WHO) statistics, every fourth of the world's population dies due to hypodynamia, 5.3 million out of 57 million or 9% deaths in 2008 occurred due to hypodynamia (Mendis S, Puska P., Norrving B. editors. 2011).

In recent years, the level of physical activity around the world has been changing according to the following manner: More than a quarter (1.4 billion) of the world's older population is physically inactive, and approximately one in three women and one in four men worldwide are not physically active, physical inactivity rates are twice as high in developed countries as in low-income countries, Since 2001, there has been no increase in the average level of physical activity among the world's population, between 2001 and 2016, the prevalence of physical activity in low-income countries increased by 5% (from 31.6% to 36.8%) when compared to

high-income countries (Regina G., Gretchen A. S., Leanne M. R., Fiona C. B., 2018).

Rising levels of physical inactivity have negative impacts on health systems, the environment, economic development, well-being, and quality of life.

Globally, 28% of people over the age of 18 had insufficient physical activity levels (23% of men and 32% of women) in 2016. This suggests that because of the lack of physical activity, people are doing less at least 150 minutes moderate and are doing less at least 75 minutes intensive exercises than the standard recommended for healthy people by WHO (Globally, 1.4 billion adults at risk of disease from not doing enough physical activity).

In high-income countries, 26% of men and 35% of women are physically inactive, compared to 12% of men and 24% of women in low-income countries. This means that as the economic indicators of the countries increase, the physical activity of the population decreases (Globally, 1.4 billion adults at risk of disease from not doing enough physical activity).

As the population's income increases, the share of their daily free time increases. At this time, many prefer a sedentary lifestyle and rest. Also, due to the advanced transport infrastructure in developed countries, the indicators of people's walking are decreasing. In the economy of industrialized countries, as production becomes increasingly automated, the proportion of robotics and smart technologies increases, and the share of the population working in professions that require physical labor tends to decrease. All of the above mentioned reasons are causing the spread of a sedentary lifestyle among the population of countries with a high gross domestic product. Admittedly, the governments of many developed countries are considering the above-mentioned trends and they have been promoting physical activity among the population, walking and using bicycles as a means of transportation (How Artificial Intelligence and Robotics Are Changing Our Lives).

The widespread use of vehicles and the increasing use of modern gadgets for work, education, and recreation are leading to a sedentary lifestyle. According to recent research, the decline in physical activity is causing the following public health problems: the prevalence of obesity in children and adolescents is increasing, the duration of sleep is decreasing, the state of cardiometabolic health and the level of social fitness in children and adolescents is decreasing. Also, it is affecting mental-emotional stability, and the probability of adult death is increasing. In addition to this, the rates of type 2 diabetes and cardiovascular diseases have been increasing dramatically in recent years (Emotional stability (the opposite of neuroticism).

Despite the many beneficial aspects of physical activity, there is a decrease in the population following a physically active lifestyle and an increase in the sedentary lifestyle in most countries of the world. Two principles are used to assess the level of physical activity: physical activity during working hours and during leisure hours. It has been proved that an increase in physical exercise during leisure time has a significant positive effect on health conditions and the prevention of chronic non-infectious diseases. The level of physical activity can change depending on the practical desire of each person (Akulova T. N., Plaksina N. V., Smirnova E. V., 2020).

In 2018, the World Health Organization announced that reducing physical inactivity by 10% among the world's population by 2030 is one of the global goals for achieving the Sustainable Development Goals. To achieve this goal, recommendations have been developed by WHO, and each country is developing national action plans based on these recommendations and implementing them among the population (Global action plan on physical activity 2018–2030).

The purpose of research. To study physical activity depending on human living conditions patients with coronary artery diseases living in rural and urban areas.

Materials and methods

The clinical material for the study was collected in the cardiology and cardio rehabilitation departments of the multidisciplinary clinic of the Tashkent Medical Academy between 2019 and 2021. 183 female and male patients with coronary artery disease (CAD), and stable tension angina pectoris I–III functional class were recruited for the study. The average age of the patients was 64.2 ± ± 5.1 years, 98 of them were men and 85 were women. According to the living conditions

of the patients, they were divided into two groups. Group № 1 consisted of 89 (47 men, 42 women) patients with CAD living in urban areas, and 94 (51 men, 43 women) patients with CAD living in rural areas were included in group № 2. All patients do not work in state organizations; they spend most of their time at home.

Patients were enrolled in the study either on admission to the hospital or the next day. Patients were treated as an inpatient for an average of 10 days, after discharge, patients were monitored, and patients underwent re-examination in 3–6 months.

All patients had no contraindications to physical activity and they were informed about the examination before exercise tests, and they signed a consent form. The following cases were not included in the study: acute forms of coronary artery disease, unstable angina, stable angina class IV, heart failure class III–IV according to NYHA, aneurysms of the left ventricle, stage 3 arterial hypertension, severe forms of heart arrhythmias and conduction disorders (all forms of ventricular fibrillation/fibrillation, coupled and early ventricular extrasystole, atrioventricular block second and third degree), an acute cerebral blood circulation disorder, transient ischemic attack, history of thromboembolism, severe concomitant diseases (diseases of the musculoskeletal system, osteoarthrosis and arthritis III X-ray stage, chronic lung, liver, kidney failure), type 1 and type 2 diabetes mellitus.

The diagnosis of CAD was based on the classification adopted at the IV meeting of cardiologists in 2000, and the functional class of the disease was based on the classification of the Canadian Society of Cardiology in 1976.

The clinical characteristics of the patients included in the study are presented in (Table 1).

Table 1. *Clinical characteristics of the patients included in the study*

Clinical features	Group № 1 (n=89)	Group № 2 (n=94)
Average age (years)	65.4 ± 4.3	63.7 ± 5.1
Male	47 (52.8%)	51 (54.3%)
Female	42 (47.2%)	43 (45.7%)
Duration of CAD (years)	4.2 ± 0.33	3.6 ± 0.26
Hypertension	75 (84.3%)	76 (80.8%)
BMI (kg/m2)	30.8	29.7
Abdominal obesity (sm)	118.4	111.8
Smoking	21 (23.6%)	29 (30.8%)

The average age of the 1st group, i.e., the patients with CAD living in the city, was 65.4 ± ± 4.3 years, and the average age of the 2nd group, the patients with CAD living in rural conditions was 63.7 ± 5.1 years. 52.8% of patients in the first group and 54.3% of patients in the second group are males. The majority of patients in both groups were patients with arterial hypertension, i.e. 84.3% and 80.8%, respectively.

Smoking was detected in 1/3 of patients living in rural areas, and in almost ¼ of those living in cities, 23.6% and 30.8%, respectively.

General clinical laboratory examinations, electrocardiogram, echocardiology, cardiac exercise stress test, and Holter monitoring were performed on the patients. Before the study, the patients included in the study underwent a cardiac exercise stress test and an individual physical activity program was created for each patient. Patients were monitored for continuous physical activity for six months.

To determine tolerance to execise stress (ES), all patients underwent a VEM test on a Kettle-ergometer RX1 bicycle ergometer (Germany) according to the protocol for determining the threshold load power with its continuous stepwise increase by 25 W every 3 minutes until the clinical or electrocardiographic criteria for stopping the load or submaximal heart rate (HR) by Andersen (1983) (Bubnova M.G., Aronov D.M., 2016). Clinical criteria for discontinuing the trial were generally accepted. An electrocardiogram (in 12 conventional leads), blood pressure – BP (according to the method of Korotkoff) and heart rate were recorded at the 3rd minute of each load stage, at the peak of the load

and in the recovery phase at 1, 3 and 5 minutes.

The following indicators were analyzed: performance and achieved load power, total volume of performed work (TVW), double systolic product (DSP), also the ratio of TVW to the number of heartbeats (HB) for the period of exercise (TVW / HBworking = [HBmax – HBrest] × t / 2) and the sum of the values of DSP during work (TVW / DSPworking = = [DSPmax – DSPrest] × t / 2), which reflect the efficiency of the internal work of the heart during exercise in dynamics or the change in the performed work in terms of one heartbeat and a unit of DSP during exercise. Previously, a bicycle ergometric study was carried out, using the formula (Nikolaeva L. F., Aronov D. M., 1988), the required walking rhythm was calculated for each patient:

$$\mathbf{X = 0.042 \times M + 0.15 \times HR + 65.5}$$

where X – the pace of walking (number of steps / min),

M – threshold load power (kgm / min),

Heart rate – at the peak of the load during bicycle ergometry.

Physical training lasting 50–60 minutes took place 3 times a week for 3 months with the use of intermittent dynamic loads. The training load was 50–60% of the individual threshold load (Bubnova M. G., Aronov D. M., 2016).

Table 2. *Physical activity program based on functional classes of coronary artery disease*

Type of physical activity	Functional class		
	I	II	III
General developmental exercises	35–45 minutes	25–35 minutes	20–30 minutes
Dosed walking exercise	30 minutes	20–30 minutes	20 minutes
Breathing exercises	+++	+++	+++
Slow walking exercises	2.5–3.0 km	2.0–2.5 km	1.5–2.0 km

General developmental exercises include small, medium, and partially large joint movements, first in the sitting position, then standing position. Light gymnastic exercises can be performed together with breathing exercises and separately.

"HealthRunApp" – a mobile application that allows the selection of physical activity individually. Prescription of physical activity on the basis of an individually selected innovative approach together with the main treatment of CAD is one of the urgent problems in modern medical healthcare. We have developed "HealthRunApp" – a mobile application that determines individual physical activity and adding these indicators in practice will be a special assistant for the general practitioner, cardiologist, and therapist to assess the positive effect of the physical activity selected for each patient on the treatment efficiency and quality of life. This mobile application can be a good practice assistant for general practitioners, cardiologists, and therapists who are now called family doctors. The mobile application is filled out by the doctor, and the changes in the indicators allow for comparing the dynamics in 3–6 months.

Daily monitoring of ECG. 24-hour ECG monitoring was carried out using the "Poly-Spektr-SM-154" Holter monitoring system (an ambulatory ECG). A 7-channel recorder was used, which allows the creation of 3 monitor connections corresponding to V5, V1, avF electrodes of the standard ECG. During the observation period, the patient's physical activity regimen was observed, they are recommended to sleep no later than 10:00 p.m. and wake up before 7:00 a.m. During the study, patients filled out a diary in which they recorded the type of their activities, their feelings, and the time they took their medications. It was used to compare retrospectively daily patient changes and the characteristics of ECG changes at a given moment of the day.

Interpretation of Holter monitoring data was performed according to the recommendations of the North American Society of Stimulation and Electrophysiology (1999). According to Holter monitoring data, the maximum, minimum and average number of heartbeats, the total number of ventricular extrasystoles and their composition, the number of single, coupled, and group supra-

ventricular extrasystoles and their composition were analyzed. Heart rhythm turbulence, variability, QT interval were evaluated.

Results and discussions

A study of the effect of physical activity on the lipid spectrum of patients with CAD. Lipid spectrum indicators were determined in all the patients included in the study. Initial and final results were compared. The results of the lipid spectrum of patients are presented in Tables 3. and 4.

Table 3. *Lipid spectrum results in urban-dwelling patients with CAD*

Indicator	Initial		After 6 months	
	Males (n=47)	Females (n=42)	Males (n=47)	Females (n=42)
Total cholesterol, mmol/l	6.54 ± 0.59	6.15 ± 0.55	5.8 ± 0.45	5.56 ± 0.55
TG	2.21 ± 0.22	2.09 ± 0.11	1.8 ± 0.17	1.67 ± 0.12
HDL	0.89 ± 0.02	0.91 ± 0.02	1.03 ± 0.03*	1.06 ± 0.03*
LDL	4.65 ± 0.45	3.73 ± 0.27	3.49 ± 0.29*	3.28 ± 0.28
VLDL	1.05 ± 0.13	1.03 ± 0.12	1.02 ± 0.08	1.01 ± 0.12
Kax	5.85 ± 0.45	5.41 ± 0.49	4.33 ± 0.36*	4.24 ± 0.41

*Note: *–$p < 0.05$; **$p < 0.01$; ***$p < 0.001$*

According to the data presented in (Table 3), it is seen that the amount of HDLP was reliably increased in all patients under the influence of continuous dosed walking exercise for 6 months in combination with standard treatment measures for urban patients with CAD ($p < 0.05$). In male patients, LDL and, correspondingly, Kax also reliably decreased ($r < 0.05$). All patients have a tendency to change the amount of total cholesterol, TG, VLDL in a positive way.

Table 4. *Lipid spectrum results of patients living in a rural area with CAD*

Indicator	Initial		After 6 months	
	Males (n=51)	Females (n=43)	Males (n=51)	Females (n=43)
Total cholesterol, mmol/l	6.67 ± 0.62	6.37 ± 0.59	5.9 ± 0.45	5.9 ± 0.45
TG	2.41 ± 0.27	2.14 ± 0.25	1.94 ± 0.18	1.88 ± 0.17
HDL	0.88 ± 0.02	0.89 ± 0.02	1.01 ± 0.02**	1.03 ± 0.02**
LDL	4.58 ± 0.39	4.27 ± 0.31	3.50 ± 0.29*	3.41 ± 0.27*
VLDL	1.33 ± 0.16	1.21 ± 0.17	1.15 ± 0.09	1.08 ± 0.08
Kax	5.89 ± 0.57	5.66 ± 0.52	4.18 ± 0.33*	4.11 ± 0.33*

Table 4. shows that as a result of continuous dosed walking exercise for 6 months in combination with standard treatment measures for rural patients with CAD, LDL, and correspondingly, Kax in both sexes reliably decreased ($p < 0.05$), it appears that the amount of HDL increased at a highly reliable level ($p < 0.01$).

In this group of patients, there is a tendency for the amount of total cholesterol, TG, VLDL to change in a positive way. Based on the above-mentioned facts, in patients with CAD, positive changes are observed not only under the influence of hypolipidemic agents but also as a result of physical activity.

Especially in HDL, LDL, and Kax indicators.

Evaluation of physical activity-induced Holter monitoring changes in patients with ischemic heart disease

All patients included in the study underwent Holter monitoring during the first

3 days of inpatient treatment. In addition, when the patient was instructed to exercise, Holter monitoring was performed to monitor the safety of exercise. During the Holter monitoring study, the maximum, minimum, and average values of heart rate, supraventricular and ventricular arrhythmias, ST-segment elevation, and QTc values were studied.

Initial and 6-month Holter monitoring results of patients included in the study. given in Tables 5. and 6.

Table 5. *Initial and final (after 6 months) Holter monitoring findings in urban patients with CAD*

Indicator	Initial		After 6 months	
	Males (n=47)	Females (n=42)	Males (n=47)	Females (n=42)
Maximum heart beat	133.9 ± 12.8	129.2 ± 13.6	100.2 ± 9.7*	107.5 ± 11.6
Minimum heart beat	56.9 ± 7.2	59.6 ± 5.7	52.3 ± 4.6	54.6 ± 4.1
Average heart beat	76.2 ± 5.8	73.5 ± 6.6	61.5 ± 4.3*	65.5 ± 5.2
Single Supraventricular extrosystole (SVE)	124.52 ± 10.3	111.6 ± 9.2	101.4 ± 8.2	96.5 ± 6.7
Coupled and group SVE	63.4 ± 5.3	64.1 ± 4.5	23.5 ± 3.1**	26.6 ± 2.3**
Single VE	106.8 ± 13.1	98.3 ± 10.1	63.5 ± 7.6*	56.7 ± 6.8*
Coupled VE	12.6 ± 1.4	7.4 ± 1.1	4.6 ± 2.3*	2.8 ± 1.1*
ST segment elevation)	0.69 ± 0.04	0.65 ± 0.03	0.61 ± 0.03	0.59 ± 0.02
QT (msec)	414.3 ± 28.9	408.3 ± 31.2	411.3 ± 26.4	408.1 ± 27.6

*Note: *– $p < 0.05$; ** $p < 0.01$; *** $p < 0.001$*

As shown in table 5, the maximum and average heartbeats, and single and coupled ventricular extrasystoles in men living in urban conditions are reliably reduced ($p<0.05$) under the influence of dosed walking and physical activity in combination with standard treatment measures carried out in patients with CAD, coupled and group supraventricular extrasystoles decrease in both sexes at a highly reliable level ($p<0.01$). All patients tend positive changes in ST segment changes, ventricular extrasystoles.

Table 6. *Results of initial and 6-month follow-up Holter monitoring of rural patients with CAD*

Indicator	Initial		After 6 months	
	Males (n=51)	Females (n=43)	Males (n=51)	Females (n=43)
Max. Heart beat	116.9 ± 10.2	131.3 ± 11.6	95.4 ± 8.8	105.4 ± 9.7
Min. Heart beat	54.5 ± 5.3	61.3 ± 5.8	51.6 ± 5.9	54.6 ± 4.1
Average heart beat	68.7 ± 7.1	78.3 ± 6.1	62.4 ± 4.7	64.5 ± 5.2
Single SVE	258.8 ± 33.4	239.6 ± 38.7	143.8 ± 12.7*	121.5 ± 14.5*
Coupled and group SVE	77.6 ± 6.5	65.8 ± 7.8	45.9 ± 5.3*	37.9 ± 4.1*
Single VE	145.7 ± 11.7	118.3 ± 12.7	101.7 ± 10.1*	74.7 ± 8.6*
Coupled VE	17.1 ± 2.4	13.4 ± 1.3	4.8 ± 0.9**	3.6 ± 0.7*
Changes of ST segment	0.64 ± 0.03	0.67 ± 0.03	0.60 ± 0.03	0.61 ± 0.02
QT (msec)	421.0 ± 24.7	419.3 ± 34.9	418.0 ± 21.3	417.6 ± 37.5

*Note: * – $p < 0.05$; ** $p < 0.01$; *** $p < 0.001$*

Table 6 shows that the number of single, coupled and group supraventricular extrasystoles in men who live in rural areas decreased significantly under the influence of a dosed walking and physical activity program, which was carried out continuously in com-

bination with standard treatment measures, ($p<0.05$), the number of single and coupled ventricular extrasystole decreased at a highly reliable level ($P<0.01$), there is a tendency to decrease the maximum, minimum and average heart beats.

In female patients living in rural areas, single, coupled, and group ventricular extrasystoles, single and coupled ventricular extrasystoles have decreased dramatically ($p<0.05$), and there is a tendency to decrease maximum, average, and minimum heartbeats. All patients tend positive changes in ST-segment change.

In **conclusion**, it can be said that, in addition to the standard treatment of patients with CAD, continuous physical activity, regardless of living conditions, has a positive effect on the amount of atherogenic and antiatherogenic lipoproteins, the number of heart contractions, supraventricular and ventricular arrhythmias.

References

Mendis S., Puska P., Norrving B. editors. Global Atlas on Cardiovascular Disease Prevention and Control. World Health Organization, – Geneva, 2011.

Regina G., Gretchen A. S., Leanne M. R., Fiona C. B. Worldwide trends in insufficient physical activity from 2001 to 2016: a pooled analysis of 358 population-based surveys with 1·9 million participants. URL: http://www. thelancet.com/lancetgh Vol 6 October, 2018.

Globally, 1.4 billion adults at risk of disease from not doing enough physical activity// The Lancet // https://medicalxpress.com/news/2018-09-globally-billion- adults-disease-physical.html

How Artificial Intelligence and Robotics Are Changing Our Lives // https://www.sam-solutions.com/blog/ai-and-robotics-impact-on-our-lives

Emotional stability (the opposite of neuroticism) is a fundamental personality trait that has to do with being even-tempered, particularly in the face of challenges and threats // Handbook of Social Status Correlates, 2018.

Akulova T. N., Plaksina N. V., Smirnova E. V. Decrease in physical activity of the population as a complex problem: solutions // Akulova T. N., Plaksina N. V., Smirnova E. V./ Society and Security Insights 2020. (In Russian)

Global action plan on physical activity 2018–2030: more active people for a healthier world// World Health Organization 2018.

Bubnova M. G., Aronov D. M. Methodological recommendations for ensuring physical activity of citizens with health limitations,– Moscow, 2016. (in Russian)

submitted 16.08.2024;
accepted for publication 31.08.2024;
published 28.09.2024

Contact: rano_uzbechka@mail.ru

The Austrian Journal of Technical and Natural Sciences, No 7–8
ISSN 2310-5607

PREMIER Publishing
ppublishing.org

DOI:10.29013/AJT-24-7.8-37-40

STUDY OF PHYSICOCHEMICAL AND TECHNOLOGICAL PROPERTIES OF DRY EXTRACT FROM ROSA RUGOSA LEAVES

Alimujiang A. [1]***, Khalilov R.M.*** [1]***, Wen Juan Xue*** [2]***, Aidarhan N.*** [2]***, Sagdullaev Sh. Sh.*** [1]

[1] Institute of the Chemistry of Plant Substances named after Acad. S. Yu. Yunusov of the Academy of the Sciences Republic of Uzbekistan, Uzbekistan

[2] State Key Laboratory Basis of Xinjiang Indigenous Medicinal Plants Resource Utilization, Xinjiang Technical Institute of Physics and Chemistry, Chinese Academy of Sciences, China

Cite: *Alimujiang A., Khalilov R.M., Wen Juan Xue, Aidarhan N., Sagdullaev Sh. Sh. (2024). Study of Physicochemical and Technological Properties of Dry Extract From Rosa Rugosa Leaves. Austrian Journal of Technical and Natural Sciences 2024, No 3–4.* https://doi.org/10.29013/AJT-24-7.8-37-40

Abstract

At the experimental and technological laboratory of the Institute of Plant Chemistry, a dry extract was obtained from the leaves of Rosa rugosa, containing the flavonoids quercetin-3-O-sophoroside and kaempferol-3-O-sophoroside. To substantiate the composition and technology of solid dosage forms, the physicochemical and technological properties of the dry extract were studied. As a result of experimental studies, the feasibility of incorporating a complex of auxiliary substances into the composition of the solid dosage form and utilizing the method of preliminary wet granulation was determined.

Keywords: *Rosa rugosa, dry extract, technological properties*

Introduction

Herbal medicines offer the advantage of providing a mild pharmacological effect, low toxicity, and are generally safer than synthetic drugs. However, developing solid dosage forms, such as tablets containing dry extracts, often presents significant challenges due to the unsatisfactory technological properties of the dry extracts. Therefore, studying the physicochemical and technological properties of these dry extracts is crucial for the accurate selection of the composition and technology of the drugs (Madrakhimov, Sh.N., Rakhimova et al., 2016). The aim of this study is to investigate the physicochemical and technological properties of the dry extract from Rosa rugosa leaves, which will help in determining the optimal selection of excipients for the development of the composition and technology of plant-based tablets.

Materials and methods

The object of the study was a dry extract from *Rosa rugosa* leaves, obtained using the following procedure: air-dried *Rosa rugosa* leaves were ground in a mill equipped with a 6

mm sieve. Ten kilograms of the ground raw material were loaded into an extractor, into which 200 liters of 70% ethyl alcohol were poured. The extraction process was carried out at a temperature of 70 °C for 6 hours. After this period, the first 180 liters of the extract were drained into a collector. Subsequently, a new portion of 200 liters of 70% ethyl alcohol was added to the extractor, and extraction was conducted under the same conditions as the first extraction. As a result, 380 liters of the combined extract were obtained, which were filtered and loaded in portions into a vacuum evaporator, where the extract was concentrated to a concentration of 0.12 g/ml at a temperature of 60–70 °C and under a vacuum of 0.04–0.08 MPa (0.4–0.8 kgf/cm²). The concentrate was then passed through a column filled with adsorption resin XAD-16N. The adsorption resin absorbed the flavonoids (quercetin-3-O-sophoroside and kaempferol-3-O-sophoroside), which were subsequently washed with distilled water in a volume ratio of sorbent to water of 1:5. Flavonoids were extracted from the purified sorbent using 50% ethyl alcohol in a volume ratio of sorbent to alcohol of 1:2. The alcohol solution of flavonoids was then concentrated using a rotary evaporator and dried in a drying cabinet at a temperature of 60–70 °C under a vacuum of 0.04–0.08 MPa (0.4–0.8 kgf/cm²). The resulting dry mass was ground in a mill and sieved, yielding 1.25 kg of dry extract.

The study of the moisture absorption kinetics of the dry extract from *Rosa rugosa* leaves was conducted using the gravimetric method (Nosovitskaya, S.A. et al., 1969). Additionally, the following physical, chemical, and technological quality indicators were examined: crystal size and shape, solubility, particle size distribution, bulk density before and after shrinkage, flowability, residual moisture, compressibility, angle of repose, accompanying impurities, authenticity, quantitative content, and other necessary characteristics according to the methods outlined in the State Pharmacopoeia of the Republic of Uzbekistan. Bulk density was determined using a 545R-AK-3 device from the Mariupol Plant of Technological Equipment. The flowability of the materials was assessed using a VP-12A device. Compressibility was evaluated by measuring the resistance to crushing of standard pressings obtained on a hydraulic press at a pressure of 1200 kg/cm². The angle of repose was measured using a special ruler and scale. Residual moisture was determined using the infrared (IR) drying method, employing an IR moisture meter from Kett (Kedika, S.A., 2011).

Results and discussion

Initially, the size and shape of the crystals in the dry extract of *Rosa rugosa* leaves were assessed. The shape of the powder crystals can significantly affect the orientation of the particles, influencing characteristics such as flowability, solubility, compressibility, and compactness. Crystallographic studies revealed that the dry extract is amorphous.

Figure 1. *Kinetics of water absorption of dry extract of Rosa rugosa leaves under experimental conditions of 58% and 100% relative humidity*

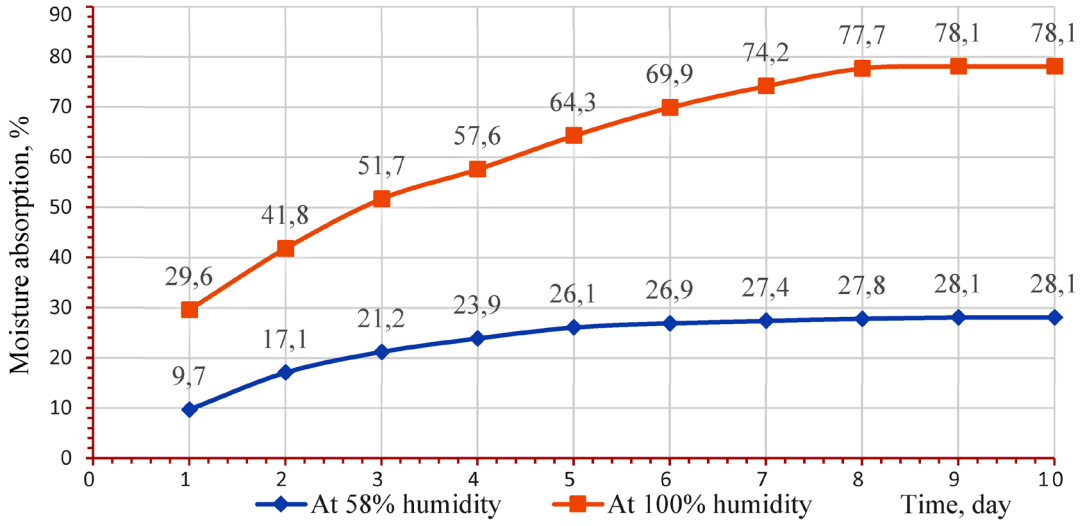

The study of the moisture absorption kinetics of the dry extract showed that under experimental conditions-58% relative humidity for 5 days, and 100% for 24 hours – the moisture content of the extract increased to over 25%, turning it into a resinous mass. These results indicate that the dry extract of *Rosa rugosa* leaves is classified as a "very hygroscopic" substance (Fig. 1).

The study then proceeded to examine the technological properties of the dry extract, with the results presented in Table 1.

Table 1. *Technological properties of the dry extract of Rosa rugosa leaves*

№	Indicators to be checked	Units of measurement	Results obtained
1	Particle shape	–	amorphous
2	Fractional composition: + 1000 – 1000 +500 – 500 +315 – 315 +250 – 250 +160 – 160	microns.%	– 2.20 11.18 35.34 44.07 7.21
3	Flowability	10^{-3} kg/s	2.28
4	Natural angle of repose	degree	62.00
5	Bulk density	kg/m^3	479
6	Compressibility	H	72
7	Compaction coefficient	K	2.68
8	Residual humidity (70 °C)	%	4.48

Analyzing the results presented in Table 1, it can be concluded that the dry extract of *Rosa rugosa* leaves exhibits unsatisfactory volumetric characteristics and poor fluidity. The high compressibility coefficient further indicates poor flowability, as confirmed by the elevated angle of repose and the irregular shape of the powder particles. However, the dry extract does show satisfactory compressibility, which can be attributed to the complex shape of its particles, large contact surface area, and cohesive forces. Based on the crystallographic and technological studies of the *Rosa rugosa* dry extract, it was determined that when developing solid dosage forms, auxiliary substances should be incorporated to improve the flowability and compressibility of the formulation mass (Table 1).

Conclusions

Thus, we have studied the physicochemical and technological properties of the dry extract of *Rosa rugosa* leaves and identified the critical characteristics of the raw material that can impact the quality of the finished product. Experimental studies have demonstrated the necessity of incorporating a complex of auxiliary substances into the dosage forms and utilizing the method of preliminary wet granulation. The data obtained should also be considered when storing the dry extract of *Rosa rugosa* leaves.

References

Madrakhimov, Sh. N., Rakhimova, O. R., Khalilov, R. M., Rakhimova, G. R. (2016). Technology of tablets flanorin. *Parmaceuticaljournal*,– 2.– P. 62–65. (in Russ).

Madrakhimov, Sh. N., Rakhimova, O. R., Khalilov, R. M., Kotenko, L. D., Rakhimova, G. R. (2016). Development of the technology and the quality assessment of ferulen tablets. *Parmaceuticaljournal*,– 4.– P. 63–69. (in Uzbek).

Pharmaceutical technology. Solid dosage forms. Textbook (2011). edited by Prof. Kedika, S.A.,– Moscow. 2011.– 661 p. (in Russ).
Nosovitskaya, S.A., Borzunov, E.E., Safiulin, R.M. (1969). *Production of tablets*.– M.: Medicine,– 136 p. (in Russ).

submitted 06.08.2024;
accepted for publication 21.08.2024;
published 28.09.2024

Contact: atux@ms.xjb.ac.cn

The Austrian Journal of Technical and Natural Sciences, No 7–8
ISSN 2310-5607

PREMIER Publishing
ppublishing.org

DOI:10.29013/AJT-24-7.8-41-45

FEATURES OF THE IMMUNE MICROENVIRONMENT IN VARIOUS MOLECULAR BIOLOGICAL SUBTYPES OF BREAST CANCER

Kahharov A.J. [1]***, Narzieva D.F.*** [2]

[1] Tashkent State Dental Institute, Tashkent, Uzbekistan,

[2] Bukhara State Medical Institute, Bukhara, Uzbekistan

Cite: *Kahharov A.J., Narzieva D.F. (2024). Features of the Immune Microenvironment in Various Molecular Biological Subtypes of Breast Cancer. Austrian Journal of Technical and Natural Sciences 2024, No 3–4.* https://doi.org/10.29013/AJT-24-7.8-41-45

Abstract

This article is devoted to the peculiarities of the immune microenvironment of a tumor in various molecular biological subtypes of breast cancer.To study the immune microenvironment, we conducted an IHC study of CD4, CD8, CD20 markers. Our study showed the presence of strong relationships between the molecular biological subtypes of breast cancer and the immune microenvironment of the tumor, which may indicate its potential role as a predictive and prognostic factor in breast cancer. Given these data, it can be assumed that this relationship creates a modern view of more effective treatment with a favorable prognosis and increases survival among patients with breast cancer.

Keywords: *microenvironment, lymphocytes, breast cancer*

Introduction

Breast cancer is the most common malignant neoplasm among women worldwide. In recent decades, there has been a trend of increasing incidence and mortality in both developed and developing countries (Li J.J., Tsang J.Y., Tse G.M. 2022; Toss M.S. et al. 2020). The course of breast cancer depends on many factors such as histologic and molecular biologic characteristics. Nevertheless, more and more studies have recently focused on the influence of tumor microenvironment on the course, response to treatment and prognosis of breast cancer (Giannoudis A. et al. 2022; Mir M.A. 2022; Russo M., Nastasi C. 2020).

Purpose of the study: To determine the relationship between immunohistochemical features of tumor cells and their cellular microenvironment in breast cancer.

Materials and methods

The study included 102 breast cancer patients who were under dispensary observation at the Tashkent city branch of the Republican Specialized Scientific and Practical Medical Center of Oncology and Radiology. In order to study the immune microenvironment, we conducted an IHC study of CD4, CD8, CD20 markers. A posteriori comparisons were performed using Pearson's chi-square criterion with Hill's correction. The strength of associ-

ation between categorical indicators was assessed using Cramer's V, whose values were interpreted according to the recommendations of Rea & Parker (2014).

Differences were considered statistically significant at $p < 0.05$.

Results

We analyzed CD4 status depending on the molecular-biological subtype.

According to the obtained data, when comparing CD4 status depending on the molecular biological subtype, we found statistically significant differences ($p < 0.001$) (Pearson's Chi-square method used).

The association between molecular biological subtype and CD4 status was strong (Cramer's V = 0.86). We analyzed the type of tumor infiltration by CD4 lymphocytes depending on the molecular biological subtype.

Figure 1. *Analysis of CD4 status according to molecular biological subtype*

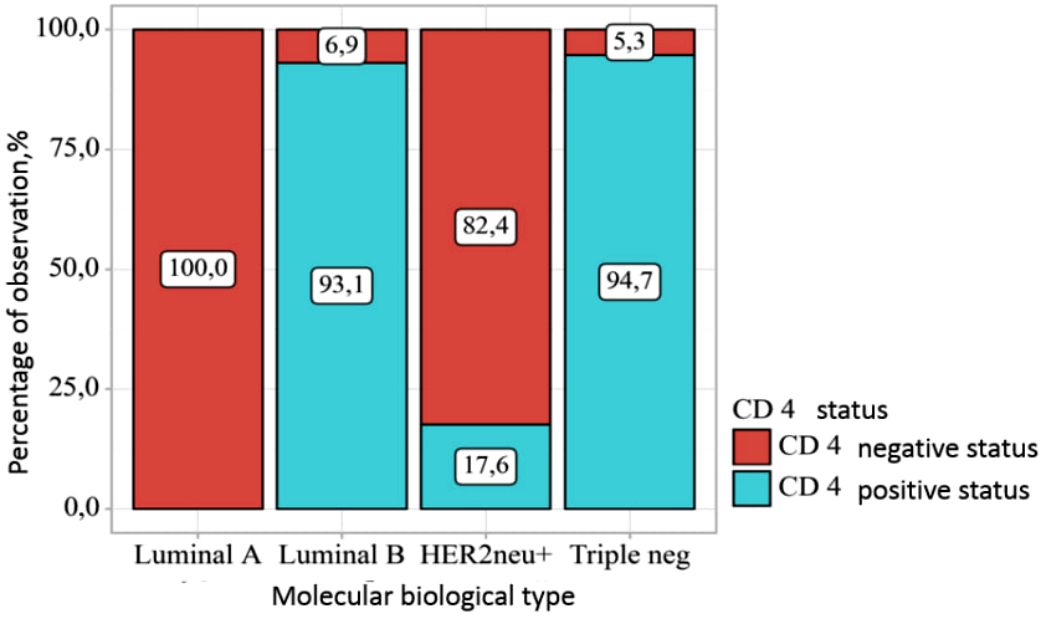

Table 1. *Analysis of the type of tumor infiltration by CD4 lymphocytes depending on the molecular biological subtype*

Indicator	Categories	Molecular biological subtype				χ2	df
		Luminal subtype A	Luminal subtype B	HER2 neu positive subtype	Triple negative subtype		
Type of tumor infiltration by CD4 lymphocytes	No lymphocyte infiltration of the tumor	18 (100.0)	2 (6.9)	14 (82.4)	2 (5.3)		
	Intratumoral infiltration with lymphocytes	0 (0.0)	18 (62.1)	3 (17.6)	28 (73.7)	76.526	6
	Intrastromal infiltration with lymphocytes	0 (0.0)	9 (31.0)	0 (0.0)	8 (21.1)		

< 0.001; pLuminal subtype A – Luminal subtype B < 0.001, pLuminal subtype A – Triple negative subtype < 0.001; pLuminal subtype B – HER2 neu positive subtype < 0.001, pHER2 neu positive subtype – Triple negative subtype < 0.001; * – differences are statistically significant (p < 0.05)*

According to the presented table, when comparing the type of tumor infiltration by CD4 lymphocytes depending on the molecular-biological subtype, we found statistically significant differences ($p < 0.001$) (Pearson's Chi-square method used).

The correlation between molecular biological subtype and the type of tumor infiltration by CD4 lymphocytes was relatively strong (Cramer's V = 0.61).

We analyzed CD8 status depending on the molecular-biological subtype.

According to the presented table, when analyzing CD8 status according to molecular biological subtype, significant differences ($p < 0.001$) were found (method used: Pearson's Chi-square).

Figure 2. *Analysis of CD8 status according to molecular biological subtype*

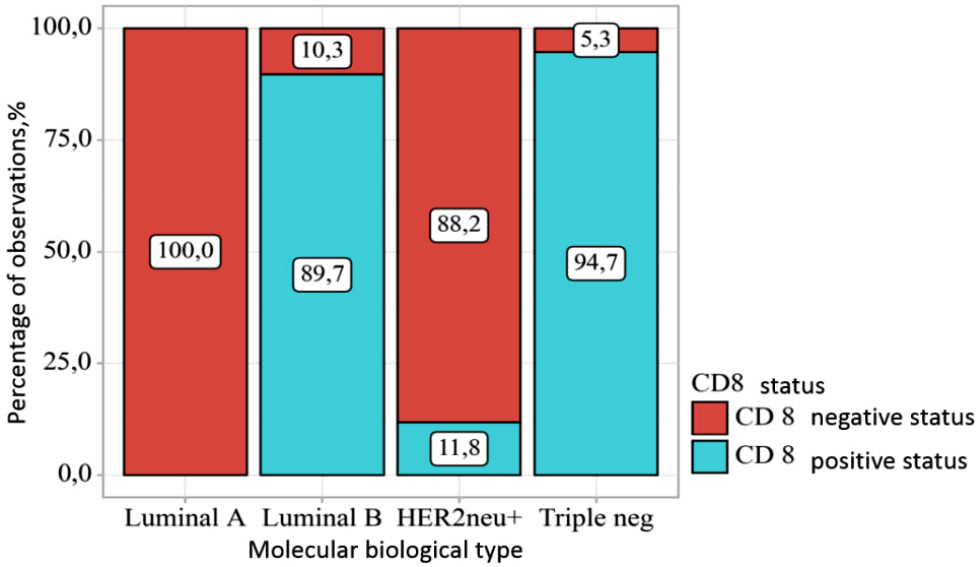

Table 2. *Analysis of the type of tumor infiltration by CD8 lymphocytes depending on the molecular biological subtype*

Indicator	Categories	Molecular biological subtype				χ2	df
		Luminal subtype A	Luminal subtype B	HER2 neu positive subtype	Triple negative subtype		
Type of tumor infiltration by CD8 lymphocytes	No CD8 lymphocyte infiltration of the tumor	18 (100.0)	3 (10.3)	15 (88.2)	2 (5.3)	79.526	6
	Intratumoral infiltration with CD8 lymphocytes	0 (0.0)	14 (48.3)	2 (11.8)	27 (71.1)		
	Intrastromal infiltration with CD8 lymphocytes	0 (0.0)	12 (41.4)	0 (0.0)	9 (23.7)		

< 0.001; pLuminal subtype A – Luminal subtype B < 0.001, pLuminal subtype A – Triple negative subtype < 0.001; pLuminal subtype B – HER2 neu positive subtype < 0.001, pHER2 neu positive subtype – Triple negative subtype < 0.001; * – differences are statistically significant (p < 0.05)*

The association between molecular biological subtype and CD8 status was strong (Cramer's V = 0.86).

We analyzed the type of tumor infiltration by CD8 lymphocytes depending on the molecular-biological subtype.

According to the presented table, when analyzing the type of tumor infiltration by CD8 lymphocytes depending on the molecular-biological subtype, we found statistically significant differences ($p < 0.001$) (method used: Pearson's Chi-square).

The correlation between molecular-biological subtype and the type of tumor infiltration by CD8 lymphocytes was relatively strong (Cramer's V = 0.62).

According to the findings, when CD20 status was compared according to molecular biological subtype, significant differences ($p < 0.001$) were found (method used: Pearson's Chi-square).

The association between molecular biological subtype and CD20 status was strong (Cramer's V = 0.78).

We analyzed the type of tumor infiltration by CD20 lymphocytes depending on the molecular-biological subtype.

Figure 3. *Analysis of CD20 status according to molecular biological subtype*

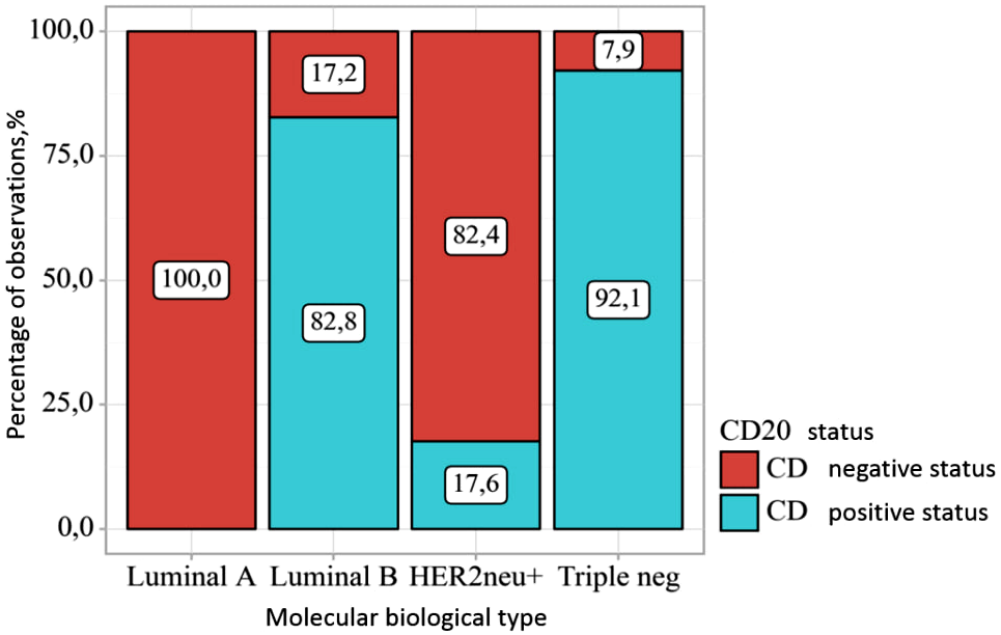

Table 3. *Analysis of the type of tumor infiltration by CD20 lymphocytes depending on the molecular biological subtype*

Indicator	Categories	Molecular biological subtype				χ2	df
		Luminal subtype A	Luminal subtype B	HER2 neu positive subtype	Triple negative subtype		
Type of tumor infiltration by CD20 lymphocytes	No CD20 lymphocyte infiltration of the tumor	18 (100.0)	5 (17.2)	15 (88.2)	1 (2.7)	72.353	6
	Intrastromal tumor infiltration by CD20 lymphocytes	0 (0.0)	19 (65.5)	2 (11.8)	27 (73.0)		

Indicator	Categories	Molecular biological subtype				χ2	df
		Luminal subtype A	Luminal subtype B	HER2 neu positive subtype	Triple negative subtype		
	Intratumoral tumor infiltration by CD20 lymphocytes	0 (0.0)	5 (17.2)	0 (0.0)	9 (24.3)		

< 0.001; pLuminal subtype A – Luminal subtype B < 0.001, pLuminal subtype A – Triple negative subtype < 0.001; pLuminal subtype B – HER2 neu positive subtype < 0.001, pHER2 neu positive subtype – Triple negative subtype < 0.001; * – differences are statistically significant (p < 0.05)*

According to the table below, when analyzing the type of tumor infiltration by CD20 lymphocytes depending on the molecular biological subtype, statistically significant differences (p < 0.001) were found (method used: Pearson's Chi-square).

The association between molecular biological subtype and type of tumor infiltration by CD20 lymphocytes was relatively strong (Cramer's V = 0.6).

Conclusion

Our study showed strong correlations between molecular biological subtypes of breast cancer and the immune tumor microenvironment, which may suggest its potential role as a predictive and prognostic factor in breast cancer. Considering these data, we can assume that this relationship creates a modern view of more effective treatment with a favorable prognosis and increases survival among patients with cancer.

References

Giannoudis A. et al. Characterisation of the immune microenvironment of primary breast cancer and brain metastasis reveals depleted T-cell response associated to ARG2 expression //ESMO open. 2022.– T. 7.– № . 6.– 100636 p.

Li J. J., Tsang J. Y., Tse G. M. Tumor microenvironment in breast cancer – updates on therapeutic implications and pathologic assessment //Cancers. 2021.– T. 13.– № 16.– 4233 p.

Mir M. A. Role of tumor microenvironment in breast cancer and targeted therapies.– Elsevier, 2022.

Russo M., Nastasi C. Targeting the tumor microenvironment: a close up of tumor-associated macrophages and neutrophils // Frontiers in Oncology. 2022.– T. 12.– 871513 p.

Toss M. S. et al. The prognostic significance of immune microenvironment in breast ductal carcinoma in situ //British journal of cancer. 2020.– T. 122.– № 10.– P. 1496–1506.

submitted 06.04.2024;
accepted for publication 21.08.2024;
published 28.09.2024

Contact: alisher1510@mail.rua, noza_2206@mail.rub

The Austrian Journal of Technical and Natural Sciences, No 7–8
ISSN 2310-5607

PREMIER Publishing
ppublishing.org

Section 4. Technical sciences in general

DOI:10.29013/AJT-24-7.8-46-51

TECHNOLOGY OF NON-TRADITIONAL BALANCED COMPOUND FOOD, WITH ENRICHED PROTEIN AND ENZYME COMPOSITION FROM THE FUNGUS PLEUROTUS OSTREATUS

Niyozov Kh.N. [1]***, Dodaev K. O.*** [1]***, Akhmedova Z.R.*** [2]***, Yakhyaeva M.A.*** [2]

[1] Technical Sciences, Tashkent Institute of Chemical Technology

[2] Institute of Microbiology of the Academy of Sciences of the Republic of Uzbekistan

Cite: *Niyozov Kh.N., Dodaev K. O., Akhmedova Z.R., Yakhyaeva M.A. (2024). Technology of Non-Traditional Balanced Compound Food, With Enriched Protein and Enzyme Composition From the Fungus Pleurotus Ostreatus. Austrian Journal of Technical and Natural Sciences 2024, No 3–4.* https://doi.org/10.29013/AJT-24-7.8-46-51

Abstract

This article is devoted to the study of the protein synthesis characteristics of the selected basidial fungus Pleurotus ostreatus producer, using microbiological methods to increase the protein content of the feed in the preparation of balanced, protein-rich, mixed feed used in fisheries.

Keywords: *Pleurotus ostreatus, balanced feed, protein, enzymatic activity, amylase, protease, basidiomycete, growth performance, protein, medium, biomass*

Introduction

All reforms carried out in the Republic of Uzbekistan are aimed at protecting the socio-economic interests of the population and improving their lifestyle. A growing population leads to an even greater increase in demand for food. Today, the growing population demand for meat products leads to the fact that supply and demand in a market economy are becoming even higher. Currently, the development of each industry and the production of quality products are the main criteria of a market economy. Therefore, when developing the main industry, it is necessary to determine the level of demand for the production of feed products, ensure it in practice and conduct a series of studies. As a result of these studies, the quantity and quality of high-quality meat products are ensured, that is, products grown in livestock, poultry and fish farms. At the same time, a number of program measures have been adopted to ensure food security in the Republic of Uzbekistan, including to increase the volume of production of high-quality fish products. As a result of the measures being implemented, thousands of hectares of new artificial reservoirs are being created, in which many new fish farms operate on a business basis.

The main factor in increasing the productivity of fisheries is its rational feeding. This situation is a current problem (Sakovskaya V.G., Voroshilina Z.P., 2010; Xolmirzayev D., Haqberdiyev P.S., Shoximardonov D.R., Shaptakov E.S., 2016).

Literature review

The effectiveness of feeding fish depends on the correct formulation of the feed: proteins, fats, carbohydrates must be rationally selected. Of course, the amount of vitamins, minerals, hormones, organic acids and biologically active substances should be based on the needs of the fish body. However, from a nutritional point of view, aquaculture animals are fed very differently from other farm animals, and even the nutritional needs of different fish are different. Fish food can be simple or complex depending on the amount of nutrients it contains. Today's feeds contain more carbohydrate-rich ingredients such as cracked grains, milling bran, rice powder, and oils and fats. A small amount of food waste from catering, wheat and barley waste from beer and wine production is also added. The bottom line is that currently, when developing feeds, local foods rich in carbohydrates are used, vitamin complexes (premixes) and a source of essential minerals (bone powder) are added to them. Naturally, the main part of the feed composition is carbohydrates, and the amount of protein is up to 19–20%. According to the requirements of the fishing industry, the protein content in feed must be higher than 32%. As a result of these analyzes, the main goal and objectives of the study are formed (Pulatov I.B., Zhuraeva K.M., Dodaev K.O., Niyozov Kh.N., 2023).

Feeds used in fisheries are divided into: natural, supplementary and balanced. Natural food resources include: phytoplankton, zooplankton, microscopic algae, benthic and benthic plants, zoobenthos, nektobenthos and aquatic insects. Additional nutrients include crops and residues, processed animal by-products and food waste. Balanced feeds include feeds with a very high nutritional level, the food unit of which is 1.5–2.0 (Niezov H.N., Dodaev K.O. 2023; Eremina I.A., Luzina N.I., Krieger O.V., 2003).

To obtain feed and food protein, you can use various types of lower and higher mushrooms grown industrially. Some types of microscopic fungi are capable of accumulating up to 50% protein. In terms of the content of essential amino acids, mushroom protein is close to protein of animal origin, the biomass is rich in vitamins, especially group B, the content of nucleic acids is low (2.5%), the cell walls are thin and easily digested in the gastrointestinal tract of animals. When growing microscopic fungi in a liquid nutrient medium, as a rule, intensive formation of biomass occurs at the first stage of cultivation. Under conditions of deep cultivation, complex intracellular transformations occur in the conidia in the first 5–6 hours, they swell, and the first hyphae appear. Next comes the rapid development and growth of the mycelial mass of the fungus. The mycelium can form in the form of balls or a porridge-like mass (Gorelikova, G.A. 2004, GOST. 20264.4–89).

Enzymes catalyze millions of chemical transformations in the cells of animals, plants, microorganisms and act on the corresponding substrates outside the cell. The advantage of using enzymes over chemical catalysts is that they operate at normal pressure, at a temperature range from 20 to 70 °C, pH from 4 to 9, in most cases they have high substrate specificity, which allows targeted action in a complex mixture of biopolymers for certain connections.

It is necessary to distinguish between two concepts: enzymes and enzyme preparations. Enzymes are found in almost all living objects: plants, animals and microorganisms (GOST. 20264.4–89).

The raw materials used in the production of compound feed for fish must be non-scarce, inexpensive, and, if possible, easily accessible. These include molasses – a by-product of sugar production, flour formed during the grinding of rice, meal from an oil extraction plant, waste from catering establishments, etc.

To achieve protein growth in feed, strains of Pleurotus Ostreatus mushrooms are used, widely cultivated throughout the world, usually in Asia, America and Europe, due to their simplicity, low cost of production technology and high biological efficiency. For the growth of oyster mushrooms, high humidity (80–90%) and a temperature of 25–30 °C are required for the formation of the fruiting body.

The spent substrate left after harvesting can be used as a soil conditioner for plants and animal feed after growing mushrooms. Substrates used for mushroom production in previous studies include rice straw, rice bran, wheat straw, pulp, corn cobs, cocoa shell waste, cotton waste, spent grains, sawdust, corn husks and cassava peels. Other substrates include soybean straw, rice straw, sunflower stalks, sugarcane bagasse, fruit waste, used tea leaves, bamboo leaves and corn stalks. Additional substrates used for oyster mushroom cultivation are enset waste, teff straw, paper waste, finger millet husks and banana pseudostems. Therefore, the present study aims to evaluate the cultivation of Pleurotus ostreatus on both different substrates and their combinations (Adenipekun, C.O. and Omolaso, P.O. 2015).

Methods

Scientific research was carried out in the laboratory "Biotechnology of Nature Conservation" of the Institute of Microbiology of the Academy of Sciences of the Republic of Uzbekistan. Using some non-pathogenic fungal cultures that exhibit the ability to synthesize active proteins, stored in the culture museum of this laboratory, synthetic work was carried out to obtain mixed nutritious, protein-rich feeds for fish farming. On a rich nutrient medium indicated in Table 1, the basidiomycete fungus Pleurotus ostreatus (common mushroom) belonging to the class of basidiomycetes was grown, and the amount of proteins formed in the culture liquid, enzyme activity and growth indices (medium pH index, biomass accumulation) were determined) (Batt C. A. & Tortorello M. L., 2014).

Table 1. *Recipe for food based on stillage*

№	Compound	Quantity	
		%	*g*
1	Barda	40	80
2	Wheat flour	1	2
3	$CaCO_3$	0.5	1
4	KH_2PO_4	0.5	1
5	$(NH_4)_3PO_4$	0.5	1
6	Distilled water	57.5	115
	Total	100	200

In this case, the proteins of the culture liquid were determined by the classical method – the Lowry method. The amount of protein was determined from a calibration curve constructed using bovine serum albumin. For analysis, 0.4 ml of filtrate is added to 2 ml of reagent C and kept at room temperature for 10 minutes. Then add 0.2 ml of Folin's reagent and leave the mixture for 30 minutes to change color. In this case, the mixture in the experiment slowly changes color from yellow to transparent blue. Optical density is determined in FEC at a wavelength of 750 nm.

Amylolytic enzymes (α-amylase) in the culture fluid, the activity of which is determined by hydrolysis of 1.0% starch paste, the activity of the α-amylase enzyme is determined by measuring the breakdown of the starch substrate into various low molecular weight dextrins and sugars, as well as the enzyme unit, add 1 ml of culture fluid, for 10 minutes, mg of dextrin or small sugars is determined.

The fermentation process was carried out for 10 minutes at a temperature of 30 °C and an acidity pH of 6,5. To do this, 1 ml of culture liquid was added to 2,0 ml of 1% starch, mixed thoroughly and incubated in a water bath at 30 °C for 10 minutes. The same amount (1 ml) of distilled water was placed on the starch in the control tube. At the end of the reaction time, an aliquot of 0.5 ml was taken, the iodine working solution was added and mixed well. In this case, the test tubes were of different colors, for example, the control tubes were blue-airy, and in the test tubes the enzyme activity changed to purple, dark red, brown and yellow, depending on the level of starch. decomposition. After color matching, the optical density of the reaction liquid was measured for 10 min using the FEC method at a wavelength of 670 nm.

The proteolytic enzymatic activity of the culture liquid was determined by the Anson method. This method is based on the cleavage and identification of sodium caseinate into a peptide or amino acid using an enzyme preparation. To conduct the experiment, 1 cm3 of substrate (sodium caseinate) is placed in test tubes and placed in a thermostat at a temperature of 30 °C. After about 10 minutes, 1 sm^3 of culture liquid was added to

each tube and incubated in a water bath at 30 °C for 10 minutes. After the fermentation process was completed, the test tubes were cooled and 2 sm^3 of 0.3 M trichloroacetic acid was poured into them; this mixture helps stop the reaction and precipitate protein and high-molecular hydrolysis products. Mix the mixture quickly and incubate in a water bath at 30 °C for 20 minutes to allow rapid sedimentation. The mixture is then filtered into dry test tubes. The filtrate should be very clear. Then 5 sm^3 of 0,5 mol/dm^3 sodium carbonate solution and 1 cm^3 of filtrate are added to the test tubes. They are mixed well and placed in foil with a reagent volume of 1 cm^3. Peptides and amino acids of the hydrolyzed protein are stained using folin reagent and the color intensity is compared with the control optical density tube at a wavelength of 670 nm using FEC (GOST 20264.2–88).

The amount of biomass formed by the fungus during the process of growth and development is determined by filtering the culture liquid of the fungus, drying the remaining fungal cells on filter paper at room temperature and measuring them on an analytical balance.

Results and discussion

Today, due to the sharp increase in population in Uzbekistan, mass food production is becoming a pressing issue. Meat and meat products make up a significant part of the food consumed by the population.

Recently, since the production of animal meat products requires a long period of time, the development of poultry farming and fishing has become more and more traditional. This makes it possible to satisfy the population's need for meat and protein-rich products.

Currently, the development of the fishing industry and the establishment of fishing in artificial reservoirs is becoming a cost-effective and profitable industry. This shows that along with the development of the industry, there are shortcomings and problems in it. The reason is that fish farms still purchase foreign protein-rich feed products, which are imported through investment. This leads to an increase in the price of products.

Figure 1. *Growth parameters, protein content and hydrolytic enzyme activities of the fungus Pleurotus ostreatus*

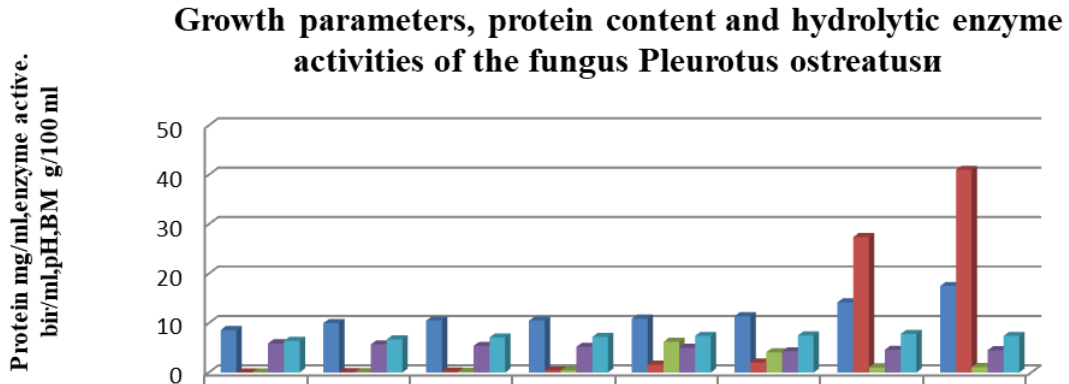

	72 hours	96 hours	120 hours	144 hours	168 hours	192 hours	216 hours	240 hours
Protein content, mg/ml	8,6	10	10,5	10,5	10,9	11,4	14,2	17,5
α-amylase bir/ml	0,006	0,08	0,2	0,41	1,6	2	27,4	41
Protease, bir/ml	0,03	0,06	0,14	0,39	6,2	4,1	1,03	1,11
pH	5,9	5,7	5,4	5,2	5	4,3	4,6	4,5
Biomass, g/100 ml	6,4	6,7	7,1	7,2	7,4	7,5	7,8	7,4

The goal of our research is to create biotechnologies based on microbiological research and solve industry problems in the production of balanced high-protein fish feeds based on local raw materials that can compete with foreign compound feeds.

In the course of scientific research, we cultivated the local basidiomycete Pleurotus ostreatus (common fungus) on some agricultural secondary materials, plant residues rich in cellulose (bran, sawdust, straw, etc.) and due to the fermentative growth process

of this fungus, cases of increasing food value of feed products by increasing the amount of protein produced (Iwase, K., Umezawa, Y. and Masuda, K., 2000).

In order to increase the protein content of fish food, we studied the dynamics of increasing the amount of protein in the food compared to the control food when growing protein-synthesizing fungi and basidiomycetes (Fig. 1).

The table below shows the growth rates of the fungus Pleurotus ostreatus, i.e. shift of the pH of the medium from neutral 5.9–6.0 to the acidic side 4.0–4.5, depending on the influence of growth factors, amount of biomass produced in the medium, 6.4 g – after 72 hours from 240 hours to 7.4 g, and the amount of monadic protein increased from 8.6 mg/ml at 72 hours to 17.5 mg/ml at 240 hours. The activity of fungal amylolytic enzymes formed in the culture liquid during the decomposition of carbohydrates present in the culture medium was studied, and it showed the highest activity of 27.4–41 units/ml at 216–240 hours of growth. In the dynamics of growth, one can observe the formation of proteolytic enzymes during the decomposition of proteins formed in the environment due to the growth of the fungus and the accumulation of biomass. Protease activity produced during fermentation showed a maximum value of 6.2 U/ml after 168 hours of growth (Moonmoon M.M., Uddin N.S., Ahmed N.J. and Khan M.A., 2010).

Based on our research, we can conclude that Pleurotus ostreatus can be used as a basidiomycete producer, producing large amounts of protein in a short period of time, when establishing the production of fish feed with balanced protein, quickly and easily digestible.

References

Sakovskaya V. G., Voroshilina Z. P. and others. “Workshop on pond fish farming”.– Moscow. VO “Agropromizdat”. 2010.

Xolmirzayev D., Haqberdiyev P.S., Shoximardonov D.R., Shaptakov E.S. Baliqchilik asoslari.– Toshkent. ILm-Ziyo. 2016.

Pulatov I.B., Zhuraeva K.M., Dodaev K.O., Niyozov Kh.N. Safety study of Uzbekistan freshwater fish and their canned fish //Bulletin of the Kazakh University of Technology and Business.– Astana, № 2, 2023.– P. 68–74. URL: https://www.researchgate.net/publication/372218330

Niezov Kh. N., Dodaev K. O. Balik uchun yaratilgan ozuka-em tarkibidagi oksil mikdorini aniklash / Yesh olimlar, undergraduate talabalarini XXXIII-ilmi-technikaviy anzhumaning makolalar typlami. “Umidli kimegarlar-2023”.– Toshkent. – B. 467-469.

Eremina I. A., Luzina N. I., Krieger O. V. Microbiology of plant products. Study guide, Kemerovo. 2003. – 94 p.

Gorelikova, G. A. Fundamentals of modern food biotechnology: textbook. manual / Kemerovo Technological Institute of Food Industry. Kemerovo, 2004. – 100 p.

GOST 20264.4–89 Group C09 Interstate standard preparations enzyme Methods for the determination of amylolytic activity. URL: https://files.stroyinf.ru/Data/112/11291.pdfAdenipekun, C.O. and Omolaso, P.O. (2015). Comparative study on cultivation, yield performance and proximate composition of Pleurotus pulmonarius Fries. (Quelet) on rice straw and banana leaves. World Journal of Agricultural Science – 11(3): – P. 151–158. URL: https://www.researchgate.net/publication/281148543

Batt C.A. & Tortorello M.L. *Encyclopedia of Food Microbiology.* Academic Press, 2014.

GOST 20264.2-88 Enzyme preparations. Methods for determining proteolytic activity. URL: http://www.omegametall.ru/Index2/1/4294833/4294833079.htm

Iwase, K., Umezawa, Y. and Masuda, K. (2000). Cultivation of Pleurotus ostreatus with beer spent grains and utilization. Mushroom Science – 15(2).– P. 819–826.

Moonmoon M.M., Uddin N.S., Ahmed N.J. and Khan M.A. (2010). Cultivation of different strains of king oyster mushroom (Pleurotus eryngii) on saw dust and rice straw in Bangladesh. Saudi Journal of Biological Science – 17.– P. 341–345. URL: https://www.researchgate.net/publication/255987189

submitted 16.08.2024;
accepted for publication 31.08.2024;
published 28.09.2024

Contact: niyozovxusan@gmail.com

The Austrian Journal of Technical and Natural Sciences, No 7–8
ISSN 2310-5607

PREMIER Publishing
ppublishing.org

DOI:10.29013/AJT-24-7.8-52-61

INTERACTION OF UREA WITH INORGANIC ACIDS

Yulbarsova M. V.[1], Kucharov B. Kh.[1], Erkayev A. U.[2], Zakirov B. S.[1]

[1] Institute of General and Inorganic Chemistry Academy of Sciences of the Republic of Uzbekistan,

[2] Tashkent Institute of Chemical Technology, Tashkent, Uzbekistan

Cite: *Yulbarsova M. V., Kucharov B. Kh., Erkayev A. U., Zakirov B. S. (2024). Interaction of Urea With Inorganic Acids. Austrian Journal of Technical and Natural Sciences 2024, No 3–4.* https://doi.org/10.29013/AJT-24-7.8-52-61

Abstract

This article presents research data on systems involving urea, nitrate, sulfuric, and phosphoric acids using the polythermal method in the production of complex fertilizers. Polythermal solubility diagrams were constructed, and the obtained data were confirmed by results from electron microscopy and X-ray structural analysis methods.

Keywords: *research, fertilizer, solution, crystallization, nitric, phosphoric, and sulfuric acids, water, solubility, polytherm, temperature, equilibrium*

Introduction

Urea, also known as carbamide, is one of the most widely used fertilizers in agriculture and industry. Urea is a white crystalline powder that is easily soluble in water. Its excellent solubility and chemical stability make it widely utilized across various industrial sectors. The high nitrogen content of urea makes it a valuable source of nutrients for plants.

Therefore, studying the physicochemical properties of urea is crucial for optimizing its use in different fields. Understanding the characteristics of this substance allows for the development of new application methods, improvement of existing technologies, and enhancement of its effectiveness in various areas of activity (Dormeshkin O. B., Mumunov N. Sh., Khoshimov B. T., 2024).

The high chemical activity of urea facilitates its ability to easily form various compounds. Numerous urea compounds with metal salts and acids have been identified in the solid state, where it can act as a neutral molecule or exhibit positive or negative charges (Molodkin A. K., Ellert G. V., Ivanova O. M., Skotnikova G. A., 1967).

The literature has explored the interaction processes of urea with sulfuric, nitric, and phosphoric acids in solution using spectrophotometric methods. The compositions of the resulting compounds have been determined, and their stability constants have been calculated (Alimova G. A., Saibova M. T., Prisekina L. I., 1982).

Methods and materials

Phase equilibrium studies in physicochemical systems were conducted using the visual polythermal method (Kirgintsev A. N., Trushnikova L. N., Lavrentieva V. G., 1972). This method involves visually observing the temperature at which the first crystals appear during uniform and slow cooling, or the disappearance of the last crystals during uniform heating with continuous stirring of solutions. The equipment used includes a test tube sealed with a stopper, a glass stirrer, and a thermometer with a scale interval of 0.1 °C. For uniform cooling, the test tube is placed in an outer test tube – called a jacket – that is immersed in a cooling mixture. Heating is also performed through the jacket. Cooling is achieved using liquid nitrogen in Dewar vessels.

Phase characteristics of the samples were measured using a powder X-ray diffractometer, Panalytical Empyrean. Equipment control was managed via a computer with the Data Collector software, and X-ray diffraction patterns were analyzed using the High Score program with the PDF 2013 database. X-ray phase analysis of the samples was performed on a Panalytical Empyrean diffractometer equipped with a Cu tube (Kα1 = 1.5406 Å). Measurements were conducted at room temperature over a 2θ angle range from 5° to 90° in step scanning mode with a step size of 0.013° and a signal accumulation time of 5 seconds per point.

Scanning electron microscopy was performed using a scanning electron microscope EVO MA-10 (Carl Zeiss, Germany), equipped with an energy-dispersive X-ray (EDX) microanalysis system (Oxford Instruments, UK), which can detect all elements of the periodic table of D. I. Mendeleev starting from boron. The microscope has a resolution of up to 2.5 nm at an accelerating voltage of 30 kV (secondary electron imaging), with accelerating voltage ranging from 1.0 to 30 kV, magnification from x10 to × 500.000, and a beam current of up to 200 nA. Sample preparation was carried out using equipment from Jeol (Japan) and Gatan (USA). Results were analyzed using specialized programs, such as INCA Point & ID for qualitative and quantitative element analysis, Mapping and QuantMap for mapping, and Feature for quantitative phase distribution and inclusions.

Results and discussion

To characterize the behavior of urea with inorganic acids in an aqueous environment, the solubility in the systems urea – nitric acid – water, urea – phosphoric acid – water, and urea – sulfuric acid – water was studied over a wide range of temperatures and concentrations using the visual polythermal method.

Binary systems of urea – water, nitric acid – water, phosphoric acid – water, and sulfuric acid – water, which are components of the studied system, have been examined by various authors (Kirgintsev A. N., Trushnikova L. N., Lavrentieva V. G., 1972).

The urea – nitric acid – water system was investigated through eight internal sections: I–IV from the side of $CO(NH_2)_2$-H_2O towards the HNO_3 pole, and V–VIII from the HNO_3-H_2O side towards the $CO(NH_2)_2$ vertex (Fig. 1).

Based on the polythermal solubility of the binary systems and internal sections, a polythermal solubility diagram for the $CO(NH_2)_2$-HNO_3-H_2O system was constructed, ranging from the complete freezing temperature (–44.8 °C) to 40 °C. This diagram delineates the crystallization fields of four solid phases: ice, $CO(NH_2)_2$, $HNO_3 \times 3H_2O$, and a new phase $CO(NH_2)_2 \times HNO_3$. Two triple points of the system, corresponding to the simultaneous crystallization of three different solid phases, were identified (Table 1). Isotherms were drawn on the polythermal solubility diagram within the crystallization fields at intervals of 10 °C. Projections of the polythermal curves on the urea – water and nitric acid – water sides were constructed.

The study revealed that the crystallization field of urea nitrate occupies a larger portion of the polythermal diagram compared to the crystallization fields of the initial components, indicating its low solubility in this system. The urea nitrate compound was isolated in crystalline form and identified using chemical and physicochemical analysis methods.

Figure 1. *Polythermal solubility diagram of the urea – nitric acid – water system*

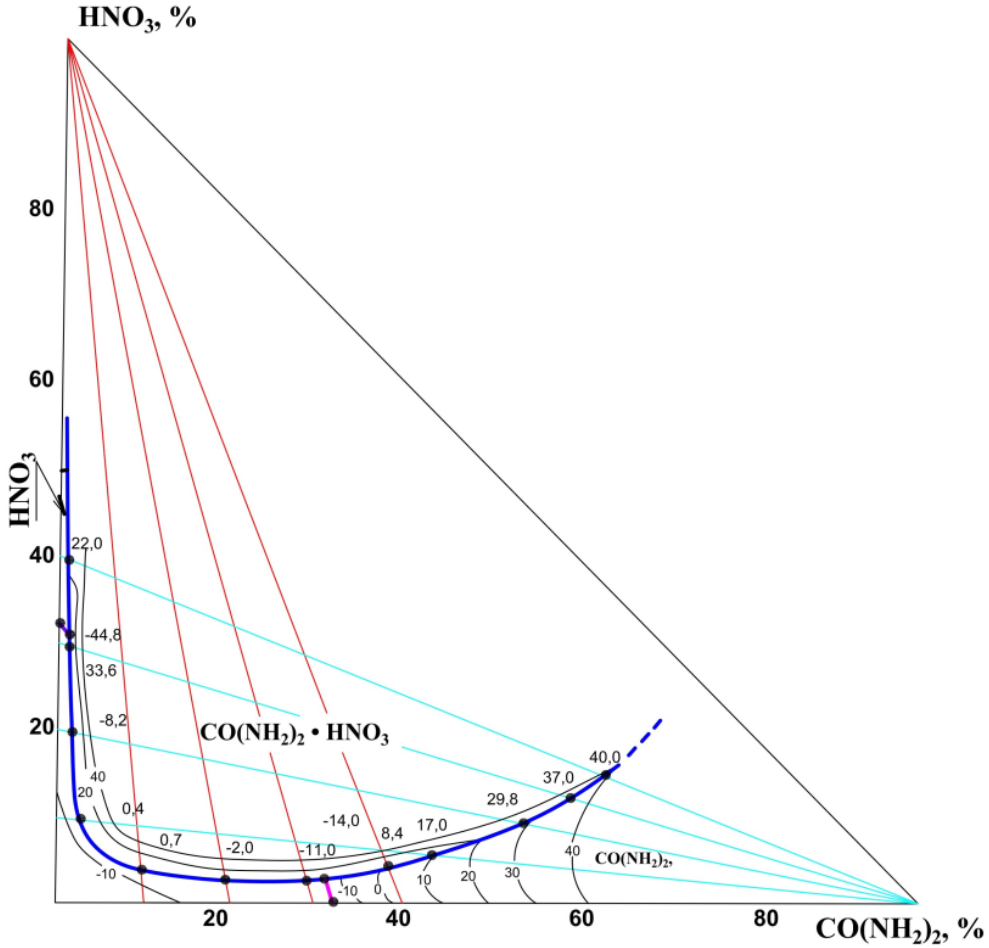

Table 1. *Double and triple points of the HNO_3-$CO(NH_2)_2$-H_2O system*

Liquid phase composition,%			Temp. crystal-lization, °C	Solid phases
HNO_3	$CO(NH_2)_2$	H_2O		
32.8	–	67.2	–43.0	Ice+$HNO_3 \times 3H_2O$
30.9	1.6	67.5	–44.8	Ice+$HNO_3 \times 3H_2O$+$HNO_3 \times$ $\times CO(NH_2)_2$
29.6	1.5	68.9	–33.4	Ice+$HNO_3 \times CO(NH_2)_2$
19.6	1.6	78.8	–8.2	Too
9.8	2.2	88.0	–0.4	Too
4.0	9.6	86.4	0.7	Too
3.0	19.6	77.4	–0.2	Too
3.0	29.8	67.2	–11.0	Too
–	32.0	68.0	–11.2	Ice+$CO(NH_2)_2$
3.6	31.0	65.4	–14.0	Ice+$CO(NH_2)_2$+$HNO_3 \times CO(NH_2)_2$
4.8	38.2	57.0	8.4	$HNO_3 \times CO(NH_2)_2$+$CO(NH_2)_2$
6.0	42.8	51.2	17.0	Too
9.8	53.0	37.2	29.8	Too
12.4	59.7	27.9	37.0	Too
15.0	63.8	21.2	40.0	Too
39.8	1.1	59.1	22.0	HNO_3+$HNO_3 \times CO(NH_2)_2$

Figure 2. *X-ray diffraction pattern of the compound: $HNO_3 \times CO(NH_2)_2$*

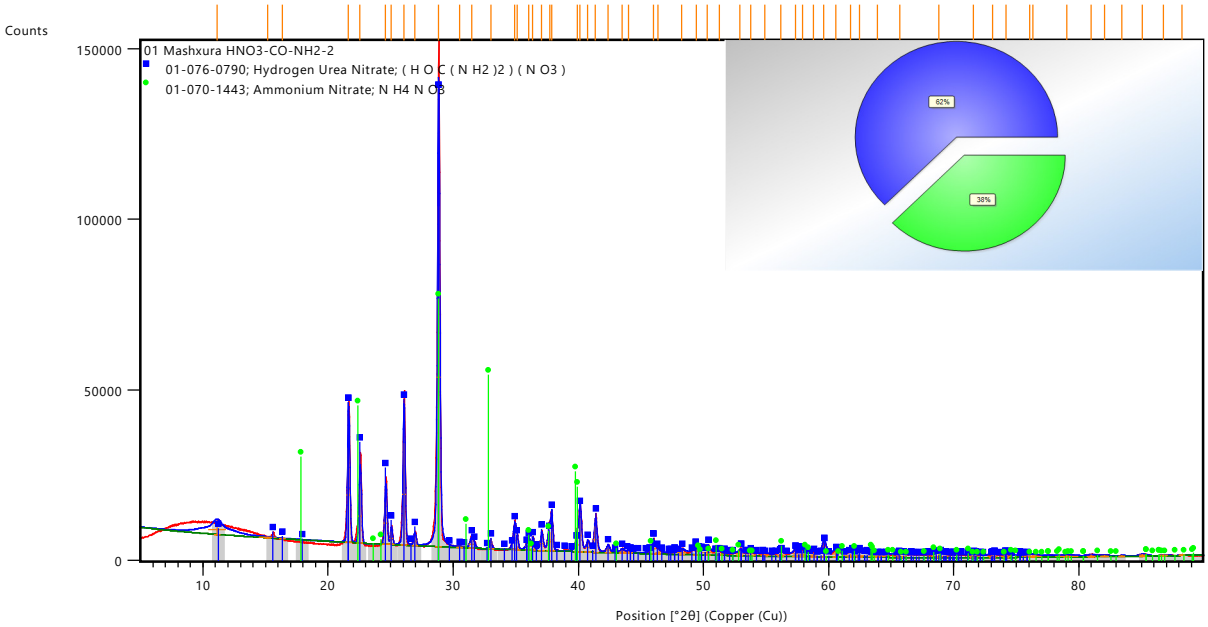

Based on the X-ray analysis, the compound contains 62% urea nitrate and 38% ammonium nitrate (Fig. 2). This is likely due to the partial decomposition of urea in nitric acid solutions. To study the elemental and mineralogical composition, a microscopic analysis was conducted using scanning electron microscopy (SEM). The elemental composition of the product was determined.

Figure 3. *Microstructure of urea nitrate*

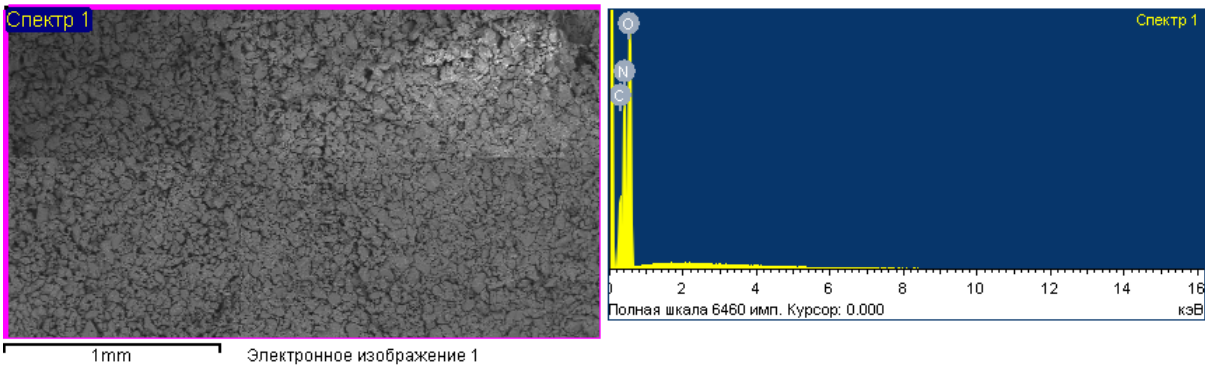

Based on the study (Fig. 3), the elemental composition of urea nitrate was determined as follows (in %): carbon (C) – 12.21, oxygen (O) – 54.46, nitrogen (N) – 33.33.

To characterize the interaction of components in the $CO(NH_2)_2$-H_3PO_4-H_2O system, the system was studied under polythermal conditions, ranging from the eutectic freezing point of –89.4 °C to 40 °C (Figure 1). The components of this system are thoroughly discussed in the literature (Kirgintsev A. N., Trushnikova L. N., Lavrentieva V. G. 1972; Yulbarsova M. V., Kucharov B. K., Zakirov B. S., Erkaev A. U., 2023; Yulbarsova M. V., Kucharov B. K., Zakirov B. S., Erkaev A. U., Nazirova R. M. 2024; Yulbarsova M. V., Kucharov B. K., Zakirov B. S., Erkaev A. U., Usmanova Z. D., 2023; Molodkin A. K., Ellert G. V., Ivanova O. M., Skotnikova G. A., 1967). Our data are consistent with the literature findings.

The authors of (Yulbarsova M. V., Kucharov B. K., Zakirov B. S., Erkaev A. U., 2023), in their study of the urea-phosphoric acid-water system, established that limited type solid solutions are formed in this system, and they also identified the eutectic point, which corresponds to a composi-

tion of 19.2% H_3PO_4, 34.3% $CO(NH_2)_2$, and 46.5% H_2O.

In our study of the urea-phosphoric acid-water system, eight internal sections were investigated, with sections I–IV ranging from the phosphoric acid-water side to the H3PO4 vertex, and sections V–VIII ranging from the $CO(NH_2)_2$-H_2O side to the phosphoric acid vertex.

Figure 4. *Polythermal Solubility diagram of the urea – phosphoric acid – water system*

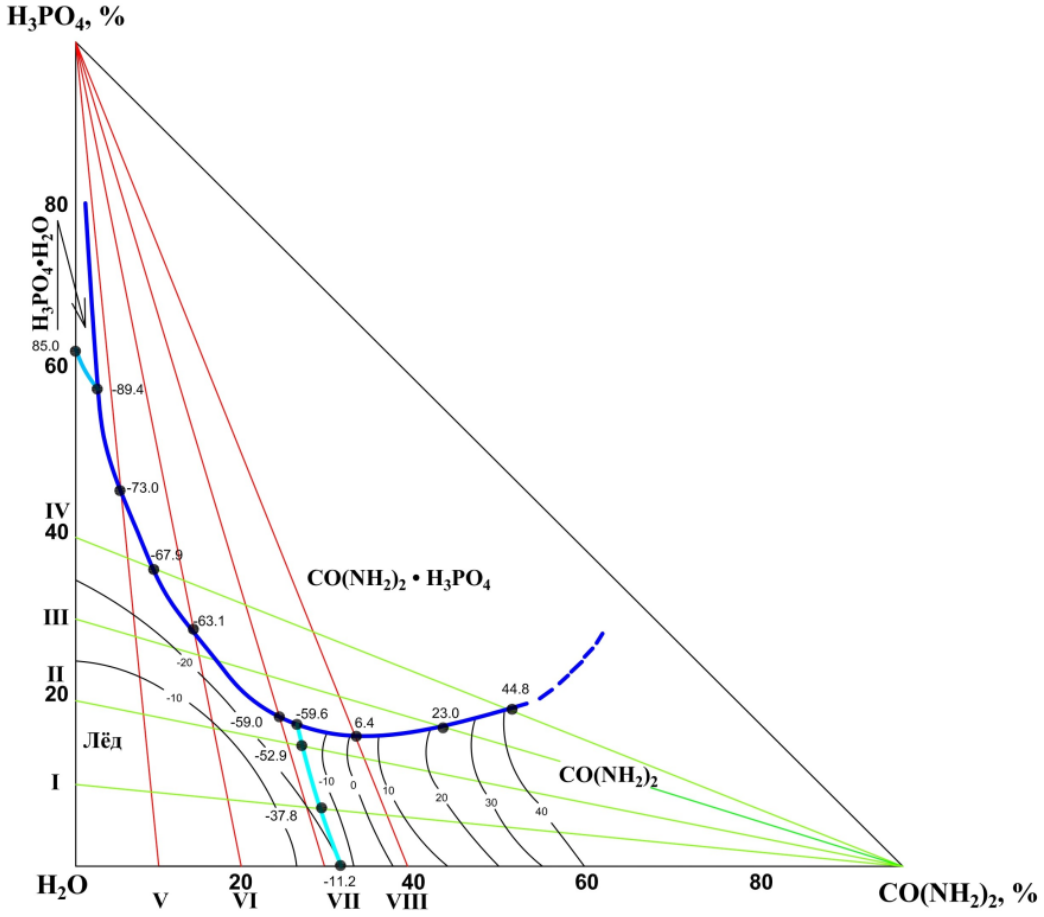

Based on the polythermal solubility data of the side systems and internal sections, a polythermal solubility diagram of the urea-phosphoric acid-water system was constructed, delineating the crystallization fields of ice, $CO(NH_2)_2$, $H_3PO_4 \times H_2O$, and the compound $CO(NH_2)_2 \times H_3PO_4$4. Two nodal triple points of the system were identified (Table 2).

Table 2. *Double and triple nodal points of the H_3PO_4-$CO(NH_2)_2$-H_2O system*

Liquid phase composition,%			Temp. crystallization, °C	Solid phases
H_3PO_4	$CO(NH_2)_2$	H_2O		
–	32.0	68.0	–11.2	Ice+$CO(NH_2)_2$
57.8	2.8	39.4	–89.4	Ice+H_3PO_4+$H_3PO_4 \times CO(NH_2)_2$
45.6	5.8	48.6	–73.0	Ice+$H_3PO_4 \times CO(NH_2)_2$
36.2	9.1	54.7	–67.9	Too
29.0	14.0	57.0	–63.1	Too
18.1	24.2	57.7	–59.0	Too
14.8	27.4	42.2	–52.9	Ice+$CO(NH_2)_2$
7.4	29.8	61.8	–37.8	Too
–	32.0	68.0	–11.2	Too

Liquid phase composition,%			Temp. crystallization, °C	Solid phases
H_3PO_4	$CO(NH_2)_2$	H_2O		
17.0	26.9	56.1	–59.6	Ice+$CO(NH_2)_2$+ $H_3PO_4 \times CO(NH_2)_2$
16.0	33.8	50.2	6.4	$H_3PO_4 \times CO(NH_2)_2$+$CO(NH_2)_2$
17.0	44.2	38.8	23.0	Too
19.1	52.8	28.1	44.8	Too
62.6	–	37.4	–85.0	Ice+$H_3PO_4 \times H_2O$

On the polythermal solubility diagram, isotherms of solubility are plotted within the crystallization fields at every 10 °C interval. Projections of the polythermal curves onto the sides of the urea-water and phosphoric acid-water systems are also constructed (Fig. 4).

In the studied system, an incongruently soluble compound of composition $CO(NH_2)_2 \times H_3PO_4$ is formed, which occupies a large area of the diagram. This is due to its lower solubility in the system compared to other components.

The compound was isolated in crystalline form and identified using chemical and physico-chemical analysis methods.

Figure 5. *X-ray diffraction pattern of the formed compound: $H_3PO_4 \times CO(NH_2)_2$*

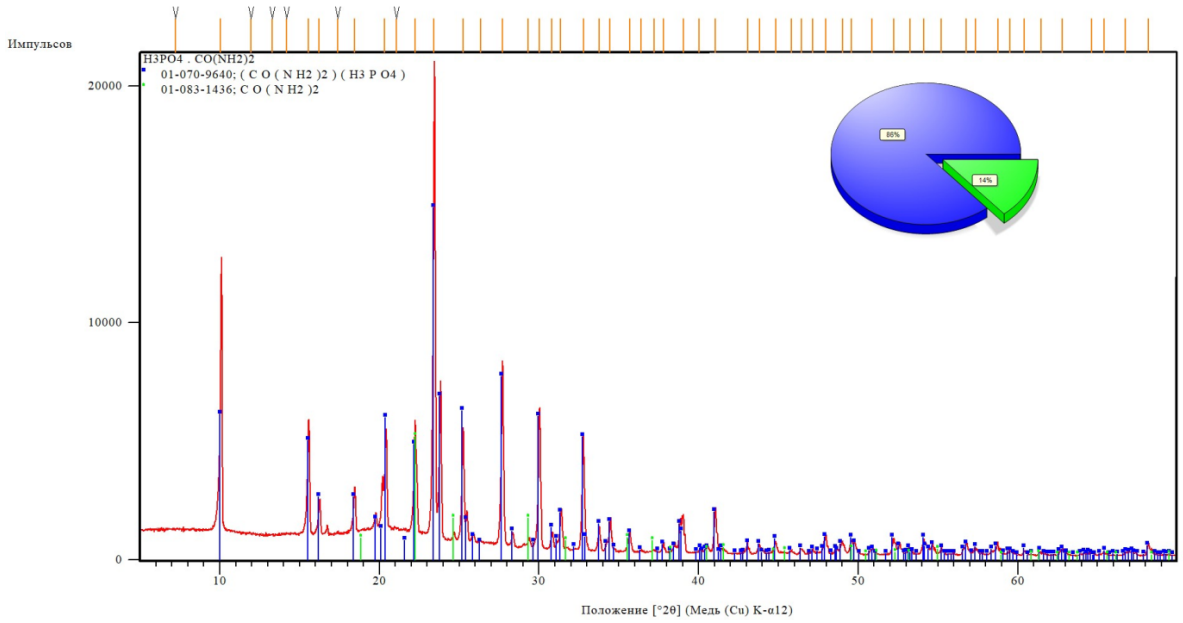

Figure 6. *Microstructure of urea phosphate*

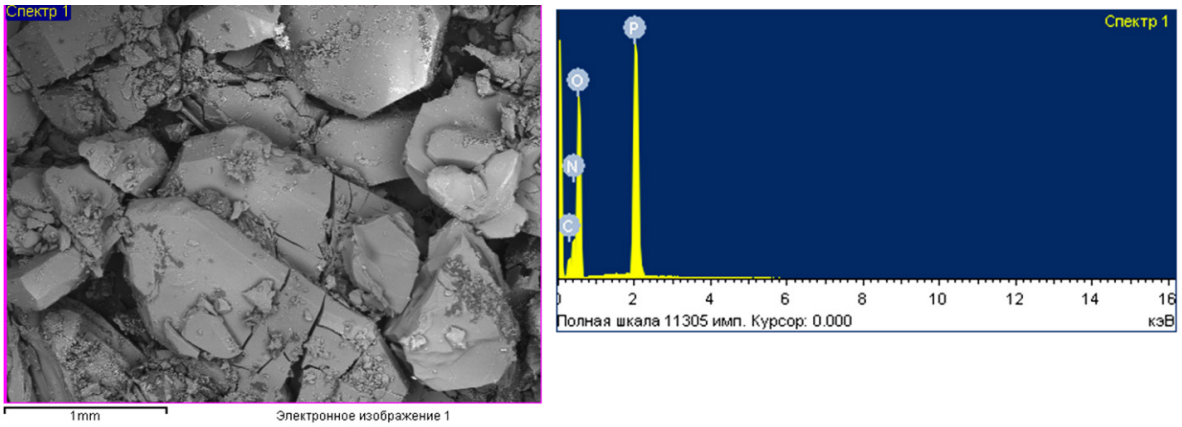

According to the X-ray analysis, the compound contains 86% urea phosphate and 14% urea (Fig. 5).

A microscopic analysis was conducted using scanning electron microscopy (SEM) to study the elemental and mineralogical composition.

Based on the study (Fig. 6), the elemental composition of urea nitrate was determined as follows (in %): carbon (C) – 13.13, oxygen (O) – 51.67, nitrogen (N) – 19.59, phosphorus (P) – 15.61.

The polythermal solubility of the $CO(NH_2)_2$-H_2SO_4-H_2O system was studied using eight internal sections (Fig. 7). Sections I–III were taken from the sulfuric acid-water side towards the urea pole, while sections IV–VIII were taken from the urea-water side towards the sulfuric acid vertex.

Based on literature data (Molodkin A.K., Ellert G.V., Ivanova O.M., Skotnikova G.A. 1967; Alimova G.A., Saibova M.T., Prisekina L.I. 1982; Nurakhmetov N.N., Beremzhanov B.A., 1978) and the polythermal solubility of binary systems and internal sections, a solubility diagram of the urea-sulfuric acid-water system was constructed for temperatures ranging from –67.8 °C to 40 °C (Fig. 7).

Figure 7. *Polythermal solubility diagram of the urea – sulfuric acid – water system*

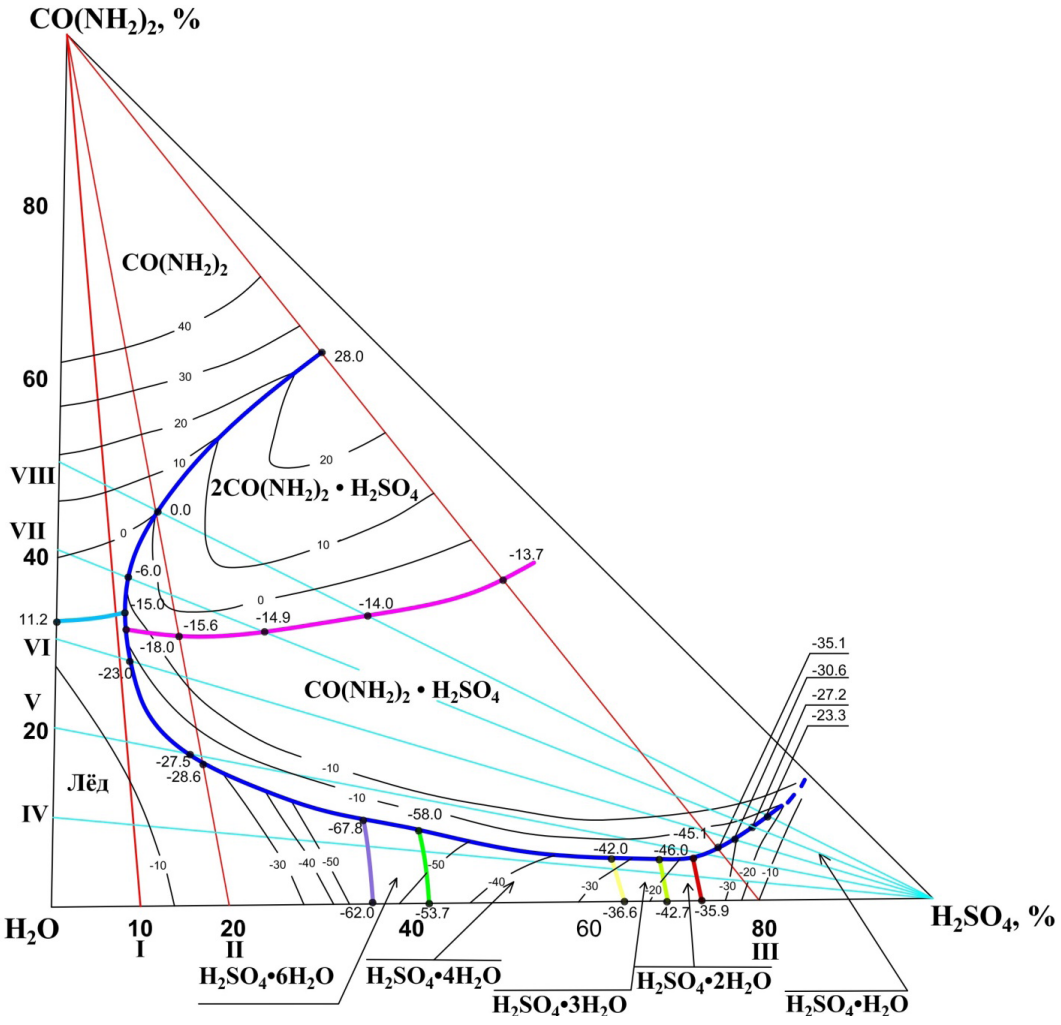

This diagram delineates the crystallization fields of ice, urea, and the six, four, three, two, and monohydrated forms of sulfuric acid, as well as two new compounds: $CO(NH_2)_2 \times H_2SO_4$ and $2CO(NH_2)_2 \times H_2SO_4$. These fields converge at seven triple points in the system, for which the crystallization temperatures and compositions of the equilibrium solution were determined. The characteristics of the double and triple nodal points of the $CO(NH_2)_2$-H_2SO_4-H_2O system are provided in Table 3.

Table 3. *Double and triple nodal points of the $CO(NH_2)_2$-H_2SO_4-H_2O system*

Liquid phase composition,%			Temp. crystallization, °C	Solid Phases
$CO(NH_2)_2$	H_2SO_4	H_2O		
32.0	–	68.0	–11.2	$Ice+CO(NH_2)_2$
32.3	8.2	59.5	–15.0	$Ice+CO(NH_2)_2+2CO(NH_2)_2 \times H_2SO_4$
31.0	7.9	61.1	–18.0	$Ice+2CO(NH_2)_2 \times H_2SO_4+CO(NH_2)_2 \times \times H_2SO_4$
27.8	8.8	63.4	–23.0	$Ice+CO(NH_2)_2 \times H_2SO_4$
16.9	15.6	67.5	–27.5	Too
16.0	17.0	67.0	–28.6	Too
9.4	35.1	55.5	–67.8	$Ice+H_2SO_4 \times 6H_2O+CO(NH_2)_2 \times H_2SO_4$
8.3	41.2	50.5	–58.0	$H_2SO_4 \times 6H_2O+H_2SO_4 \times 4H_2O+CO(NH_2)_2 \times \times H_2SO_4$
5.1	63.2	31.7	–42.0	$H_2SO_4 \times 4H_2O+H_2SO_4 \times 3H_2O+CO(NH_2)_2 \times \times H_2SO_4$
5.0	68.4	26.6	–46.0	$H_2SO_4 \times 3H_2O+H_2SO_4 \times 2H_2O+CO(NH_2)_2 \times \times H_2SO_4$
5.2	72.5	22.3	–45.1	$H_2SO_4 \times 2H_2O+H_2SO_4 \times H_2O+CO(NH_2)_2 \times \times H_2SO_4$
6.1	75.6	18.3	–35.1	$H_2SO_4 \times H_2O+CO(NH_2)_2 \times H_2SO_4$
6.9	77.1	16.0	–30.6	Too
8.1	79.2	12.7	–27.2	Too
9.6	81.3	9.1	–23.3	Too
30.1	9.8	60.1	–15.6	$2CO(NH_2)_2 \times H_2SO_4+CO(NH_2)_2 \times H_2SO_4$
30.8	23.6	45.6	–14.9	Too
32.2	35.8	32.0	–14.0	Too
36.4	51.1	12.1	–13.7	Too
36.9	8.4	54.7	–6.0	$CO(NH_2)_2+2CO(NH_2)_2 \times H_2SO_4$
63.2	29.9	6.9	28.0	Too
–	35.9	64.1	–62.0	$Ice+H_2SO_4 \times 6H_2O$
–	42.6	57.4	–53.7	$H_2SO_4 \times 6H_2O+H_2SO_4 \times 4H_2O$
–	64.7	35.3	–36.6	$H_2SO_4 \times 4H_2O+H_2SO_4 \times 3H_2O$
–	69.5	30.5	–42.7	$H_2SO_4 \times 3H_2O+H_2SO_4 \times 2H_2O$
–	73.6	26.4	–39.9	$H_2SO_4 \times 2H_2O+H_2SO_4 \times H_2O$

On the polythermal solubility diagram, isotherms of solubility are plotted within the crystallization fields at every 10 °C interval. Projections of the polythermal curves onto the sides of the urea-water and sulfuric acid-water systems have also been constructed.

The formed compound with the composition $H_2SO_4 \times {}_2CO(NH_2)_2$ was isolated in crystalline form and identified using chemical, X-ray, and physico-chemical analysis methods.

The chemical and physico-chemical analysis of the solid phase, isolated from the presumed area of existence of the formed compounds, confirmed the formation of this compound.

Figure 8. *X-ray diffraction pattern of the formed compound:* $H_2SO_{4\times2}CO(NH_2)_2$

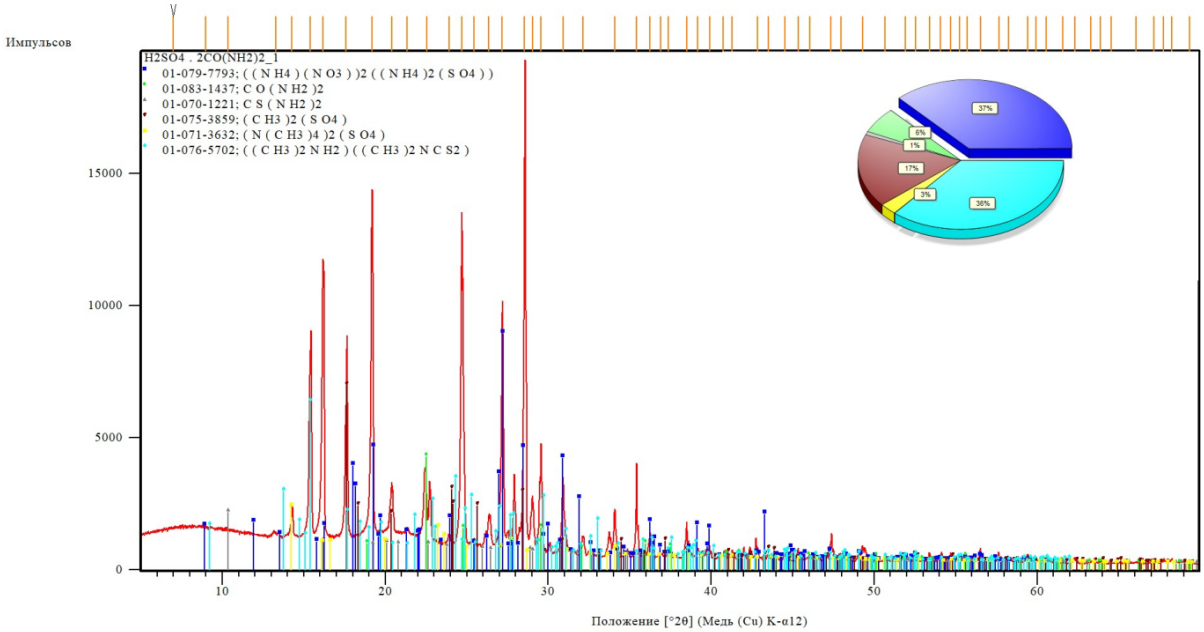

The X-ray phase analysis data of the urea-sulfuric acid compound indicate that all the reflections on the diffractograms are typically characterized by their specific reflection angles, sets of interplanar spacings, and intensities of diffraction lines (Fig. 8). This suggests the uniqueness of the crystal lattices of the obtained compounds.

A microscopic analysis using scanning electron microscopy (SEM) was conducted to study the elemental and mineralogical composition of the compound.

Figure 9. *Microstructure of urea sulfate*

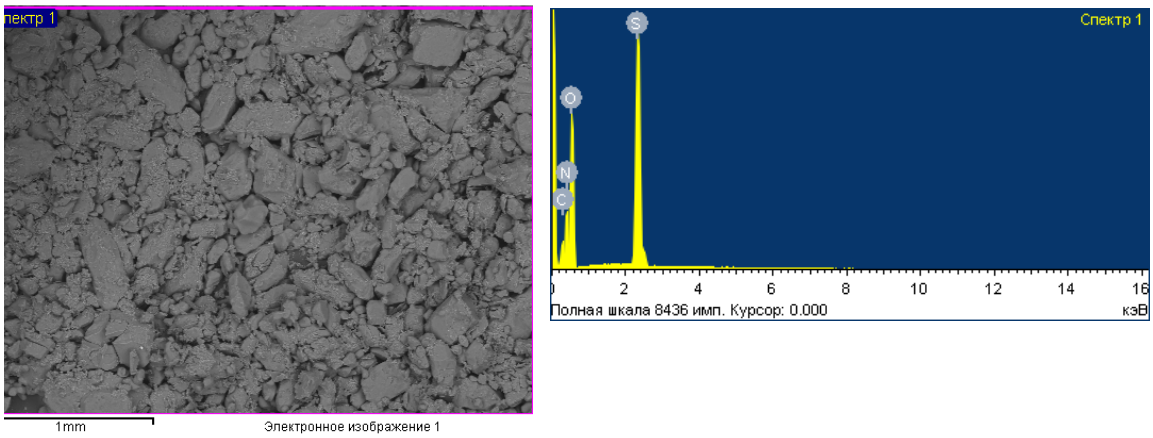

Based on the study (Fig. 9), the elemental composition of urea sulfate was determined as follows (in %): carbon (C) – 14.80, oxygen (O) – 45.69, nitrogen (N) – 26.32, sulfur (S) – 13.19.

Conclusion

The solubility of components in systems composed of urea, nitric, phosphoric, and sulfuric acids was studied using the visual-polythermal method. Polythermal solubility diagrams were constructed based on solubility data of binary systems and internal sections. In the studied systems, the formation of four new chemical compounds was established: $CO(NH_2)_2 \times HNO_3$, $CO(NH_2)_2 \times \times H_3PO_4$, $CO(NH_2)_2 \times H_2SO_4$, and $2CO(NH_2)_2 \times \times H_2SO_4$ from the original components. The formed compounds were isolated from the presumed crystallization areas in crystalline form and identified using chemical and physico-chemical analysis methods.

References

Dormeshkin O. B., Mumunov N. Sh., Khoshimov B. T. Investigation of the physicochemical properties of urea // Universum: Technical Sciences: Electronic Scientific Journal, 2024.– 6(123).– P. 53–58.
Molodkin A. K., Ellert G. V., Ivanova O. M., Skotnikova G. A. On the compounds of urea with acids // Journal of Inorganic Chemistry, 1967. XII,– P. 947–957.
Alimova G. A., Saibova M. T., Prisekina L. I. On the interaction of urea with mineral acids // Journal of Inorganic Chemistry, 1982, XXVII,– P. 1864–1865.
Kirgintsev A. N., Trushnikova L. N., Lavrentieva V. G. Solubility of inorganic substances in water. -L.: Chemistry, 1972.– 248 p.
Yulbarsova M. V., Kucharov B. K., Zakirov B. S., Erkaev A. U. Study of component interactions in the urea – nitric acid – water system // International Journal of Multidisciplinary Research in Science, Engineering, Technology & Management (IJMRSETM),– Vol. 10.– Issue 8. August 2023.– P. 2898–2901.
Yulbarsova M. V., Kucharov B. K., Zakirov B. S., Erkaev A. U., Nazirova R. M. Study of component interactions in the urea – nitric acid – water system // Scientific-Technical Journal (STJ FerPI,), 2024.– Vol. 28.– No. 3.– P. 152–156.
Yulbarsova M. V., Kucharov B. K., Zakirov B. S., Erkaev A. U., Usmanova Z. D. Polythermal solubility diagram of the urea – nitric acid – water system // International Scientific and Technical Conference on «Computer Science and Engineering Technologies» at the Jizzakh Branch of Mirzo Ulugbek National University of Uzbekistan, October – 13, 2023.– Jizzakh,– P. 237–240.
Molodkin A. K., Ellert G. V., Ivanova O. M., Skotnikova G. A. On the compounds of urea with acids // Journal of Inorganic Chemistry, 1967. XII,– P. 947–957.
Alimova G. A., Saibova M. T., Prisekina L. I. On the interaction of urea with mineral acids // Journal of Inorganic Chemistry, 1982. XXVII,– P. 1864–1865.
Nurakhmetov N. N., Beremzhanov B. A. On the interaction of inorganic acids with amides // Journal of Inorganic Chemistry, 1978. XXIII,– P. 504–514.

submitted 16.08.2024;
accepted for publication 31.08.2024;
published 28.09.2024

Contact: mashhura_1909@mail.ru

Contents